OPEN ACCESS
IOP Publishing | IMMT International Journal of Extreme Manufacturing
Int. J. Extrem. Manuf. 7 (2025) 032003 (44pp) https://doi.org/10.1088/2631-7990/ada857

Topical Review

Manufacturing high-performance flexible sensors via advanced patterning techniques

Xiaokun Qin[1,2], **Bowen Zhong**[1,2], **Hao Xu**[1,2,*], **Joshua A Jackman**[3], **Kaichen Xu**[4], **Nam-Joon Cho**[5,*], **Zheng Lou**[1,2] and **Lili Wang**[1,2,*]

[1] State Key Laboratory for Semiconductor Physics and Chip Technologies, Institute of Semiconductors, Chinese Academy of Sciences, Beijing 100083, People's Republic of China
[2] Center of Materials Science and Optoelectronic Engineering, University of Chinese Academy of Sciences, Beijing 100049, People's Republic of China
[3] School of Chemical Engineering and Translational Nanobioscience Research Center, Sungkyunkwan University, Suwon 16419, Republic of Korea
[4] State Key Laboratory of Fluid Power and Mechatronic Systems, School of Mechanical Engineering, Zhejiang University, Hangzhou, People's Republic of China
[5] School of Materials Science and Engineering, Nanyang Technological University, Singapore 637553, Singapore

E-mail: haoxu19@semi.ac.cn, njcho@ntu.edu.sg and liliwang@semi.ac.cn

Received 12 July 2024, revised 11 October 2024
Accepted for publication 9 January 2025
Published 27 January 2025

Abstract
Sensors play an important role in information perception during the age of intelligence, particularly in areas such as environmental monitoring and human perception. To meet the huge demands for information acquisition in the whole society, the development of elaborated sensor structures using patterned manufacturing technology is important to improve the performance of sensors. Creating patterned structures can enhance the interaction between the sensitive material and target matter, increase the contact area between the sensor and the target matter, amplify the effect of target matter on the sensor structure, and enhance the density of information sensing by building arrays. This review presents a comprehensive overview of patterned micro-nanostructure manufacturing techniques for performance enhancement of flexible sensors, including printing, exposure lithography, mould method, soft lithography, nanoimprinting lithography, and laser direct writing technology. Meanwhile, it introduces the evaluation methods of flexible sensor performance and discusses how patterned structures influence this performance. Finally, some practical application examples of patterned manufacturing techniques are introduced according to different types of flexible sensors. This review also summarises and provides an outlook on the role of these techniques in enhancing

* Authors to whom any correspondence should be addressed.

Original content from this work may be used under the terms of the Creative Commons Attribution 4.0 licence. Any further distribution of this work must maintain attribution to the author(s) and the title of the work, journal citation and DOI.

© 2025 The Author(s). Published by IOP Publishing Ltd on behalf of the IMMT
2631-7990/25/032003+44$33.00

sensor performance offering valuable insights for future developments in the patterned manufacturing of flexible sensors.

Keywords: patterned process, flexible sensor, patterned structure, performance enhancement

1. Introduction

Digital construction in the intelligent era is based on information perception, information transmission and information processing [1]. As key devices in the field of information perception, sensors have been broadening and replacing the human body's own level of perception of the surrounding environment since their birth, and have become an indispensable part of modern society [2]. A sensor is a device that converts a signal to be measured into another usable signal with a certain regularity [3]. According to the mechanical properties of sensor materials, sensors can be categorised into rigid and flexible sensors [4]. Rigid sensors are usually based on rigid materials such as metals, ceramics, and semiconductors. The device structure is fixed and fails in complex deformations, which limits the application scenarios of traditional sensors [5]. Flexible sensors are made of flexible materials and have a flexible structure that can adapt to complex shapes and dynamic environments. With the increasing demand for wearable electronic systems [6] as well as portable medical diagnostic devices [7, 8], enhancing the performance of flexible sensors has become a growing concern [9].

In the process of information perception, sensors are expected to reflect the changes in the environment realistically. The evaluation system of the sensor includes sensitivity, resolution, response time, relaxation time, and detection range, etc [10]. Sensitivity represents the ratio of the amount of change in the output signal to the amount of change in the input signal when the sensor is operating [11]. Limit of detection (LOD) represents the minimum amount of change that can be measured by the sensor [12]. Response time and relaxation time represent the detection speed of the sensor, which is an important parameter for real-time sensing [13]. Meanwhile, in order to ensure the accurate operation of the sensor, the sensor needs to work in a suitable detection range. Currently, the demand for information perception in the electronic information society is driving the development of flexible sensors toward high performance, high density, miniaturisation and low cost [14]. Among them, the patterned micro-nanostructure construction of active materials and structures has become one of the breakthrough directions for researchers [15, 16].

The patterning of flexible sensors often focuses on the sensitive element and electrode materials. The introduction of finely patterned structures can enhance the interaction between the material and the measured source [17], amplify the sensor's response to the measured signal [18], increase the specific surface area of the material and enhance the contact between molecules and the material [19], and enhance the mechanical stability of flexible sensors. Additionally, applying the patterned process to the manufacturing of sensor arrays can improve the density of information sensing and reduce the cross-influence of multiple objects to be measured [16, 20]. Thus, a judicious patterned structure design can significantly improve the performance of the sensor (figure 1).

Compared to traditional rigid sensors, flexible sensors are applied in more complex and diverse scenarios, and the processing constraints of flexible materials are more limited. The patterned micro-nanostructure interacts directly with the external surroundings, imposing higher requirements on the patterned manufacturing process of flexible sensors [21]. Common patterning processes typically comprise exposure lithography [22, 23], printing [24, 25], mould method [26, 27], soft lithography [28, 29], nanoimprint lithography (NIL) [30, 31], and laser direct writing (LDW) [32, 33]. Over time, the application of patterned manufacturing processes has become more finely categorised, with special manufacturing techniques emerging for specific materials involving the sensitive, structure and electrode parts of the sensor (figure 2) [34–53]. The selection of a specific patterned process often depends on material properties, processing cost, and difficulty of mass production [54]. This review provides a detailed overview of the commonly used manufacturing process for patterned micro-nanostructures, discusses the significance of patterned structures for flexible sensor performance enhancement, and presents practical applications of various patterned manufacturing technologies in flexible sensor preparation. Finally, we summarise the patterned techniques used for flexible sensor enhancement, and predict future directions in this field.

2. Patterned manufacturing method

Traditional methods for the manufacturing patterned micro-nanostructures for rigid sensors are compatible with rigid electronic systems and semiconductor manufacturing processes. In contrast, the manufacturing techniques applied to flexible materials usually face challenges such as reduced material stability, lower temperature tolerance, and increased process complexity [55]. These constrain the large-scale manufacturing and application of flexible sensors. After decades of development, micro-nano processing technology has derived customised new process technologies based on traditional processes to cope with different usage scenarios and processing materials. These new process technologies are complex and have some differences in classification. Here, we summarise from the level of key processes and introduce six common manufacturing methods: printing, exposure lithography, soft lithography, mould method, NIL and LDW. Specific comparisons are shown in table 1 [34, 39, 45, 56–99], and we will describe the various methods in detail next.

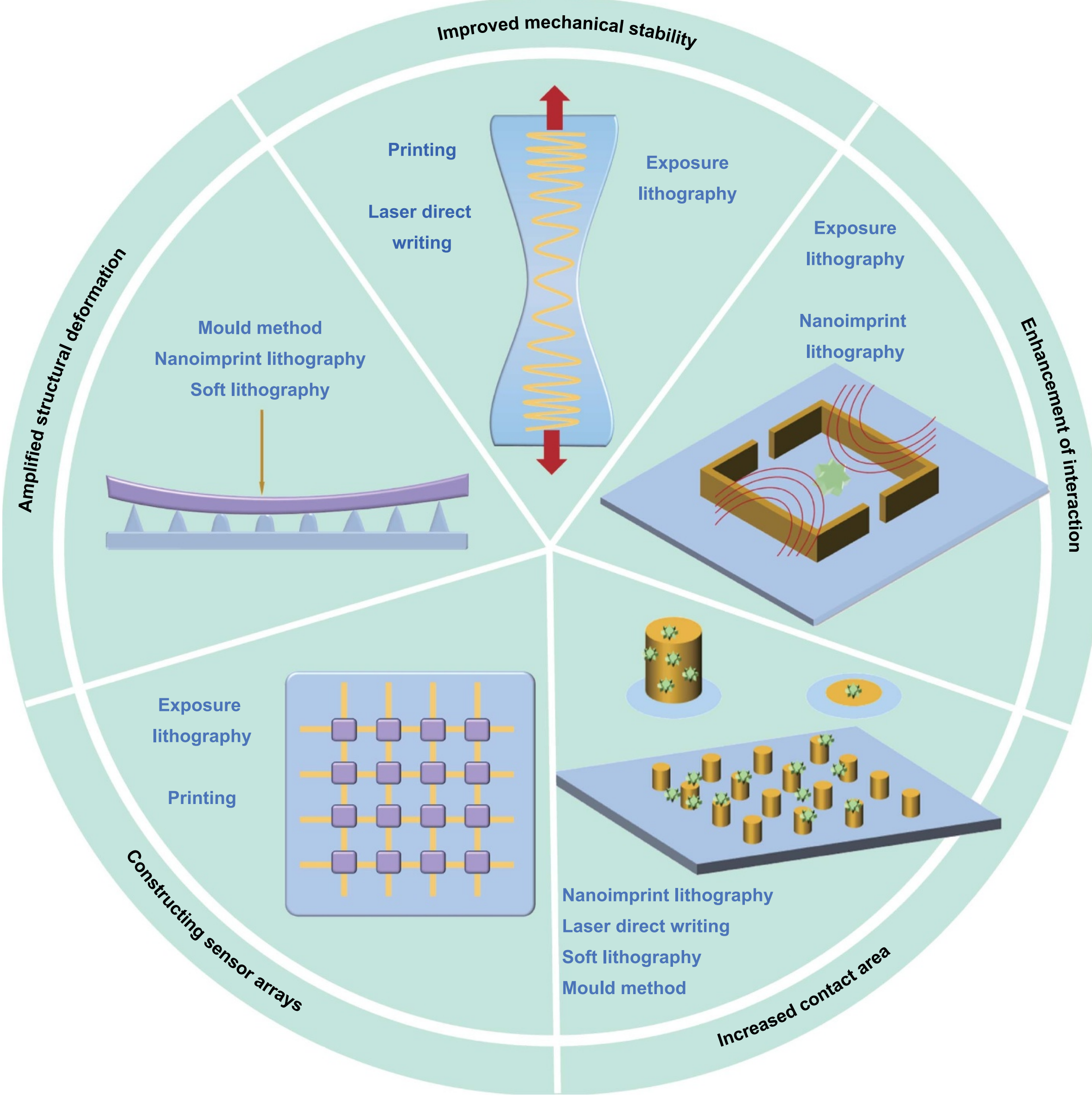

Figure 1. The role of patterned micro-nanostructures in flexible sensor performance enhancement. This mainly includes improved mechanical stability, enhancement of interaction, increased contact area, constructing sensor arrays, and amplified structural deformation. Also, common types of processes are listed in the figure for different parts.

2.1. Printing

Similar to traditional graphic printing used in books, the printing technology used in micro-nano processing is also a material deposition technology using liquid phase 'ink', which is a type of additive manufacturing technology [100]. Here, 'ink' stands not for ordinary ink, but for a category of functional materials, including metal nanoparticle inks, polymer inks, semiconductor inks, carbon inks, ceramic inks and a series of liquid-phase functional materials [101]. Depending on whether a masked version of the process is required or not, the printing processes include direct writing of patterns without a mask as well as printing patterns with a mask [102]. It is important to note here that we present scanning probe lithography separately as a maskless printing technique as well.

2.1.1. Inkjet printing. Inkjet printing belongs to a kind of plateless printing, and non-contact printing, through the computer control of the print head movement, with the worktable, can be directly nano-size solution sprayed on the rigid or flexible substrate to form the required pattern [103]. The inkjet printing device mainly includes an ink cartridge and an inkjet print head. To obtain suitable and high-resolution print patterns, the density of the ink, solution surface tension, ink viscosity, and nozzle diameter need to be considered [104]. Parameters describing the properties of the ink mainly

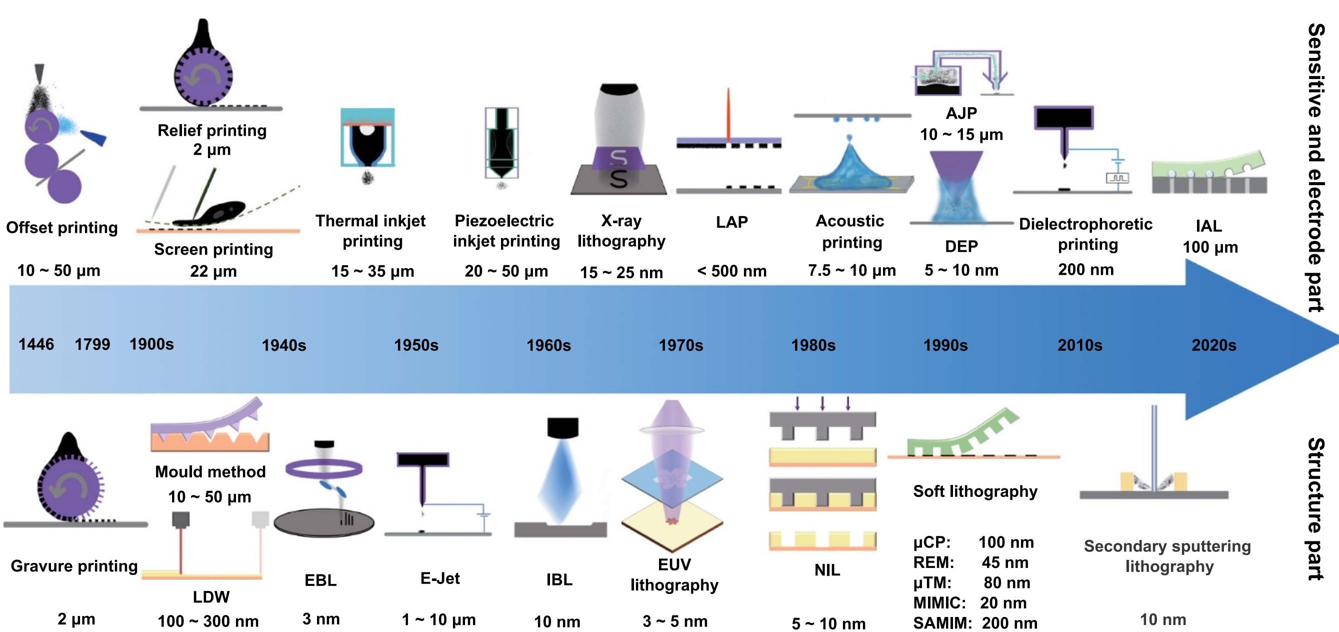

Figure 2. The timing of the large-scale application of the sensor patterning preparation process and the application areas of the process for sensors. The information in the figure also includes the minimum machining accuracy of the patterned manufacturing process [34–53].

Table 1. Patterned micro-nanostructure manufacturing method.

Patterned preparation method	Minimum size	Process feature	References
Piezoelectric inkjet printing	20–50 μm	Room temperature, non-contact	[34, 79, 80]
Thermal inkjet printing	15–35 μm	High temperature, low cost	[56, 81]
Laser-assisted printing (LAP)	<500 nm	Nozzle less	[57, 82]
Acoustic printing	7.5–10 μm	Nozzle less, biofriendly	[58, 83]
Aerosol jet printing (AJP)	10–15 μm	Atomised ink	[59, 84]
Electrohydrodynamic jet printing (E-Jet)	1–10 μm	Electric fields, non-contact	[60, 85]
Dielectrophoretic printing	200 nm	Applicable to uncharged particles	[39]
Screen printing	22 μm	High viscosity and low volatility inks	[61, 86]
Offset lithography printing	10–50 μm	Large-scale preparation, indirect printing	[62, 87]
Gravure/relief printing	2 μm	Large-scale preparation	[63, 88]
Dip-pen nanolithography	5–10 nm	Probe, low cleanliness requirements	[64]
EUV lithography	3–5 nm	High resolution, high productivity, high energy consumption, high cost.	[65, 89]
X-ray lithography	15–25 nm	1:1 proximity exposure	[45]
Electron beam lithography (EBL)	3 nm	Low throughput	[66]
Ion beam lithography	10 nm	No proximity effect of resist	[67, 68, 90]
Microcontact printing (μCP)	100 nm	Contact process, molecular self-assembly, fast, low-cost	[69, 91]
Replica moulding (REM)	45 nm	Easy peeling process	[70, 92]
Microtransfer moulding (μTM)	80 nm	Easy preparation of high aspect ratio structures	[71, 93]
Micromoulding in capillary (MIMIC)	20 nm	Spontaneous flow	[72, 94]
Solvent-assisted micromoulding (SAMIM)	200 nm	No temperature or UV effects.	[73, 95]
Sacrificial moulding method	12–100 μm	The minimum pattern size is related to the mould.	[74, 75]
Reusable moulding method	10–50 μm	The moulds are reusable and the sizes are related to lithography and etching	[76, 77]
Shadow masks technique	$\sim$5 nm	Reusable and fast	[96]
Thermal nanoimprinting lithography	5–10 nm	Fast, low cost, heat	[97]
Ultraviolet nanoimprinting lithography	5–10 nm	Fast, low cost, UV	[98]
Laser direct writing	100–300 nm	Reduced and modified manufacturing can be accomplished.	[78, 99]

include the Reynolds (Re), Weber (We), Ohnesorge (Oh) and Z parameter [105]:

$$Re = \frac{\upsilon \rho d}{\eta} \quad (1)$$

$$We = \frac{\upsilon^2 \rho d}{\gamma} \quad (2)$$

$$Oh = \frac{\sqrt{We}}{Re} \quad (3)$$

$$Z = \frac{1}{Oh} \quad (4)$$

where ν is the liquid flow rate, ρ is the density of the ink, d is the nozzle diameter, η is the ink viscosity and γ is the solution surface tension. The printing characteristics of an ink are usually related to the Z parameter. A synthesis of the data from related studies has led to the conclusion that $1 < Z < 14$ is a suitable printing interval for inks, which ensures better droplet outflow and reduces the production of satellite droplets [106]. When the ink containing nanodispersed particles comes into contact with a substrate, the solutes in the solution will be deposited on the contact line to form a ring-shaped deposit, which is the 'coffee ring effect' [107]. By using a solvent with a higher boiling point and heat of vaporisation than water, the effects of the coffee ring effect can be reduced [108].

According to the ejection mode of ink, inkjet printing can be divided into continuous inkjet (CIJ) and drop-on-demand inkjet (DOD) [34]. In the past, CIJ was often used in traditional printing processes, and DOD was often used in the field of high-resolution pattern printing due to the controllable ink volume. However, in recent years, with the continuous improvement of electric field theory and technology, the CIJ mode also has high-resolution printing technology, which is used together with DOD technology in micro-nano manufacturing processes [60]. Next, we will introduce a detailed classification based on the jet actuation method of the inkjet printhead.

Piezoelectric inkjet printing technology is a room temperature and pressure printing technology that contains piezoelectric material within the print head (figure 3(a)) [34]. Piezoelectric materials have the inverse piezoelectric effect. When polarised in an electric field, the material will deform due to the displacement of the charge centre within the material [109]. According to the way the piezoelectric material drives the ink in the print head, it can be divided into shear mode, squeeze mode, bending mode, push mode (figures 3(a-i)–(a-iv)) [110]. When a voltage pulse is applied to the piezoelectric material within the printhead, it causes a sudden change in volume within the printhead, which ejects droplets of ink. The pattern information is converted into a voltage and input to the piezoelectric material [111]. The deformation of the piezoelectric material is related to the pattern, and the ink in the print head is ejected according to a predetermined time and volume. Piezoelectric inkjet printing technology has the characteristics of fast response speed, strong anti-electromagnetic interference ability, simple structure and convenient control. It can control the volume of ejected ink by accurately controlling the driving voltage to achieve high-precision printing [112]. But in high-precision printing, the contradiction between smaller nozzles and nozzle clogging has always existed. Methods to reduce the solution viscosity (20–40 mPa s) only limit the types of printable materials [113]. To address the aforementioned issues, Bernasconi *et al* [114] designed a piezoelectric-driven print head capable of ejecting high-viscosity fluids, and achieved piezoelectric ejection of solutions with viscosities exceeding 200 cP.

Thermal inkjet printing is a low-cost printing technology. Its basic principle is to use ink vapour bubbles generated by heating to eject ink droplets from a chamber (figure 3(b)) [122]. The key to thermal inkjet printing equipment is the print head, which consists of an ink cartridge, a heater, and an ink nozzle that stores ink [123]. Through the power input controller, microsecond-level electrical pulses are quickly applied to the heating resistor, generating a high-temperature pulse of 300 °C [56]. The high-temperature heat flow on the heater surface will cause the temperature of the nearby ink to rise, thereby forming high-pressure ink vapour bubbles. As the bubbles gather and grow, the ink is ejected from the nozzle. The ejection of ink is accompanied by the collapse of the bubbles, and the ink is re-injected into the nozzle for the next printing process [115]. It is commonly believed that the drawback of thermal inkjet printing lies in the high temperatures that can damage the ink components, which limits its application in certain scenarios. However, Setti *et al* [124] found that thermal inkjet printing technology is compatible with the deposition of enzyme β-galactosidase and PEDOT: PSS, and they used inkjet printing technology to fabricate a glucose biosensor.

Laser-assisted printing (LAP) is a nozzle-less printing technology that is independent of the ink substrate (figure 3(c)). The LAP technology is developed based on the method of laser-induced forward transfer [57]. The printing system consists of a pulsed laser source, a ribbon and a receptor substrate [125]. The ribbon is usually made of quartz material as the support material. A metal film is used as the laser absorption layer, and the ink to be printed is deposited on the surface of the metal film [126]. When the pulsed laser is focused on the ribbon, the high temperature induces the formation of bubbles between the support material and the material to be printed. The bubbles rapidly expand and eject ink downwards [127]. Compared with conventional inkjet printing technology, LAP is capable of printing high-viscosity inks. Research by Makrygianni *et al* [128] has demonstrated that LAP can achieve a printing resolution of 30 μm using inks with viscosities ranging from 30 mPa s to 1700 mPa s. Additionally, the printing resolution can be flexibly adjusted by modulating the laser energy density. With its high precision and ease of operation, LAP holds significant potential for future applications [116].

Acoustic printing is a technology that uses sound waves to push ink jets. Elrod *et al* [129] and Hadimioglu *et al* [130] reported that a focused acoustic beam on the surface of a liquid can generate droplets with controllable diameters. This has propelled the development of acoustic inkjet printing

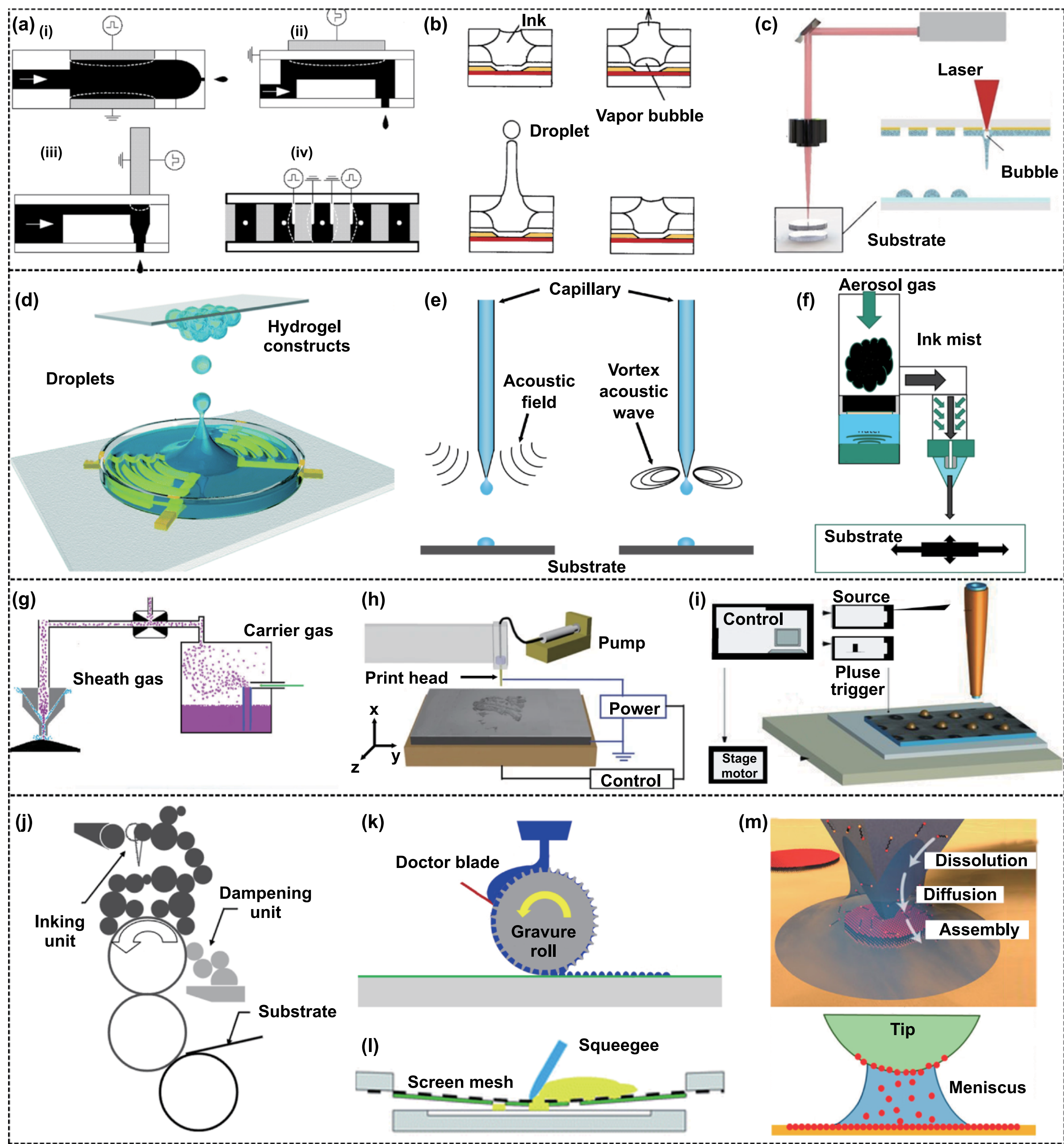

Figure 3. Printing process schematic. (a) Piezoelectric inkjet printing technology. (i) Squeeze mode. (ii) Bend mode. (iii) Push mode. (iv) Shear mode. Reprinted from [34], Copyright © 2010 Elsevier B.V. All rights reserved. (b) Thermal inkjet printing. Reprinted from [115], Copyright © 1997 Published by Elsevier Ltd. (c) Laser-assisted printing (LAP). [116] John Wiley & Sons. © 2021 Wiley-VCH GmbH. (d) Surface acoustic printing. Reproduced from [58] with permission from the Royal Society of Chemistry. (e) Acoustically driven microfluidic nozzles. (f) Aerosol jet printing with ultrasonic atomisation. Reproduced from [117]. © 2021 The Electrochemical Society ("ECS"). Published on behalf of ECS by IOP Publishing Limited. (g) Aerosol jet printing with pneumatic atomisation. [118] John Wiley & Sons. © 2021 Wiley-VCH GmbH. (h) Electrohydrodynamic jet printing (E-Jet). Reproduced from [60], with permission from Springer Nature. (i) Dielectrophoretic printing (DEP). [39] John Wiley & Sons. Copyright © 2010 WILEY-VCH Verlag GmbH & Co. KGaA, Weinheim. (j) Offset lithography printing. Used with permission of [ACM (Association for Computing Machinery)], from [119]; permission conveyed through Copyright Clearance Center, Inc. (k) Gravure printing. Reproduced from [120]. © IOP Publishing Ltd. All rights reserved. (l) Screen printing. Reproduced from [121] with permission from the Royal Society of Chemistry. (m) Dip-pen nanolithography. Reprinted (adapted) with permission from [64]. Copyright (2020) American Chemical Society.

technology. This printing method does not cause nozzle clogging, thereby getting rid of the limitation of nozzle diameter [110]. According to the ejection method of sonic wave-driven droplets, it can be roughly divided into two categories: (1) using a focused acoustic transducer, the sound waves are focused on the surface of the ink liquid to overcome the surface tension of the liquid and achieve liquid ejection (figure 3(d)) [58, 131]. Including acoustic focusing technology using concave acoustic transducers; use ring-shaped electrodes to clamp a piezoelectric film to form a Fresnel half-wave band source

to realise the acoustic focusing technology of self-focusing acoustic transducers [130]; place the acoustic lens in front of the transducer to achieve acoustic focusing technology; surface acoustic wave acoustic focusing technique using a single-phase transducer controlled by electrode width [132, 133]. (2) Using an acoustic microfluidic inkjet printing system with nozzles. Acoustophoretic or vortex acoustic wave induces droplet generation at the tip of the capillary tube (figure 3(e)) [134].

Aerosol jet printing (AJP) is a technology that prints ink in the form of an aerosol. Matters suspended in aerosols can be directly written in the form of aerosol jets [117]. According to the aerosol generation method, it can be divided into ultrasonic atomisation or pneumatic atomisation (figures 3(f) and (g)) [59]. During ultrasonic atomisation, the transducer is placed in the transmission medium. The electrical signal causes the transducer to produce high-frequency oscillations, and the superposition of continuous waves in the ink liquid causes the ejection of small droplets, and then a carrier gas is used to eject the aerosol onto the deposition substrate [135]. Bappy *et al* [136] utilised AJP technology with ultrasonic atomisation to fabricate a multimodal sensor integrated with strain and temperature. In the process of the pneumatic atomisation, the high-speed carrier gas impacts the top of the ink, and the top layer of the ink produces a series of dispersed small droplets. Among them, low-mass small droplets are deposited on the surface of the deposition substrate along with the carrier gas in the form of aerosol [118].

Electrohydrodynamic jet printing (E-Jet) is an inkjet printing technology driven by an electric field (figure 3(h)). The E-Jet system mainly consists of an ink tank, a pressure propulsion device, a glass nozzle with metal deposited on the tip, a substrate, and a high-voltage power supply [137]. The ink is injected into the glass nozzle tip by the pressure propelling device. An electric field is applied between the substrate and the nozzle, and the liquid at the nozzle tip is affected by gravity, surface tension, electromagnetic forces, and adhesion forces [138]. Under the combined action of these forces, the liquid interface forms a cone, which called a Taylor cone [139]. The ink jet is ejected from the Taylor cone surface onto the substrate. E-Jet printing can realise CIJ and DOD. Constant DC electric field can realise CIJ, and pulsed DC and AC electric fields can realise DOD [110]. Because the jet size based on the Taylor cone is much smaller than the nozzle diameter, the E-Jet printing can achieve high-resolution printing while reducing the risk of nozzle clogging [60, 140]. Guo *et al* [141] employed the E-jet technique to fabricate an array of microstructured electrodes that cure under ultraviolet light, constructing a capacitive pressure sensor with high sensitivity and excellent mechanical properties.

Dielectrophoretic printing (DEP) is an improvement over conventional electric field-driven inkjet printing (figure 3(i)). E-Jet relies on charged particles in the suspension, which is not friendly to ink suspensions composed of uncharged particles, and it is difficult to control the angle of the jet generated at the tip of the Taylor cone [142]. A uniform electrostatic field cannot control uncharged particles in the ink suspension, but a non-uniform electrostatic field will exert a DEP force on the particles by affecting the polarisability of the particles, which is applicable to all particles [143]. By applying pulsed DC power between the submicron capillary tip and the substrate, sufficiently large dielectrophoretic forces can result in ejection of the ink liquid [144]. DEP printing enables on-demand printing with high precision and controllability [39]. Chen *et al* [145] successfully fabricated a CMOS-compatible capacitive immunosensor array using DEP assisted manufacturing methods.

2.1.2. Coating printing. Coating printing is a contact printing method that requires a mask. Compared with inkjet printing, coating printing can achieve large-scale, high-throughput, and high-speed material printing. According to different printing moulds, coating printing can be divided into four types: offset lithographic printing, gravure printing, relief printing and screen printing [119].

Offset lithographic printing is a flat indirect printing technology. It realises printing based on the principle of water-oil incompatibility. The offset lithographic printing device mainly includes a water supply system, an ink supply system, a plate cylinder, a blanket cylinder and an impression cylinder [119]. The water film first adheres to the blank areas on the printing plate, and then the ink adheres to the patterned areas on the printing plate. The patterned water-oil film is transferred from the printing plate cylinder to the rubber cylinder. And then through the rubber cylinder and impression cylinder, the patterned ink is transferred to the substrate to be printed (figure 3(j)) [62]. Offset lithographic printing technology, known for its low cost and high speed, is commonly used in the process of printing books and magazines. It is currently also applied to the printing of electrode materials on large-area polymer films. Harrey *et al* [146] have prepared a capacitive humidity sensor, in which the patterned electrode film is deposited using a high-speed offset lithographic printing process.

Gravure printing and relief printing are direct printing technologies based on three-dimensional templates (figure 3(k)) [63]. The roller is a key device in the gravure and letterpress printing processes. Patterned pits or bumps are usually prepared using laser engraving, wet etching and dry etching processes [119]. Their basic printing process includes four steps: filling a patterned cell with ink; squeegee wipes the ink; ink is transferred to the substrate; and the ink solidifies on the substrate [120]. Gravure printing and relief printing require inks with low viscosity, high fluidity and fast drying characteristics [147]. Both of them are suitable for high-precision and large-scale printing scenarios, but the cost of preparing high-precision rollers is higher, so their development is slow [61]. As the demand for disposable wearable sensors continues to grow, the gravure printing technology, with its advantages of low cost and high efficiency, has gradually been applied to the preparation of patterned electrodes. Bariya *et al* [148] used gravure printing technology to fabricate electrode materials for disposable electrochemical sensors, which exhibit excellent mechanical properties.

Screen printing device consists of a patterned template screen, a rigid frame that supports the grid, and a matching scraper (figure 3(l)). During the screen-printing process, ink is placed on a patterned screen, and the patterned screen is closely attached to the substrate to be printed. A squeegee is used to apply shear force to the ink, squeezing the ink through the patterned screen and depositing onto the substrate [149]. The ink particles of screen-printing include metal particles, carbon materials, ceramic materials, semiconductor materials, and polymer materials [121, 150]. The ink solvent needs to have high viscosity and low volatility properties to ensure that the ink can be placed on the surface of the patterned screen without clogging the mesh [61]. Like conventional coating techniques, screen printing technology also has the advantages of low cost and high efficiency, and is commonly used in the field of disposable sensor preparation. Beniwal *et al* [151] used screen-printing technology to prepare a humidity sensor based on graphene carbon ink on paper substrates. The sensor has the advantages of high flexibility, high stability, and low cost.

2.1.3. Scanning-probe lithography (SPL). SPL is a maskless material patterning manufacturing method. With the advent of scanning probe microscopes (SPMs) and atomic force microscopes (AFMs), researchers used the nanotips of probes to pattern the surface of materials. Since then, the development of SPL in the field of micro-nano structure preparation has been initiated [152]. Although lithography is in the name, the basic principle of this technology is to use probes to affect the physical or chemical structure of a material's surface [64, 153]. This technology is mainly divided into destructive material manufacturing and additive manufacturing [154]. Damage material manufacturing technology involves etching, oxidation, and heating of the material surface by the probe [155–157]. Because the damage manufacturing technology is environmentally demanding, difficult to prepare and involves fewer sensor fields, we will not introduce too much here and refer to related research articles for details [158–161]. Here we focus on SPL additive manufacturing.

Dip-pen nanolithography (DPN) is a material deposition technology. Its basic working process is similar to ink direct writing, so here we classify it as printing technology. DPN mainly relies on AFM probes. Ink is applied to the tip of the probe. When the probe and the substrate are close to each other, a meniscus is formed between the probe and the substrate for the ink to move [64]. With a computer-controlled drive, the probe moves in a set path and can complete the deposition of ink on the surface of the substrate (figure 3(m)) [162]. As a direct writing patterning preparation technique, the DPN requires minimal ink material. Through the joint manipulation of multiple probes, DPN can achieve large-scale patterned material preparation [153]. Leveraging the advantages of ultra-high resolution and ultra-low loss, Saban *et al* [163] utilised DPN technology to pattern a mixture of glucose oxidase and PMMA into nanoclusters, creating an efficient working electrode that significantly enhanced the sensitivity of the sensor.

2.2. Exposure lithography

Exposure lithography is an image reproduction technique. The exposure lithography process described in this chapter refers specifically to the non-contact exposure etching process of photoresists using a photon sources or energetic particles sources as the irradiation source. Irradiation sources are irradiated on photosensitive materials, causing physical or chemical properties of the materials to change, thereby achieving patterned preparation of the substrate [164, 165]. The exposure lithography process mainly includes the following nine steps [166]: substrate cleaning, substrate surface treatment, spin coating, soft bake, alignment, exposure, post-exposure bake, stripping, hard bake. The current advanced exposure lithography technology is mainly based on projection exposure system, which has better process robustness and higher accuracy [65, 167]. The main development direction based on projection lithography technology is the continuous reduction of the resolution limit [65]. The resolution formula is as follows [168, 169]:

$$R = k_1 \frac{\lambda}{N_A} \tag{5}$$

where k_1 is the constants related to process parameters and photoresist type, λ is the exposure wavelength, N_A is the numerical aperture of the system. Under similar numerical aperture and process conditions, the shorter wavelength can bring better resolution [170]. Different radiation sources imply different wavelengths, and according to the type of radiation source exposed, exposure lithography can be divided into photons as a radiation source (photolithography) and energetic particles as a radiation source [171].

2.2.1. Photon radiation sources. Photon radiation sources mainly include ultraviolet light, deep ultraviolet light, extreme ultraviolet light and x-rays. The early photon light source is the ultraviolet light source generated by a mercury lamp, including the G-line at 436 nm, the H-line at 405 nm, and the I-line at 365 nm [172, 173]. As the demand for high resolution continues to increase, photon radiation sources have evolved into deep ultraviolet light sources based on excimer lasers, including KrF at 248 nm [174], ArF at 193 nm [175], F_2 at 157 nm [176], and the combination of immersion technology with ArF to achieve an equivalent of 134 nm wavelength [167]. And in the present day, the industry is beginning to adopt 13.5 nm extreme ultraviolet light sources to produce patterned processes with extremely high precision and resolution [164, 177]. The basic configuration of the system is shown in figure 4(a). X-ray lithography is a technology in which the radiation source is extended to shorter wavelengths, and the x-ray radiation used corresponds to wavelengths between 0.1 nm and 10 nm. X-ray has strong penetrability and the refractive index in materials is close to 1, so x-ray lithography uses a 1:1 proximity exposure technique (figure 4(b)). X-ray lithography technology can currently reach the ultimate resolution of 15 nm, and mainly performs patterning processes with high depth-to-width ratios [45, 178].

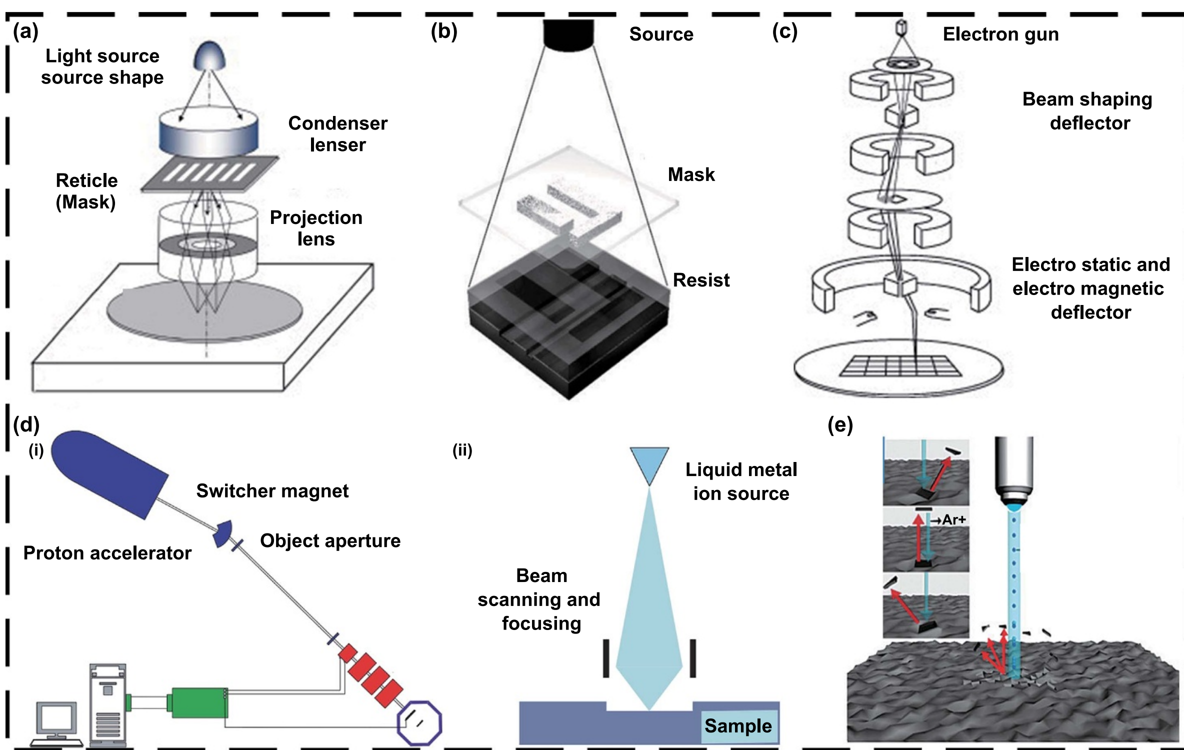

Figure 4. Exposure lithography schematic. (a) Standard lithography. Reprinted from [65], Copyright © 2014 Elsevier B.V. All rights reserved. (b) X-ray lithography. Reproduced from [178]. © IOP Publishing Ltd. All rights reserved. (c) Electron beam lithography. Reprinted from [65], Copyright © 2014 Elsevier B.V. All rights reserved. (d) Lithography based on energetic particles radiation sources. (i) Proton beam lithography. (ii) Focused ion beam lithography. Used with permission of [World Scientific Publishing Co. Pte. Ltd], from [47]; permission conveyed through Copyright Clearance Center, Inc. (e) Secondary sputtering lithography. Reprinted with permission from [52]. Copyright (2010) American Chemical Society.

2.2.2. Energetic particles radiation sources. Energetic particles radiation sources are currently mainly electron beams and ion beams. Electron beam lithography (EBL) is a maskless patterned direct writing technique using a focused electron beam as a radiation source, often used in the laboratory preparation of ultra-high precision sensors, integrated circuits and memories [179, 180]. EBL uses an electron gun to emit electrons, and its direct writing scanning method can be divided into raster scanning and vector scanning (figure 4(c)) [70]. The electron gun acceleration voltage affects the resolution of EBL and the sensitivity of the resist [65]. Currently, TEM can achieve an electron beam resolution limit of 0.1 nm. But due to resist proximity effects and sensitivity, the resolutions close to 3 nm can currently be achieved [66]. Feng *et al* [181] employed a two-step EBL nanofabrication technique to prepare ZnO-based gas sensors with a dense sub-nanometer structure, which offer the advantages of low power consumption and high resolution. The disadvantage of EBL is that the throughput is too low, and the main improvement method is to upgrade the single-beam system to a multi-beam system [182].

Ion beam lithography (IBL) technology achieves patterned manufacturing based on ion beams (figure 4(d)). The ion beam generated by the ion source is accelerated and focused through electric and magnetic fields, and projected onto the surface of the substrate [183]. Common ion types can be divided into slow heavy ions and slow heavy ions [184, 185]. IBL can be divided into focused IBL, proton beam lithography and ion projection lithography [47]. Because ions are heavier than electrons, matter waves have smaller wavelengths. At the same time, there is no proximity effect of the resist, so higher-resolution patterning manufacturing can be achieved [67, 68]. In addition, to achieve ultra-high resolution and high aspect ratio micro-nanostructures, researchers have developed a secondary sputtering lithography technique (SSL) [52]. By utilizing the secondary sputtering phenomenon during ion bombardment, 3D ultra-thin layers are prepared (figure 4(e)). Kang *et al* [186] used the SSL technique to fabricate SnO_2 nanochannels at the 10 nanometer scale, which can achieve highly sensitive H_2S detection.

2.3. Soft lithography

Soft lithography is a non-photolithographic patterning manufacturing technique using soft elastomers as moulds or stamps [73]. Commonly used elastomers are mainly polydimethylsiloxane (PDMS) [187], Ecoflex [188], polyurethane (TPU) [189], perfluoropolyethers (PFPEs) and etc [190]. The soft lithography process involves the preparation of the elastomer moulds and the patterning of the substrate using the elastomer moulds [191]. Among them, the master mould required for the elastomer moulds are usually achieved with the help of a lithography process. Compared with traditional lithography processes, soft lithography has lower environmental cleanliness requirements, lower time costs and capital costs.

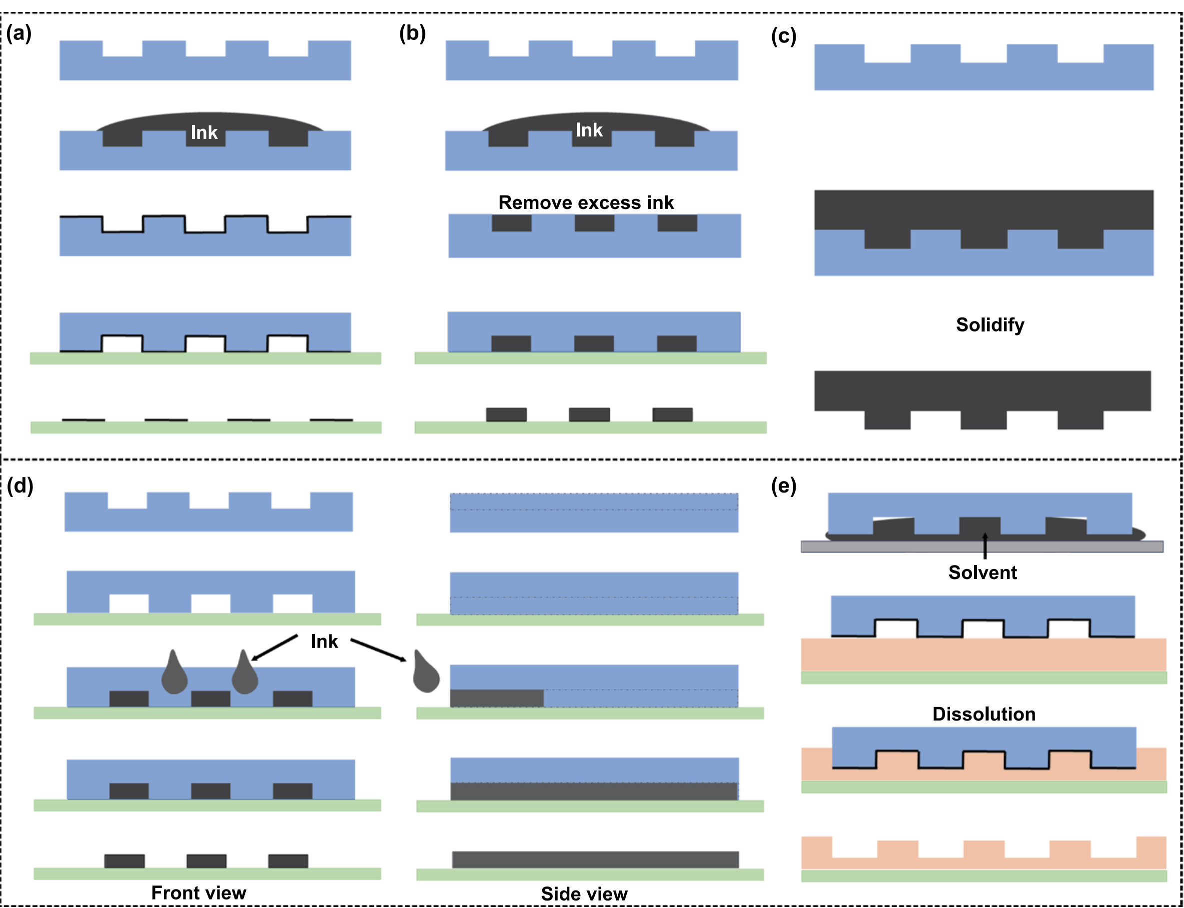

Figure 5. Soft lithography schematic. (a) Microcontact printing (μCP). (b) Replica moulding (REM). (c) Microtransfer moulding (μTM). (d) Micromoulding in capillary (MIMIC). (e) Solvent-assisted micromoulding (SAMIM).

At the same time, the elastomer moulds can achieve conformal contact with non-flat surfaces, greatly broadening the types of substrate structures that can be patterned [71, 192]. To achieve a reasonable classification of patterned manufacturing processes, soft lithography mainly refers to the micro-nano-processing technology using elastomers as stamps or moulds, and mainly contains the following five processes.

2.3.1. Microcontact printing (μCP). μCP uses an elastomer stamp with ink to contact the surface of the substrate to form a patterned, self-assembled monomolecular layer. Inks are ligand solutions that can self-assemble with the surface material of the substrate. The process is to immerse the elastomer stamp in ink and then press the stamp on the surface of the substrate (figure 5(a)) [69]. The raised patterned area of the stamp adheres the ligand to the substrate, and the contact area can form a self-assembled molecular layer within 1 s [193]. μCP is fast and low-cost. Du *et al* [194] used μCP technology and laser-induced graphene technology to fabricate ultra-thin graphene films with highly ordered micro-stripe arrays, and assembled a graphene-based liquid sensor with a sensitivity of 2.7% μl^{-1}. But the disadvantage of μCP is that the stamp will deform during the contact between the stamp and the substrate. At the same time, lateral ink diffusion occurs when ink is transferred from the elastomer stamp surface to the substrate surface [195]. These can cause errors in the patterning process, which are particularly significant at sub-micron sizes. Solutions include upgrading the Young's modulus of the elastomer and using high-speed printing strategies [196, 197].

2.3.2. Replica moulding (REM). REM is a technique of re-moulding using a patterned elastomer mould as a master mould, where the elastomer mould used as a master is formed by casting on a rigid mould (figure 5(b)) [192]. The advantage of the REM technology is the easy peeling process of the replica on the elastomer mould [198]. At the same time, by performing operations such as compression and stretching on elastomer moulds, it is possible to obtain replica sizes that can be reduced or enlarged in equal proportions, providing a high degree of flexibility [199]. Dervisevic *et al* [200] used REM technology to fabricate a microneedle array with conductive recessed microcavities, capable of monitoring urea concentration in the interstitial fluid of the skin.

2.3.3. Microtransfer moulding (μTM). μTM is a patterned manufacturing process similar to the reverse mould technique. The prepolymer is deposited onto the surface of the elastomeric mould. Excess prepolymer liquid is then removed by employing an elastic spatula or by directing a stream of inert

gas across the mould's surface. Subsequently, an elastomer mould filled with the prepolymer solution is placed in contact with the substrate, and solidified the prepolymer by light or thermal curing. Finally, the elastomer mould is peeled off to achieve patterned microstructures on the surface of the substrate (figure 5(c)) [201]. The advantage of μTM is that it can quickly and conveniently prepare high aspect ratio structures without special requirements for the substrate surface. However, a prepolymer film similar to the micro-contact printing process is easy to form on the surface of the substrate, which affects the subsequent process [71].

2.3.4. Micromoulding in capillary (MIMIC).

MIMIC is a patterned manufacturing technology that utilises spontaneous flow of capillary phenomena. An elastomer mould with a recessed structure is brought into conformal contact with the surface of the substrate and a cavity is formed between the mould and the substrate. By dropping the prepolymer solution into the openings of this composite structure, the prepolymer fills the entire cavity structure by capillary action [72]. Subsequently, through curing and peeling of the elastomer mould, a patterned structure is formed on the surface of the substrate (figure 5(d)). The processing speed and the quality of the patterned structure of MIMIC are closely related to the surface tension and the viscosity of the prepolymer liquid as well as the cavity size [71, 202]. In practice, it is necessary to select suitable moulding conditions in conjunction with the patterned structure. Heule and Gauckler [203] employed MIMIC technology to integrate an array of 12 tin oxide gas sensors on a single substrate, reducing power consumption while enhancing sensor density.

2.3.5. Solvent-assisted micromoulding (SAMIM).

SAMIM is a patterning manufacturing technique using elastomer moulds for embossing. Prior to embossing, the surface of the elastomer mould is dipped in a solvent that dissolves the polymer on the surface of the substrate. The elastomer mould is then pressed firmly onto the surface of the substrate. The solvent dissolves the polymer on the surface while the undissolved polymer fills in the cavity of the mould. After stripping the mould, a patterned structure is formed that complements the mould (figure 5(e)) [204]. Compared to embossing with rigid moulds, SAMIM avoids the influence of temperature or UV light on the material, and at the same time has a better fit, making it suitable for patterned embossing preparation on uneven surfaces [73].

2.4. Mould method

Mould method is a widely used class of processes for the preparation of complex structures. It is essentially a pattern reproduction technique. The mould method is low cost, simple and allows for rapid preparation of 2D and 3D patterning [205]. It is also highly compatible with pattern size, from micro-nano size to metre scale [206, 207]. To differentiate between the mould method and the photolithography and soft lithography techniques, here we describe the mould method which requires only one step of the process for the patterned manufacturing. At the same time, the moulds or masks used are rigid or sacrificial materials [208]. Common mould methods are mainly divided into fill-moulding techniques and shadow masks techniques.

2.4.1. Fill-moulding technique.

Fill-moulding technique is commonly used for the fabrication of patterned 3D structures, such as hemispheres, pyramids, cubes, etc., which amplify the effect of material deformation [209]. The process involves making a mould with the target structure in advance and pouring the liquid to be prepared into the mould cavity [210]. Demoulding of the poured material after curing allows for a patterned structure that complements the mould. Depending on the repetitive characteristics of the mould, it can be divided into the sacrificial moulding method and the reusable moulding method [211].

Sacrificial moulding method usually uses dissolvable, fusible or volatile mould materials, including water beads, air bubbles, polymer beads etc. (figure 6(a)) [74, 75, 212]. During the preparation of micro-nano structures, these micro-nano scale moulds are usually subjected to liquid surface tension or intermolecular forces to achieve a regular arrangement. After the sacrificial mould structure is lined up, the liquid material is poured, and after the liquid material has cured, the mould is removed by methods such as heating or high pressure, thus forming a three-dimensional patterned structure inside the cured material. This technology requires that the mould cannot be sacrificed before the pouring material solidifies, and the disappearing conditions of the mould cannot affect the solidified material. It is worth noting that Bubble template-assisted assembly is a patterned manufacturing process that uses bubbles as templates. The ultrathin interface of the bubble wall is used as a constrained template for molecular arrangement and distribution [213, 214]. Combining the molecular solution to be assembled with a surfactant can form an ordered ultrathin molecular film on the bubble surface [54]. In the process of using bubble arrays as patterning templates, to avoid the influence of the Oswald ripening process, the strategy of increasing the viscosity of the liquid and using micron arrays is usually adopted [215]. Bubble template-assisted assembly can generate ultra-high-precision pattern arrays that are not inferior to traditional photolithography technology, and the bubble preparation is simple and the bubble template is easy to remove (figure 6(b)) [75]. This is a novel sacrificial moulding method for the preparation of molecular level patterned structures.

Reusable moulding method typically uses rigid mould machined by lithography and etching processes. The inner walls of rigid mould cavities are coated with surfactants to increase the efficiency of the de-moulding process (figure 6(c)) [76]. Common reusable rigid moulds are silicon wafers with patterned structures prepared on the surface by an etching process, in addition to metal moulds, 3D printed moulds, and natural material moulds [17, 27, 77, 217]. The technology needs to reduce the residue of cured material in rigid moulds, while the mould is designed to ensure the

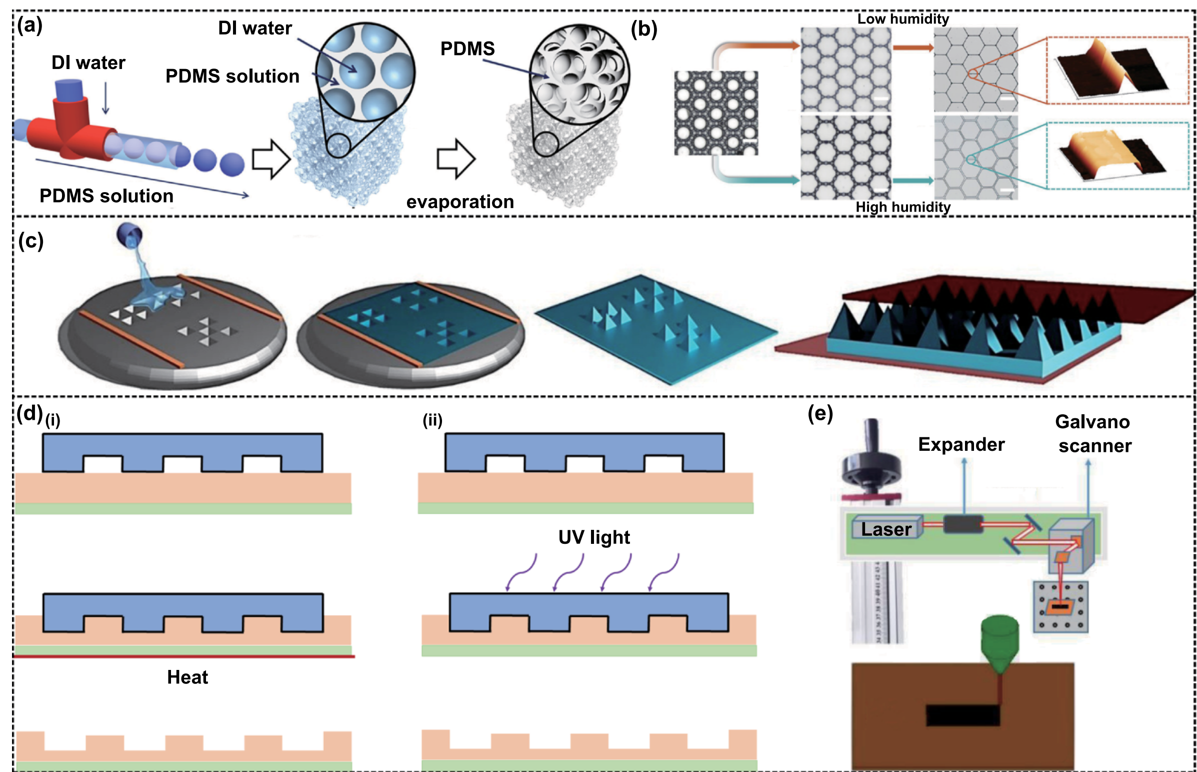

Figure 6. Mould method schematic. (a) Sacrificial moulding method. The sacrificial moulds are water droplets. Reprinted with permission from [74]. Copyright (2019) American Chemical Society. (b) Bubble mould-assisted assembly technology. [75] John Wiley & Sons. © 2023 Wiley-VCH GmbH. (c) Reusable moulding method. Reprinted from [76], © 2020 Elsevier B.V. All rights reserved. (d) Nanoimprint lithography (NIL). The left side is thermal nanoimprint lithography, and the right side is ultraviolet nanoimprint lithography. (e) Laser direct writing (LDW). Reproduced from [216]. CC BY 4.0.

feasibility of de-moulding [211]. Recently, researchers have developed a technique known as isolated air-pocket lithography (IAL) [53]. By growing isolated micro-bubbles within high-precision master mould holes, this method can produce 3D micro-patterns with complex structures and high curvature. The approach is precise, uniform, and suitable for large-area production, potentially offering new solutions for the manufacturing of sensor patterned micro-nanostructures in the future.

2.4.2. Shadow masks technique. Shadow masks technique is a two-dimensional patterned structure forming technique. Shadow masks are typically placed on the surface of a substrate to enable additive or subtractive manufacturing on the substrate surface using spray, spin, drop, deposition or etching processes [218–220]. Unlike lithography for the preparation of disposable mask layers, the shadow masks technique allows direct completion of patterned material preparation and the shadow masks can be reused [221].

2.5. NIL

NIL is a contact compression moulding technology. In this review, we distinguish between NIL and soft lithography. The concept of NIL that we describe involves only rigid moulds, and soft lithography uses elastomers as moulds. Compression moulding is a very old technique of pattern preparation. The wood, wax and metal stamping are all products of compression moulding [222]. After entering the micro-nano size, Compression moulding technology is called NIL. NIL consists of three main processes. First, a polymer coating is applied to the substrate surface. Subsequently a rigid mould with patterned structures is brought into contact with a polymer coating on the surface of the substrate, and special equipment is used to apply uniform pressure to the mould. Finally, the mould is separated from the polymer coating under high temperature or UV light conditions, and the polymer on the substrate surface forms a patterned structure complementary to the mould structure (figure 6(d)) [223, 224]. NIL is considered a favourable competitor to lithography due to its fast-processing speed, low cost and high resolution [225]. Canon's latest NIL equipment currently enables the preparation of patterning processes at the 5 nm node. The commonly used NIL includes thermal NIL (T-NIL) and ultraviolet NIL (UV-NIL).

2.5.1. Thermal NIL (T-NIL). NIL is a high-temperature, high-pressure compression moulding technique. First, a layer of thermoplastic polymer resist is spin-coated on the surface of the substrate, and then the substrate is heated above the glass transition temperature of the polymer. The mould with the surface pattern is placed in contact with the surface of the substrate. Pressure is applied and the pattern on the mould is pressed into the softened polymer. The patterning transfer

process is completed when the overall material cools and the template is removed [226]. Zanut *et al* [227] utilised T-NIL to create an array of nanoelectrodes with small dimensions, fabricating a highly sensitive and high-grade biochemical sensor. This process has been proven to possess high reliability and repeatability. Currently, the difficulty with NIL is the patterning of highly viscous polymer films, which is often achieved by treating the mould surface with a release agent to reduce polymer adhesion [228].

2.5.2. Ultraviolet NIL (UV-NIL). UV-NIL is a compression moulding technique at room temperature and low pressure [222]. Firstly, liquid polymer resist that can be light-cured is spin-coated on the surface of the substrate, and the transparent mould is pressed onto the polymer. The resist is gradually cured by UV light. After removal of the mould, the cured resist exhibits an established patterned structure. The transparent mould improves alignment accuracy on the one hand and ensures uniform transmission of UV light on the other.

2.6. LDW

LDW is a non-contact material patterning processing technology. A laser is essentially an amplification of light by stimulated radiation, which is a beam of light with good monochromaticity, good coherence, high brightness and good directionality [229]. Depending on the wavelength of the laser, it can be divided into infrared LDW, visible LDW and ultraviolet LDW technology. The choice of laser wavelength depends on the range of light wavelengths that can be absorbed by the materials and structures to be processed (figure 6(e)) [216]. Depending on the mode of operation, LDW can be classified as continuous laser processing [230], long-pulse laser processing (milliseconds, microseconds) [231], short-pulse laser processing (nanoseconds) [232] and ultra-short-pulse laser processing (picoseconds, femtoseconds) [233]. The narrower the pulse width is, the higher the machining accuracy. In terms of building patterned structures on the surface of materials, LDW can complete processes such as surface modification and surface material etching [234]. Next, each of these two laser processes will be described.

2.6.1. Laser induced technology. In contrast to conventional thermal methods, lasers have a high peak power that induces photochemical and photothermal reactions for material synthesis [235]. The technology of laser modified materials usually focuses on the manufacturing of electrodes for devices, with the fastest development in the preparation of carbon material [236, 237]. In 2014, Lin *et al* [238] prepared patterned porous graphene films on polymer surfaces for the first time using CO_2 lasers, which greatly reduced the difficulty of preparing graphene electrode materials. Since then, laser modification techniques based on a variety of polymer materials have been developed and are gradually being applied to sensors [239]. Yang *et al* [240] used LDW technology to transform a mixture of self-assembled block copolymers and resins into porous graphene foam. The sensor exhibits high sensitivity and selectivity for nitrogen oxides. The patterned structure obtained directly on the substrate material by laser modification technology has strong adhesion and good flexibility, which is particularly suitable for the manufacturing of flexible sensor arrays [241].

2.6.2. Laser etching. Laser etching is a micromachining technique that utilises a laser beam to remove the surface of a material [242]. During laser etching, a high-power density laser beam irradiates the surface of the material, causing localised areas of the material to heat up, resulting in melting and evaporation of the material [243]. During the manufacturing of patterned micro-nanostructure for sensors, short-pulse laser processing and ultra-short-pulse laser processing techniques are usually used to ensure the resolution of patterned micro-nanostructures. At the same time, the reduction of the pulse width reduces the influence of thermal effects [244], which is particularly important for the processing of flexible materials. Laser etching techniques can be used to construct patterned active materials directly [245] or to assist in the preparation of patterned structures by constructing patterned templates [246].

3. Comparison of manufacturing methods and techniques

When selecting a method for manufacturing patterned micro-nanostructure, several factors must be considered, including material compatibility, resolution, uniformity, cost, production efficiency, scalability and environmental impact. The relative importance of different factors depends on the performance requirements of the flexible sensor and the actual application scenario. Processes are usually classified and ranked according to the degree of concern in order to select a suitable method for the fabrication of patterned micro-nanostructure. For example, commercial sensor fabrication usually requires multifactor coordination and mutual compromise to maximise benefits. Sensor preparation in the laboratory is usually based on performance as the primary metric, and the appropriate fabrication technique is selected with the aim of optimizing performance. In the following section, we will analyse the different patterned manufacturing process in detail from seven aspects. The relevant analyses are also presented in tabular form for easy reference (table 2).

3.1. Material compatibility

The material compatibility of patterned manufacturing techniques represents the universality of the methods. The materials involved in process mainly include patterning materials and substrate materials. Among them, the printing methods have extremely high material compatibility. Based on the material requirements of the different sensors, printing inks include metallic materials [247], carbon materials [248], organic polymer materials [249], semiconductor materials [250], ceramic materials [251], inorganic metal salts [252] as well as mixtures of different material compositions, etc., and the physical characteristics of the inks are adjusted according to the process

Table 2. Comparative analysis of patterned manufacturing processes.

Method	Material compatibility	Resolution	Uniformity	Cost	Production efficiency	Scalability	Environmental impact	References
Printing	Multi-type materials	Large resolution span	Standard, influenced by inks	Cheap	Rapid	Large-scale	Eco-friendly	[64, 110, 111, 247–253]
Exposure lithography	Flat surfaces	Ultra-high	Ultra-high	Exorbitant	Slow, and the EBL is very slow	Large-scale, but the EBL and IBL are limited	Polluting	[250, 254–258]
Soft lithography	PDMS	Standard	Standard	Moderate	Fast	Small-scale	Low-impact	[259, 260]
Mould method	Depend on natural or artificial moulds	Standard	Standard	Moderate	Fast	Medium-scale	Low-impact	[225, 261]
NIL	Thermoset or photoset material, rigid substrate	High	Ultra-high	Expensive	Fast	Large-scale	Neutral	[73, 262–265]
LDW	Multi-type materials	High	High	Expensive	Slow	Small-scale	Eco-friendly	[266–269]

temperature and nozzle diameter. During the manufacturing of sensors, the ink types may be complex and varied to prepare different functional structures. Ma *et al* [270] prepared a fully printed and multiplexed sensing system that enabled continuous monitoring and analysis of sweat markers. The flexible sensors integrated in the system are prepared by inkjet printing, for which they have specially designed 11 printable functional inks. At the same time, the printing process can be done on both flat and curved surfaces [254]. As a non-contact processing technology, LDW method can be applied to a wide range of materials and can even manipulate biomolecules and living cells and keep them biologically active [266]. At the same time, laser-induced technology does not require precursor materials, and can directly realise patterned functional material preparation on the substrate material, with lower material requirements [267]. Other manufacturing technologies, which have certain requirements on the machinable material, are suitable for a specific range of machining. NIL requires that the patterned material be thermoset or photoset. Meanwhile, the polymer viscosity is low and the coefficient of thermal expansion of the thermosetting polymer is different from that of the stamps, and the purpose of these is to improve processability and processing accuracy [73]. Soft lithography typically uses PDMS as a mould. Thanks to the better flexibility of PDMS, it has advantage in the curved materials' patterned manufacturing [259]. In the mould method, the mould materials are categorised into natural and artificial materials. Natural materials are simple to obtain but cannot be customised. Shi *et al* [271] prepared flexible piezoresistive pressure sensors with micro-nanostructures using lotus leaves as templates. Artificial materials are usually manufactured by photolithography, printing or LDW techniques and are available in a wide variety of materials. However, the materials for reproducing patterns are mainly based on curable materials such as PDMS or PI. Photolithography, EBL and IBL have high requirements for the processing environment and processing materials. The substrate material usually has a flat surface [255]. Photoresist is the key to the exposure lithography process, and it is a photosensitive mixture with complex composition. According to the type of exposure lithography process, photoresist is mainly categorised into chemically amplified resists (CAR) and non-CA resist [256]. Its complex material requirements reduce the material compatibility of exposure lithography technology.

3.2. Resolution

The resolution is a reflection of the precision of the process and represents the minimum machining line width of the patterning process. The higher the resolution is, the more accurate the patterning structure, which is critical for sensors that are partially based on physical field coupling [272], and the increased resolution also enhances sensor integration. The photolithography process is one of the highest resolution patterning manufacturing processes available. At the same time, the EBL technique has high resolution and is commonly used for mask plate preparation for photolithography and NIL [257]. Manfrinato *et al* [273] used EBL to achieve an isolated feature size of 2 nm and a half pitch of 5 nm. EUV photolithography, which uses extreme ultraviolet light at a wavelength of 13.5 nm as a light source, has the smallest resolution currently available for large-scale commercial production, with a resolution limit of 3–5 nm [258]. Rigid moulds for NIL are prepared by photolithography or EBL, resulting in high resolution of NIL. Canon produces commercialised NIL equipment with a resolution of 5 nm to 10 nm [262], and has become a

strong contender for photolithography in the field of micro-nanostructure manufacturing. Soft lithography uses flexible materials as mould, and flexible mould is prepared using high-precision rigid mould as masters, resulting in high resolution of flexible mould. However, there is deformation of the flexible mould during the transfer of the patterned structure, which greatly reduces the resolution of the soft lithography technique [260]. Therefore, soft lithography is suitable for patterning manufacturing of sensors with low resolution requirements and flexible structures. LDW technology can obtain patterned structures with submicron resolution, where the heat affected zone is an important factor affecting the accuracy of laser processing. By reducing the laser pulse duration and incorporating aids such as microlens arrays (MLAs), femtosecond laser processing can be achieved with feature sizes on the order of a hundred nanometres [274]. Hong *et al* [275] fabricated submicron-sized metamaterial terahertz resonant cavities using femtosecond laser beam irradiation through the MLA, which can be used for ultrasensitive biosensing. The resolution of the printing process is generally at the micron level, limited by the nozzle diameter or the erratic movement of the ink. Fine control of the ink is required to realise a high-precision printing process. DPN using microscope probes can achieve resolutions of 5–10 nm [64]. E-jet and DEP printing can achieve sub-micron processing accuracy [39, 60]. The resolution of the mould method is mainly dependent on the machining accuracy of the mould and the filling capacity of the fluid to be cured. Therefore, the resolution of mould method spans a wide range, with a minimum of nanometer resolution achievable.

3.3. Uniformity

Uniformity is the error between the same structures between different regions during the processing of patterned micro and nanostructures. The processing uniformity of the manufacturing process enhances the ability to prepare sensors on a large scale, and is critical for sensor integration. Exposure lithography has extremely high uniformity, high resolution and high automation, which can realise the preparation of large-scale patterned structures with high precision. The LDW technology enables highly uniform patterned micro-nanostructures to be realised on flat substrate surfaces by relying on a stable laser light source. NIL is an effective means of reproducing nanoscale patterns [263]. In contrast to photolithography, NIL has a layer of residual polymer underneath the stamp after demoulding, which can lead to defects and affect the uniformity of the micro-nanostructures [264]. The uniformity of the printing process is strongly influenced by the ink. The infiltration and movement of ink during the printing process can lead to a coffee ring effect or satellite droplets that affect the uniformity of the patterned structure [111]. The state of the ink is usually changed according to the substrate material for better continuous printing. The uniformity of the mould method depends mainly on the preparation process of the mould. Uniform templates can be prepared using photolithography or LDW techniques. At the same time, the process of material filling and moulding often lacks precise control of bubble size as well as structure, which can affect the uniformity of the sensor's micro-nanostructure [268].

3.4. Cost

Cost is an important consideration for commercialised sensor manufacturing. Photolithography is a high-resolution and high-cost technology. The high cost of photolithography is mainly reflected in the high cleanliness requirements of the production environment, expensive equipment and complex systems [257]. At the same time, the photolithography process is always accompanied by the removal of materials, the consumption of such materials is expensive and wasteful [250]. An equally high-cost technique for the manufacturing of patterned micro-nanostructures is LDW. To achieve the highest resolution fabrication, femtosecond laser equipment is costly. Also, due to the slow processing speed of LDW technology, it is relatively more costly in large-area manufacturing. To reduce environmental, equipment and production costs, reusable moulds can be processed using lithography or LDW technology. Currently, NIL, soft lithography, and mould methods all reduce the cost-per-use in mass production by using moulds with micro-nanostructures, and have lower process environmental requirements [261]. The printing process is an additive manufacturing process with low material loss [110]. Meanwhile, the printing equipment has low cost and low environmental requirements, which makes it a low-cost patterned micro-nanostructure manufacturing technology [250].

3.5. Production efficiency

Production efficiency affects the cost of time in sensors production. LDW technology is a point-by-point, line-by-line scanning maskless processing technology with slow processing speeds. Scaling of productivity is usually achieved through parallel processing [266]. High-resolution photolithography is a less production efficiency micro-nanostructure processing technique due to the complex processing steps and the preparation of a high-clean environment during processing [254]. The maskless writing of EBL is very slow, and is not suitable for the preparation of large-area patterns [168]. In order to solve the problem of low throughput of the above two processing techniques, high precision moulds are prepared by high resolution processing technique, which can save processing time [261]. Soft lithography, NIL and mould method technologies transfer high-precision nanoscale patterns to substrate materials quickly and efficiently, making them ideal for commercial mass production [225]. Printing process is technically mature, easy to operate, and can integrate thousands of high-density nozzles for mass production [111].

3.6. Scalability

Scalability represents the ability of a patterned manufacturing technology to scale up from small-scale laboratory production to large-scale commercial production, and is influenced by cost, production efficiency, and uniformity. Printing process has been in commercial use for a long time due to its low

cost and high-speed production capabilities. However, ultra-high-resolution SPL has not yet solved the problem of simultaneous realisation of high speed, high resolution and low cost, large-scale manufacturing needs further development [253]. Photolithography has become an important component in the preparation of patterned micro-nanostructures due to its ultra-high resolution and great commercial value. EBL and IBL are less efficient for industrialised mass production due to their slow speed and complex systems [257]. In order to reduce the production cost of EUV technology and increase the production speed of EBL technology, NIL technology has emerged as a key candidate for the commercial production of patterned micro-nanostructures, and has been gradually scaled up to mass production [265]. Soft lithography and mould methods are low cost and can be used in the production of flexible devices, but are more suitable for laboratory use due to the low level of standardisation in the production process. LDW technology has high resolution, but is limited by production speed issues and is not suitable for cost-effective mass production [254].

3.7. Environmental impact

The environmental impact of process production is mainly reflected in the emission of pollutants and the waste of resources during the production process. Exposure lithography process is a material reduction process for the photoresist, so the photoresist consumption is high, and the cleaning process consumes a large amount of DI water and hazardous chemical solutions, which have a high impact on the environment [254]. Printing and LDW technologies have less surface contamination than processes involving direct contact between chemicals and substrate materials [269].

4. Significance of patterned micro-nanostructure for sensor performance enhancement

4.1. Sensor performance evaluation parameters

4.1.1. Sensitivity. The sensitivity of a sensor is the ability of the sensor to respond to changes in the measured value, representing the amount of change in the sensor output signal when the measured value changes. The generalised formula for sensor sensitivity is as follows:

$$Sensitivity = \frac{\Delta S/S_0}{M} \tag{6}$$

where ΔS is the change value of the output signal, S_0 is the initial output signal value, and M is signal to be measured. The units of sensitivity depend on the sensor type and what is being measured. For example, pressure sensor is typically measured in $\mathrm{kPa^{-1}}$ [10], gas sensors in $\mathrm{ppm^{-1}}$ [23], temperature sensors in $^{\circ}\mathrm{C}^{-1}$ [221], humidity sensors in $\mathrm{RH^{-1}}$ [276] and magnetic sensors in $\mathrm{Oe^{-1}}$ [277].

4.1.2. LOD. LOD refers to the minimum concentration or amount of the component to be measured that can be detected by the sensor from the sample to be measured at a given level of confidence. The LOD is a key technical metric for evaluating sensors, and can help determine if the output data is of value. LOD is calculated by counting the measured values where the output signal is k times the baseline noise value. The value of k depends on the type of sensor and the usage scenario. Typically, k takes the value of 3 according to the International Union of Pure and Applied Chemistry (IUPAC) standard [12].

4.1.3. Response time. In sensors, response time refers to the time it takes for a sensor to react to changes in external inputs (such as temperature, pressure, light, biochemical, etc.) and stabilise to a new output state. Specifically, response time is often defined as the time required for the sensor's output to reach a certain percentage (e.g. 90%, 95%, or 99%) of its final steady-state value. In different research works, special values are usually set as the end point of response time calculation. A shorter response time represents a faster response speed and better signal processing capability of the system. In evaluating their prepared fibre optic temperature sensor, Liu *et al* [278] defined the response time as the time it took for the output signal to reach 63% of the total change.

4.1.4. Cycle stability. Cyclic stability in sensors refers to the ability of a sensor to maintain consistent performance over multiple repeated operating or working cycles. It measures the reliability and consistency of the sensor's response after being used or tested many times, and whether its output can remain stable throughout repeated cycles. Cyclic stability is primarily used for assessing long-term performance retention, evaluating performance degradation, and statistically analysing differences across various application scenarios. Good cyclic stability ensures the reliability and durability of the sensor in practice [279]. Cyclic stability is tested by subjecting the sensor to specific operating conditions, then the signal to be measured is loaded and unloaded in multiple cycles, and the output signal error is evaluated according to the application requirements. Usually, the error of a cycle stability test is determined by the researcher. The self-powered pressure sensor prepared by Lin *et al* [280] showed only a slight degradation of 6.7% in voltage response after 30 000 cycle tests, which is in accordance with the design as well as usage requirements.

4.1.5. Other evaluation parameters. The above four items are common evaluation indexes for sensors, while some sensors also have special evaluation systems. The resonance characteristics of an electromagnetic wave sensor based on resonance mechanism can be estimated by the quality factor (Q). Q is defined as follow [281]:

$$Q = \frac{f}{FWHM} \tag{7}$$

where f is the resonance, $FWHM$ is the full width half maximum. Superior preparation of patterned structures results in sensors that possess high Q. A high Q-factor indicates that the sensor is very sensitive to changes in frequency and can distinguish between very close frequencies. The responsivity (R) and specific detectivity (D^*) are the key performance parameters for the photodetector. The R is the ratio of the power of the electrical signal output by the photodetector to the power of the incident light [282]. R is defined as follow [283]:

$$R = \frac{I_{\text{photo}} - I_{\text{dark}}}{P_{\text{input}}} \quad (8)$$

where I_{photo} is the photocurrent, I_{dark} is the dark current, P_{input} is the incident light power, and its unit is AW^{-1}. R reflects the efficiency of the photodetector in converting light energy into electrical energy. The D^* is a parameter that measures the performance of a photodetector, taking into account the signal-to-noise ratio (SNR) of the sensor, the sensor area and the operating wavelength. D^* is defined as follow [284]:

$$D^* = \frac{R\sqrt{S}}{\sqrt{2eI_{\text{dark}}}} \quad (9)$$

where S is the effective illuminating area, e is the elementary charge, and its unit is Jones. The high D^* means that the sensor can have good signal detection in low light or high background noise.

4.2. Significance of patterned micro-nanostructure

The core of the sensor to realise the information perception is the sensitive material. Sensitive materials convert changes in physical and chemical signals into changes in electrical or electromagnetic wave signals. For the patterning of sensors, it mainly includes the patterned of sensitive layers of individual devices as well as the patterned of prepared sensor arrays. The advantages of sensor patterning will be described separately next.

4.2.1. Change the sensor structure. The deformation capability of the material is enhanced by building patterned structures, and structural deformation gradients are constructed. This is mainly reflected in flexible force sensors. Due to the low compressibility of homogeneous materials, pressure sensors without patterned structures have low sensitivity and slow response. By building patterned structures on the material surface, the porosity of the pressure sensor can be increased significantly, which in turn improves the compressibility of the structure. Yang *et al* [77] conducted a comparative study of the enhancement effects of sensor patterning structures. They prepared smooth graphene electrodes, graphene electrodes with non-homogeneous structures, and graphene electrodes with patterned structures, respectively. And three capacitive pressure sensors were constructed with these three materials respectively. The capacitive pressure sensor with patterned structure was tested to have the greatest sensitivity of 3.19 kPa^{-1}, which is 319 times higher than that of smooth graphene electrodes and 11 times higher than that of non-homogeneous structured graphene electrodes, respectively. And it had been demonstrated that a high aspect ratio structure had many advantages for the improvement of sensor performance. This suggests that the improvement in material deformation capability brought about by the patterned structure of the flexible sensor is the key to the improvement in sensor performance.

4.2.2. Increase the contact area. By patterning the surface of the sensor, the contact area between the flexible sensor and the target matter can be increased, thereby improving the sensitivity and response speed of the sensor. Liu *et al* [285] constructed an electrochemical sensor based on a 3D graphene structure for phenol detection. After testing, it was found that the three-dimensional 3D graphene structure could significantly increase the enzyme loading compared to the planar graphene structure, while enhancing the contact area of phenol with the material. The sensor achieved a sensitivity of 3.9 nA $\mu\text{M}^{-1}\cdot\text{cm}^{-1}$ and a minimum detection concentration of 50 nM. Therefore, the increase in contact area due to patterned microstructures is important for chemical sensors using contact sensing.

4.2.3. Enhance the interaction of sensing signals with matter. This focuses on electromagnetic wave sensors that use electromagnetic waves as the sensing signal. Electromagnetic wave sensors often require reasonable and precise structural design to enhance the interaction between electromagnetic waves and matter, amplify changes in electromagnetic wave characteristics, and realise ultra-high precision sensing. Electromagnetic wave sensors are usually based on metamaterials [286], photonic crystal structures [22], waveguide structures [287], and surface plasmon resonance structures for sensing [288]. For these structures, fine patterning designs as well as manufacturing processes are essential and enable sensors to sense molecular weights at the fg level [289].

4.2.4. Improve sensor stability. The ability of flexible sensors to measure accurately in complex environments is a key requirement for real-world applications [290]. By constructing patterned electron transport materials or structural materials, it is possible to broaden the applicability range of the sensors, enhance the robustness and mechanical deformation stability of the sensors, and reduce the sensing hysteresis phenomenon due to the increase in resistance [291, 292]. For example, we have constructed a flexible photodetector based on a 3D wrinkled-serpentine interconnect structure for fingertip physiological signal acquisition. The wrinkled-serpentine electrode constructed using a shadow masks technology and a pre-stressed shrinking polymer substrate with outstanding ductility and structural stability to enable fingertip encapsulation, while having a responsivity of 120.7 $\text{mA}\cdot\text{W}^{-1}$ at 635 nm [293].

4.2.5. Construct patterned sensor arrays. Array preparation of flexible sensors using a patterned manufacturing process enables sensors to leapfrog from one-dimensional sensing to multidimensional sensing capabilities. For sensors, sensing arrays can realise signal distribution imaging, realise the perception of regional information, and increase the dimension of information perception [294]. Meanwhile, by integrating different sensing units, multi-target object sensing or multi-modal sensing can be realised [20, 295, 296]. In 2024, Xu *et al* [297] reported a comprehensive artificial-intelligence-reinforced electronic skin. The sensing system combines pressure sensors, electrical response sensors, temperature sensors, and electrochemical biosensors to noninvasively detect three vital signs in the body and six biochemical markers in sweat. Meanwhile, combined with machine learning algorithms, it can classify stressors and enable highly accurate prediction of anxiety states.

5. Application of patterned manufacturing

The sensing structure of the flexible sensor mainly consists of substrate layer, electron transport layer, sensitive layer, and additional layer [298]. The patterning process of sensors includes the patterning of the sensitive elements, the electron transport layer, and the structural material. The patterned structure of the sensitive elements can be directly or indirectly affected by the sensing source, including the structural changes caused by the sensing source as well as the interaction between the sensing source and the particular sensitive structure. Patterning the electron transport layer and the structural material can improve device stability and assist in enhancing the sensing performance of the device. In addition to the patterned construction of individual sensing elements, the construction of flexible sensing arrays by a patterning process is also a common method. Patterned flexible sensor arrays can enhance the integration and resolution of information sensing, which are an important means of information sensing from one-dimensional to two-dimensional and three-dimensional space [299]. Based on the type of change signal output from the sensor, the flexible sensors can be classified into those based on electrical response signals and those based on electromagnetic wave response signals.

Electrically responsive sensors sense signals based on changes in electrical characteristics, whose direct readout signals are current or voltage values [300]. In power supply systems, changes in electrical parameters include resistance, capacitance, and chemical reaction in the electrolytic cell. In systems without an external power source, currents or voltages are usually generated directly by physical or chemical processes, including piezoelectricity, triboelectric, thermoelectricity, and electrochemical reactions in the device [301]. Flexible sensors with electrical characteristics as response signals are common types of sensors and have the advantage of low cost and simplicity of principle.

Electromagnetic wave responsive sensor are sensors that sense changes in electromagnetic characteristics. Based on wavelength, electromagnetic wave can be classified as millimetre wave, microwave, infrared light, visible light, ultraviolet light, x-rays and so on. Electromagnetic wave interacts with matter or structures, changing their amplitude, phase, wavelength or polarisation characteristics through processes such as reflection, scattering, transmission or absorption. Electromagnetic wave responsive sensors are frequently utilised as wireless transmissions and are well-suited for long-distance signal detection in complex and harsh environments. In 2024, Ma *et al* [302] presented the inaugural millimetre-wave wireless sensor capable of continuous operation at exceedingly high temperatures. The sensor exhibits sensitivity to aluminium oxide-based 3D photonic crystals and is capable of functioning in environments exceeding 1000 °C. The matter to be measured is usually regarded as a dielectric matter, and different types and different concentrations of the matter change the dielectric properties of the surroundings [303, 304]. Similarly, changes in the physical parameters of the surrounding environment can alter the surface properties of a substance or structure, such as temperature, light, and humidity. During the interaction of electromagnetic waves with matter or structures, the surrounding environment can be sensed by monitoring the characteristic parameters of electromagnetic waves. Electromagnetic wave sensors can be categorised into radio frequency sensors, microwave sensors, millimetre wave sensors, terahertz sensors and optical sensors and so on. Rationally designed patterned structures of electromagnetic wave sensors can enhance wave-matter interaction and achieve high sensitivity sensing.

Thanks to the continuous progress in the manufacturing process of patterned micro-nanostructures, electromagnetic wave sensors based on a variety of high-precision structures have appeared, constantly refreshing the sensitivity limit of flexible sensors. Metamaterials are man-made electromagnetic materials with characteristic dimensions in the sub-wavelength range, whose properties are related not only to the nature of the material, but also to the structure of the metamaterial [305]. The geometric resonant cavity structure of the metamaterial exhibits local field enhancement under electromagnetic wave irradiation, which greatly improves the detection performance of the sensor [306]. To achieve CMOS compatibility, reduce metal loss, and improve Q, as well as to solve the problem of high absorption loss of terahertz waves in water, the waveguide resonant cavity system becomes the key [287, 307, 308]. Waveguide-coupled resonator terahertz sensors reduce the loss in the propagation path, while using the evanescent field on the waveguide surface for solution sensing, which can overcome the absorption loss of terahertz waves by water [309, 310]. Photonic crystals are a class of man-made crystals with a periodic dielectric structure on the optical scale [311], which can control the interaction of light with matter at the nanoscale. The period of the photonic crystal is similar to the wavelength. When the matter to be measured is in the environment of the photonic crystal, it causes a change in the refractive index around the photonic crystal, or changes in the resonant frequency of the resonant cavity of the photonic crystal, thus enabling sensing [312]. Electromagnetic wave sensors based on surface plasmon resonance are also highly sensitive techniques for analysing matter [313]. Among them, optical

excitation methods for surface plasmon excitations are classified into prism coupling and grating coupling techniques. Surface plasmon resonance sensors measure changes in the refractive index of a dielectric near the interface using an evanescent field excited by electromagnetic waves at the interface between the metal and the medium [314]. Therefore, it has an ultra-high sensitivity to changes in the material at the interface [315].

Next, we will describe the practical application of the patterned micro-nanostructure manufacturing process based on the flexible sensor type and process type. We also summarise all the applications in table 3 to facilitate comparative analysis. Notably, the patterning structure of a flexible sensor often exists in multiple parts, and the following presentation focuses primarily on the patterning part that directly enhances the performance of the sensor. At the same time, since the preparation of patterned sensor materials often includes a multi-step process, the presentation focuses mainly on the key processes for forming patterned structures.

5.1. Strain sensor

Flexible strain sensor can measure the deformation of an object due to a force, usually through the deformation of their own structure to convert the force signals into response signals. They are mainly categorised as resistive strain sensors, capacitive strain sensors, piezoelectric strain sensors, triboelectric strain sensors and electromagnetic wave strain sensors [353]. According to the law of resistance, the resistance of a material is related to the shape and resistivity. Changes in material conductive pathways and material resistivity caused by deformation of material geometry and material microstructure are both sensing mechanisms for resistive strain sensors [354]. Capacitive strain sensors are based on the parallel-plate capacitor principle and are associated with changes in capacitance under strain [355, 356]. Piezoelectric strain sensors are based on the principle that a piezoelectric material generates an electrical charge under mechanical stress, and are mainly used for dynamic strain measurement [357]. Triboelectric strain sensors exploit the triboelectric effect that arises from the contact between two distinct materials [358, 359]. Upon contact and subsequent separation, a transfer of charge occurs on the surface of the materials, resulting in a potential difference [360]. This potential difference can be utilised to detect mechanical strain [361], as well as to harvest the energy of mechanical motion to build self-powered sensor systems [362]. Electromagnetic wave sensors change the properties of the electromagnetic waves they propagate, such as intensity, phase, state of polarisation, and frequency, in response to changes in external environmental parameters. Patterned micro-nanostructures are usually three-dimensional to amplify the structural deformation effects caused by large forces. By increasing the contact area, concentrating the stress region and dividing the deformation space, the LOD and sensitivity of the strain sensor is improved [363]. Currently, combined with deep learning algorithms, the flexible strain sensor system can recognise complex and rapid changes in the human body, and is expected to be used for practical applications in areas such as gesture recognition and sign language translation [364]. In the following sections, we will discuss separately the application of patterned micro-nanostructure manufacturing methods in the preparation of flexible strain sensors.

5.1.1. Printing.

Printing techniques are commonly used to construct triboelectric strain sensors. Jing *et al* [321] constructed triboelectric-based strain sensors by printing silver nanoparticles and polyimide inks on polyimide substrates using AJP. Thanks to the fine comb structure, the sensor had a sensitivity of 630 μV μm^{-1}. We printed silver AgNWs/thermoplastic polyurethane (TPU) composites on a substrate using an electrostatic spinning process in a previous study to form a composite film with a three-dimensional structure. Flexible capacitive pressure sensors were prepared by using the 3D AgNWs@TPU composite film as a dielectric layer. Thanks to the construction of an excellent 3D structure, our sensor exhibits a sensitivity of 1.21 kPa^{-1}, a LOD of 0.9 Pa, a response time of 100 ms and a stability of more than 10 000 cycles [322]. The printing process is mainly used for the fabrication of two-dimensional structures. Therefore, it is commonly used for the manufacturing of triboelectrical sensors as well as sensor arrays.

5.1.2. Photolithography.

Photolithography technology is one of the important ways to prepare high resolution, high uniformity patterned micro-nanostructures. It is usually used to fabricate patterned electrodes in flexible sensors as well as fine microstructures. Cai *et al* [316] used a photolithography process to prepare SU-8 photoresist-based micro-projections as well as patterned metal films on the surface of flexible PDMS. The spatially distributed micro-projections on the metal films amplify the force-induced out-of-plane compression into bending deformation, giving the devices pressure-sensitive properties. The piezoresistive sensor has a linear response range of $<$80 kPa, a sensitivity of 2.02×10^{-4} kPa^{-1}, a response time of 100 ms, a recovery time of 200 ms, and no significant performance degradation after 10 000 cycle stability tests.

Strain sensors based on electromagnetic waves as the sensing medium have complex resonance structures, so lithography process is commonly used for the preparation of such sensors. The need for remote wireless strain measurement in industrial production, aerospace and human health has driven the development of wireless strain sensors using electromagnetic waves as the sensing medium. The change in resonant frequency due to structural deformation is the basis for sensing by electromagnetic wave strain sensors. Finely patterned structures can amplify the deformation, leading to higher sensitivity. Since resonant structures have complex shapes, photolithographic processes are the most common patterning preparation method. Melik *et al* [317] prepared wireless strain sensors based on flexible metamaterials (figure 7(a)). The strain sensing units are a split ring resonators (SRRs) prepared

Table 3. Application of patterned process.

Sensor type	Patterned process	Structures	Sensitivity[a]	LOD	Response time	Cyclic stability	References
Piezoresistive strain sensor	Photolithography	Micro-projections	2.02×10^{-4} kPa^{-1}	10 kPa	100 ms	10 000	[316]
Metamaterial sensor	Photolithography	Split ring resonators	0.292 MHz·kgf^{-1}				[317]
Piezoresistive pressure sensor	Fill-moulding	Pyramid	S: 10.3 kPa^{-1}	23 Pa	0.2 s	400	[318]
Capacitive pressure sensor	Fill-moulding	Micro-convex	S: 131.5 kPa^{-1}	1.12 Pa	43 ms	7000	[319]
Capacitive pressure sensor	Sacrificial moulding method	Microporous	S: 0.63 kPa^{-1}	2.42 Pa	40 ms	10 000	[212]
Capacitive pressure sensor	REM	Micro-convex	S: 1.194 kPa^{-1}	0.8 Pa	36 ms	100 000	[320]
Triboelectric-based strain sensors	AJP	Strip structure	S: 630 μV μm^{-1}	/	/	/	[321]
Capacitive pressure sensors	E-Jet	3D nanowire	S: 1.21 kPa^{-1}	0.9 Pa	100 ms	10 000	[322]
Capacitive pressure sensor	REM, sacrificial moulding method	Microsphere protrusion	S: 30.2 kPa^{-1}	0.7 Pa	28 ms	100 000	[323]
Capacitive pressure sensor	NIL, sacrificial moulding method	Porous pyramid	S: 44.5 kPa^{-1}	0.14 Pa	50 ms	5000	[324]
Piezoresistive pressure sensor	NIL, sacrificial moulding method	Porous pyramid	S: 449 kPa^{-1}	0.14 Pa	9 ms	/	[324]
Triboelectric pressure sensor array	LDW	Array	S: 0.016 V·kPa^{-1}	/	/	6000	[325]
Flexible tactile sensor	LDW	Micropyramids	2.78 kPa^{-1}	3 Pa	80 ms	10 000	[326]
Capacitive strain sensor array	μCP	Array	S: 0.42 MPa^{-1}	50 kPa	/	/	[327]
Multiplexed Biosensors	Inkjet printing	Array	Triglyceride: 7.49 μA·mM^{-1}·cm^{-2} Glucose: 5.03 μA·mM^{-1}·cm^{-2} Lactate: 3.94 μA·mM^{-1}·cm^{-2}	Triglyceride: 0.07 mM Glucose: 0.2 mM Lactate: 0.06 mM			[328]
Lead electrochemical sensor	Dip-pen nanolithography	Nanoclusters	/	0.49 ppb	/	/	[329]

(Continued.)

Table 3. (Continued.)

Metamaterial biosensor	EBL	Split ring resonators	BSA: 4.5 nm nM^{-1}				[330]
Metamaterial biosensor	UV photolithography	Spiral-shaped strips	0.37 THz: 0.09 THz·RIU^{-1} 1.13 THz: 0.28 THz·RIU^{-1}				[331]
Metamaterial biosensor	Photolithography	Cut wire resonator and two split semicircle resonators		10.6 fg ml^{-1}			[332]
Metasurface biosensor	Photolithography	Cut wire resonator and split-over ring resonators		42.3 pg ml^{-1}			[333]
Metamaterial biosensor	Shadow mask method	Split ring resonators	14.3 GHz $mmol^{-1}$	0.35 mmol·l^{-1}			[334]
Solution-gated FET biosensor	MIMIC	Strip structure	0.02 mM^{-1}				[335]
Electrochemical biosensor	REM	Micro-bumps		100 fM		1000	[336]
LSPR biosensor	NIL	Nanopillar		1.0 ng·ml^{-1}			[337]
Terahertz Metamaterial Sensor	LDW	U-shaped split-ring resonators	Low-frequency Fano resonance: 60 GHz·RIU^{-1} High-frequency EIT: 100 GHz·RIU^{-1}				[338]
SO_2 sensor	Laser direct writing	Square box	S: 0.63 μA·ppm^{-1}	10 ppb	6 s		[339]
Gas sensor array	Inkjet printing	Array	/	<ppb	/	/	[340]
NO_2 sensor	Gravure printing	Microscale stripe	6.5	30 ppb	45.1 s		[341]
NO_2 sensor	μTM	Nanoflowers	218.1		25 s	10 000	[342]
Nanowire electronic nose system	MIMIC	Nanowire		1 ppm	p-xylene: 10 s acetone: 12 s ethanol: 8 s n-hexane: 10 s		[343]
Photodetector	E-jet	Array	Responsivity: 14.97 AW^{-1} D^a: 1.41 × 10^{12} Jones				[344]
GaAs photodetector	Printing	Array	Responsivity: 10^4 AW^{-1} D^a: 10^{14} Jones		2.5 ms	500	[345]

(Continued.)

Table 3. (Continued.)

Sensor type	Patterned process	Structures	Sensitivity[a]	LOD	Response time	Cyclic stability	References
Perovskite-based photodetectors	Mould method	Array	Responsivity: 2.17 AW^{-1} D^{a}: 9.4×10^{11} Jones		0.48 s	>100	[346]
Solar-blind photodetector	Mould method	Array	Responsivity: 62 AW^{-1}	6.1 $nW \cdot cm^{-2}$			[347]
Photodetector array	MIMIC	Array	D^{a}: 2.78×10^{13} Jones Responsivity: 1207 AW^{-1}	/	3.9 ms	/	[284]
Resistive temperature sensor	E-Jet	Bending electrodes	Temperature coefficient: 0.000 768 7 $°C^{-1}$	/	/	/	[348]
Thermocouple temperature sensor	Lithography	Bending electrodes	S: 76.5 $\mu V\ °C^{-1}$	/	/	1000	[349]
Temperature sensor array	Shadow masks technique	Array	Temperature response coefficient: 20.4	/	/	/	[221]
Humidity sensor	E-jet and mould method	Rhombic structure	83%		38 s	1000	[350]
Humidity sensor	MIMIC	Nanowires			0.63 s	1000	[351]
Magnetic sensor	Mould method	Pyramid	1507.9% mT^{-1}		1 ms	5000	[352]

[a] Due to the different evaluation systems of different sensors, the sensitivity column will also include quality factor (Q), Detectivity, Responsivity, Temperature response coefficient, etc. The sensitivity will be expressed by S.

using a photolithography process. The sensitivity of this sensing is 0.292 MHz·kgf^{-1}, which is a six-fold increase in sensitivity and a 16-fold decrease in percent error compared to conventional strain sensors.

5.1.3. Soft lithography. Soft lithography is also commonly used in the preparation of patterned enhanced strain sensors because of its inherent advantages in the de-modelling of 3D structures. Wan *et al* [320] demonstrated a capacitive pressure sensor prepared by REM technology using a lotus leaf as a master mould (figure 7(b)). Rigid PDMS was first used to replicate the surface structure of the lotus leaf, and then standard PDMS was used to replicate the rigid PDMS surface structure. PDMS with a microtower structure was used as the bottom electrode substrate layer. Pressure could affect the distance between the upper and lower electrodes by compressing the PDMS, which in turn caused a change in the capacitance value. The capacitive pressure sensor had a sensitivity of 1.194 kPa^{-1}, a LOD of less than 0.8 Pa, a response time of 36 ms, and a stable pressure cycle of more than 100 000 cycles. At the same time, soft lithography also has the ability of planar pattern manufacturing, which can meet the needs of the manufacturing of sensor arrays on flexible and rigid material surfaces. Woo *et al* [327] prepared capacitive strain sensor arrays using a process of μCP (figure 7(c)). The patterned structure was a conductive PDMS (CPDMS) material. The PDMS mould with the patterned structure was gently contacted with CPDMS ink to form the patterned electrode layers. The strain sensor could achieve a minimum detection limit of 50 kPa, a strain factor of ~0.55 and a sensitivity of 0.42 MPa^{-1}. Compared to the mould method technology, which prepares the complementary structure of the mould, soft lithography can completely replicate the mould structure through a two-step process, while also preparing flat patterns.

5.1.4. Mould method. The mould method technique is a common process for the preparation of patterned structures for strain sensors. The cost is low, the manufacturing process is simple and the environmental impact is low. Choong *et al* [318] fabricated a piezoresistive pressure sensor based on PDMS with a pyramidal structure on the surface (figure 7(d)). The pyramid-structured PDMS was prepared using a silicon mould, and then the PDMS surface was conformally coated with a layer of elastically conductive polymer consisting of a mixture of PEDOT: PSS and PUD. The pressure sensor could achieve a maximum sensitivity of 10.3 kPa^{-1}, a LOD of 23 Pa, a response time of 0.2 s and a cycle stability of 400 cycles. Chhetry *et al* [319] demonstrated a capacitive pressure sensor based on iontronic film with microstructures (figure 7(e)). Composite material based on the composition of P(VdF-HFP) polymer matrix and 1-ethyl-3-methylimidazolium bis(trifluoromethylsulfonyl)imide polymer electrolyte was spin-coated onto the surface of silicon carbide abrasive sandpaper which as the mould. The obtained microstructured iontronic thin film was used as dielectric materials for pressure sensors. The sensor had a pressure sensitivity of 131.5 kPa^{-1} in the low-pressure range of <1.5 kPa, a response time of ~43 ms, a LOD of 1.12 Pa and a cycle stability of 7000 cycles. Preparation of sensitive layer materials with internally patterned microstructures by the sacrificial mould method can also enhance the compressibility of the sensor and achieve pressure amplification effects. Kang *et al* [212] used uniformly stacked polystyrene beads as a sacrificial mould. After filling with PDMS and heated curing, the PDMS was placed in an organic solvent to dissolve the polystyrene beads (figure 7(f)). The capacitive pressure sensor based on a patterned porous PDMS had a sensitivity of 0.63 kPa^{-1}, a LOD of ~2.42 Pa, a response time of ~40 ms, and achieved cycle stability of 10 000 cycles.

Patterned micro-nanostructures prepared by the mould method for strain sensors are usually three-dimensional and have excellent mechanical properties with large height-to-width ratios. These structures include pyramidal, cylindrical, hemispherical and porous structures, which have a large strain response to slight forces and can withstand large deformations.

5.1.5. LDW. LDW technology is also categorised into additive and subtractive manufacturing. The surface of the material is usually modified to prepare patterned electrode materials during the preparation of the sensor array. Yan *et al* [325] prepared flexible triboelectric pressure sensor arrays based on patterned graphene. The patterned graphene arrays were obtained by direct CO_2 laser irradiation of a polyimide (PI) film. The resistance of the graphene films obtained by laser modification of the PI surface was as low as 7.0 Ω sq^{-1}. The sensor array has a sensitivity of 0.016 V kPa^{-1} and maintains cyclic stability of 6000 cycles and bending stability of over 5000 cycles. Zhang *et al* [326] constructed a highly sensitive flexible tactile sensor (figure 7(g)). The electrodes of the sensor were gallium-based liquid metals and the dielectric layer was a double-sided PDMS micropyramids array of super-sparse metals fabricated using a femtosecond laser. The micropyramids structure fabricated using a femtosecond laser has an abundance of nanoparticles on the surface, and thus has an ultra-hydrophobic metal capability, which improves the durability of the liquid metal electrodes and enhances the pressure sensitivity. The sensor has a sensitivity of 2.78 kPa^{-1}, a LOD of 3 Pa, a response time of 80 ms as well as demonstrated performance output stability after 10 000 cycles of testing.

5.1.6. Multiple processes. The preparation of patterned microstructures often involves multiple processes as well. Xiong *et al* [323] designed a low-cost capacitive pressure sensor by combining the sacrificial moulding method and the REM technique. Liquid PDMS was spin-coated onto a glass substrate with uniform polystyrene beads on the surface. The PDMS was heated curing and then immersed in a toluene solution to obtain a PDMS film with concave arrays by removing the polystyrene beads. Then, another liquid PDMS was spin-coated on the cured PDMS with concave arrays to obtain a PDMS film with convex arrays after heated curing. The capacitive pressure sensor consisting of two PDMS with convex arrays had a sensitivity of 30.2 kPa^{-1} over a range of <130 kPa, a minimum detection limit of 0.7 Pa, a response

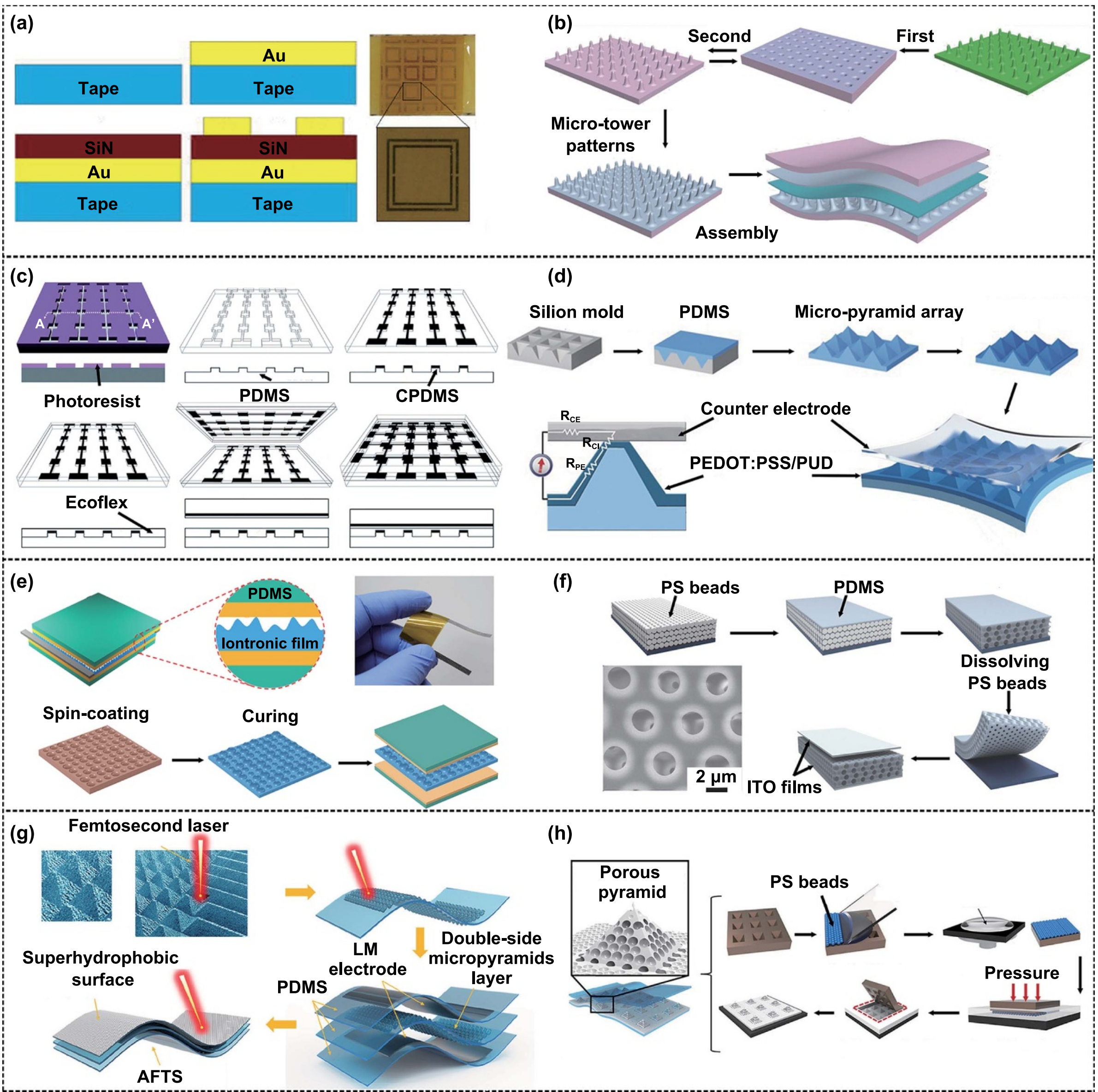

Figure 7. Strain sensor. (a) Wireless strain sensors based on flexible metamaterials prepared by photolithography. Reprinted from [317], with the permission of AIP Publishing. (b) Capacitive pressure sensor prepared by REM technology. [320] John Wiley & Sons. © 2018 WILEY-VCH Verlag GmbH & Co. KGaA, Weinheim. (c) Capacitive strain sensor arrays using a process of μCP. Reproduced from [327] with permission from the Royal Society of Chemistry. (d) Piezoresistive pressure sensor with pyramidal structures. [318] John Wiley & Sons. © 2014 WILEY-VCH Verlag GmbH & Co. KGaA, Weinheim. (e) Capacitive pressure sensor based on moulding method. Reprinted with permission from [319]. Copyright (2019) American Chemical Society. (f) Capacitive pressure sensor based on sacrificial moulding method. The polystyrene beads as the sacrificial mould. [212] John Wiley & Sons. © 2016 WILEY-VCH Verlag GmbH & Co. KGaA, Weinheim. (g) Flexible tactile sensor prepared by LDW. Reprinted with permission from [326]. Copyright (2022) American Chemical Society. (h) Capacitive pressure sensor prepared with NIL and sacrificial moulding method. Reprinted with permission from [324]. Copyright (2019) American Chemical Society.

time of 28 ms, and was stable over 100 000 cycles. Yang *et al* [324] prepared a capacitive pressure sensor with a porous pyramidal PDMS as the dielectric layer using NIL and sacrificial moulding method (figure 7(h)). Silicon mould with pyramidal micropatterns filled with polystyrene microbeads was placed on the surface of liquid PDMS. After applying pressure and heat, the cured PDMS was inlaid with polystyrene microbeads. It was then immersed in a toluene solution to remove the polystyrene microbeads to obtain a porous pyramid-structured PDMS material. The capacitive pressure sensor has a sensitivity of 44.5 kPa^{-1} at <100 Pa, a LOD of 0.14 Pa, a response time of 50 ms, and remained stable for 5000 cycles. Meanwhile, the researchers designed a piezoresistive pressure sensor based on a porous pyramid-structured PDMS, achieving a sensitivity of 449 kPa^{-1}, a response time of 9 ms and a LOD of 0.14 Pa.

5.2. Biochemical sensors

In this review, biochemical sensors represent sensors for the specific detection and concentration sensing of biomolecules and chemical molecules in liquid environments. Biochemical sensors are important in areas such as human health and water quality monitoring [365]. Meanwhile, the neuromorphic system constructed on the basis of biochemical sensors has a number of advantages in simulating biological neural networks, which can be used to optimise the way and speed of current information processing [366]. The main components of biochemical sensors are biochemical recognition elements and signal transduction elements [367]. Currently, the main categories are electrochemical biochemical sensing technology and electromagnetic wave biochemical detection technology. In electrochemical biochemical sensors, the signal is usually related to the transfer of electrons or ions in a biochemical reaction, including voltage, current, capacitance, impedance and optical signals [368, 369]. Electrochemical biosensor technologies involve amperometry, voltammetry, potentiometry, organic electrochemical transistor technology [370], photoelectrochemical and electrochemiluminescent [371]. In electromagnetic wave biochemical sensors, biochemical substances can be used as dielectric substances. Changes in the dielectric constant can be converted into changes in optical properties by techniques such as metamaterials, surface plasmon resonance, and surface-enhanced Raman scattering to enable sensing [372]. The development of biochemical sensors with high specificity, high sensitivity and fast response is the goal of researchers. Next, we will introduce biochemical sensors based on the patterned preparation process.

5.2.1. Printing. The printing process is a commonly used technique for the manufacturing of patterned electrodes. Electrically responsive sensors generally utilise electrochemical principles of operation. Chemical reactions of biochemical molecules in the vicinity of the electrode cause changes in the electronic state of the electrode surface. Thus, the patterned structures of electrochemical sensors exist mainly in the electrode materials. Li *et al* [328] prepared multiplexed biosensor arrays using a multi-nozzle inkjet printing system. The sensor preparation process takes only ~5 min and can simultaneously detect glucose, lactate and triglycerides. The sensitivity of glucose was 5.03 μA mM^{-1} cm^{-2} with a LOD of 0.2 mM, lactate was 3.94 μA mM^{-1} cm^{-2} with a LOD of 0.06 mM, and triglyceride was 7.49 μA mM^{-1} cm^{-2} with a LOD of 0.07 mM. Scanning probe lithography, as the highest resolution technique in the printing process, is gradually applied to prepare electrode materials with micro- and nanostructures. Yadav *et al* [329] used DPN to prepare electrochemical sensors for leading monitoring in water (figure 8(a)). The nanoclusters on the electrode surface have high specific surface area and can show high detection sensitivity. The sensor exhibited a detection limit LOD of 0.49 ppb for leading in water.

5.2.2. Exposure lithography. The high resolution of exposure lithography processes has driven the development of biochemical sensors using electromagnetic waves as a sensing medium. Xu *et al* [330] prepared flexible sensors based on 30 nm thick metal SRRs on poly (ethylene naphthalate) substrates using an EBL process. The SRRs of the metamaterial structure exhibited a sensitivity response of up to 436 nm RIU^{-1} to strains in the visible-infrared region, localised dielectric environments, and surface chemical variations. In addition, the sensor exhibits a sensitivity of ~4.5 nm nM^{-1} for non-specific BSA protein binding. Wang *et al* [331] prepared a dual-band flexible terahertz metamaterial sensor based on a PI film using UV photolithography (figure 8(b)). The sensitivities to pesticides were 0.09 THz·RIU^{-1} and 0.28 THz·RIU^{-1} at 0.37 THz and 1.13 THz, respectively. Liang *et al* [332] prepared metallic metamaterial flexible biosensors with a cut wire (CW) resonator and two split semicircle resonators (SCRs) on a PI film by a standard photolithography process. At 1.15 THz, the electric field strengths in the CW and SCR resonators were suppressed due to the phenomenon of interference phase cancellation, and the transparent windows formed were unusually sensitive to external substances. Its LOD for detecting aspartic acid was 10.6 fg·ml^{-1}. Yao *et al* [333] prepared a flexible biosensor based on a metasurface using photolithography (figure 8(c)). The patterned structure is a cut wire resonator (CW) and two split-over ring resonators (SORR) periodically arranged structures. The LOD of this sensor for the detection of plant protein molecules was 42.3 pg ml^{-1}.

5.2.3. Mould method. In the mould method, shadow masks are prepared by a high-resolution photolithography process with high resolution, so they are also commonly used for the manufacturing of electromagnetic wave-based biosensors. Tao *et al* [334] prepared micrometre-sized patterned metamaterial resonators on paper substrates using the shadow masking method, which can achieve high sensitivity for glucose detection (figure 8(d)). The sensitivity of the system was 14.3 GHz mmol^{-1} and the LOD was 0.35 mmol l^{-1}.

5.2.4. Soft lithography. Soft lithography uses flexible PDMS materials as moulds and is particularly suitable for the manufacturing of patterned structures on flexible material surfaces. At the same time, soft lithography is compatible with the manufacturing of two-dimensional and three-dimensional structures, which can enhance the contact area between biochemical molecules and materials in biochemical sensors and improve the sensitivity of the sensors. He *et al* [335] have prepared solution-gated FET based on graphene materials using MIMIC, which can enable the sensing of biomolecules in solution. Patterned graphene structures directly on a polymer substrate can be conformally attached to the human skin surface. Its maximum sensitivity to dopamine was 0.02 mM^{-1}. Kim *et al* [336] prepared PDMS substrates with three-dimensional micro-bumps using REM technique

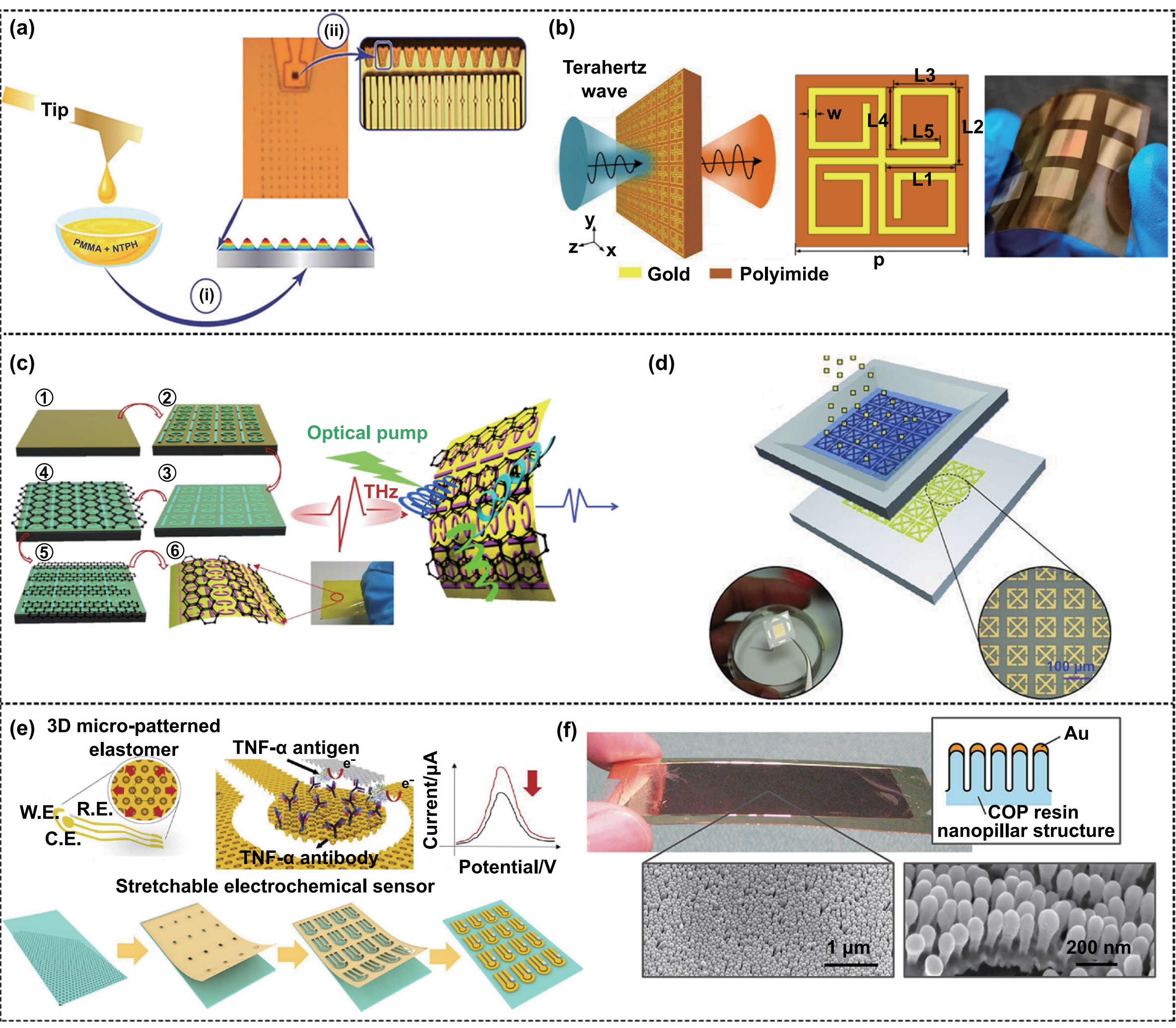

Figure 8. Biochemical sensors. (a) An electrochemical sensor for lead detection prepared using dip-pen nanolithography technique. Reproduced with permission from [329]. © 2023 The Authors. Small Methods published by Wiley-VCH GmbH. CC BY-NC-ND 4.0. (b) Dual-band flexible terahertz metamaterial sensor using UV photolithography. Reprinted (adapted) with permission from [331]. Copyright (2024) American Chemical Society. (c) Flexible biosensor based on a metasurface using photolithography. Reprinted from [333], © 2022 The Author(s). Published by Elsevier B.V. (d) Glucose metamaterial sensor prepared by shadow masking method. [334] John Wiley & Sons. Copyright © 2011 WILEY-VCH Verlag GmbH & Co. KGaA, Weinheim. (e) Stretchable electrochemical biosensor prepared by REM technology. Reprinted from [336], © 2018 Elsevier B.V. All rights reserved. (f) Biosensor based on LSPR prepared by NIL. Reprinted with permission from [337]. Copyright (2012) American Chemical Society.

(figure 8(e)). Subsequent deposition of metal electrodes onto the patterned substrate material resulted in a high-performance and stretchable electrochemical biosensor. The sensor showed ultra-high biochemical molecular sensing resolution and could detect TNF proteins below 100 fM. The linear correlation coefficient was 0.9792 when the results were compared with those of a commercial assay instrument.

5.2.5. NIL. NIL, as a strong alternative to photolithography, is suitable for the construction of micro-nanostructures with high depth-to-width ratios and high resolution for the manufacturing of highly sensitive biochemical sensors based on surface plasmon resonance. Saito *et al* [337] designed a biosensor based on localised surface plasmon resonance (LSPR) (figure 8(f)). Their substructure is a polymer nanopillar prepared by the NIL process. The LSPR enhances the real-time change of refractive index at the interface of the surrounding circuit medium and is therefore sensitive to the attachment of biomolecules. In the detection of antigenic IgG concentration, the sensor has a linear detection range of 100 μg ml^{-1} and a LOD of 1.0 ng ml^{-1}. Zhu *et al* [373] investigated flexible plasma metasurfaces for the highly sensitive detection of tumour markers in human serum samples. They prepared periodic arrays of nanocylinders on a polycarbonate substrate using T-NIL followed by thermal evaporation of metal as the metasurface. The metasurface was used to excite plasma resonance by coupling incident light, which provided strong detection of carcinoembryonic antigen (CEA). The linear correlation coefficient between its spectral inclination and CEA concentration was 0.995.

5.2.6. LDW. The simple process and high resolution of LDW technology, especially the processing of polyimide substrates by femtosecond laser etching technology, allows the construction of electromagnetic wave-based biochemical sensors with high-accuracy micro-nanostructures [374]. Yao *et al* [338] prepared a terahertz metamaterial sensor with a flexible substrate using a femtosecond laser etching technique, which demonstrated a low-frequency Fano resonance and a high-frequency electromagnetically induced transparent resonance. The refractive index sensing sensitivities based on these two resonances were 60 $GHz \cdot RIU^{-1}$ and 100 $GHz \cdot RIU^{-1}$, respectively. At the same time, the ability to utilise laser modification allows the preparation of carbon electrodes directly on polymer substrates, enabling more convenient manufacturing of sensor arrays. Yu *et al* [375] prepared flexible sensor arrays on PI substrates using a LDW process that induces porous graphene materials as electrode materials. Functionalizing different sensing units, this sensor array can detect salty, sweet as well as sour and the output signal changes with concentration.

5.3. Gas sensors

The gas sensor is a sensor that detects the presence or absence of a specified gas molecule, or detects the concentration of a gas within a certain range. Flexible gas sensors mainly include semiconductor gas sensor, electrochemical gas sensor, colorimetric gas sensor and electromagnetic wave gas sensor. Semiconductor gas sensors work on the principle that gas molecules adsorb or react on the surface of the material, causing changes in carrier motion characteristics, which in turn produce changes in conductivity or volt-ampere characteristics. Electrochemical gas sensors detect the gas concentration by sensing the current generated by the redox reaction of the gas at the electrode. In colorimetric gas sensors, the gas undergoes a redox reaction with the detection substance, changing the colour of the compound [376]. The concentration of the gas is determined by the colour change, allowing for zero-power gas detection [377]. In electromagnetic wave sensors, gas molecules act as dielectric substances inside a specially designed material structure, which causes a change in the electromagnetic wave parameters and realises the detection of gas molecules [378]. At the same time, to expand the types of detectable gases, gas sensor arrays can be constructed to realise multi-gas detection. Recently, Wang *et al* [379] fabricated a 100×100 nanotube sensor array that accurately identifies the composition and concentration of a gas mixture and recognises 24 typical odours. The fabrication of this type of sensor improves the problems of miniaturisation and poor recognition ability of electronic nose system, and is expected to be used in intelligent robotic patrols as well as rescue operations. Next, we will describe the application of the patterning process for performance enhancement of gas sensors.

5.3.1. Printing. The printing process is more often used in gas sensors for the preparation of electrode materials to build gas sensor arrays for the detection of multiple gases. The development of gas sensor arrays can compensate for the low cross-sensitivity of individual sensors and enable the detection of mixed gases. Li *et al* [340] prepared a gas sensor array based on silver nanoparticles containing various capping agents using inkjet printing (figure 9(a)). Eleven common contaminants can be detected by observing the colour change of the array. The gas sensor array enables ultrasensitive detection of gas molecules at sub-ppb levels and continuous detection for up to several days. At the same time, changing the structure of the plate pattern during coating printing allows the introduction of printing ink with microstructures on the substrate. This high aspect ratio structure increases the contact area of the gas molecules with the material. Lin *et al* [341] prepared gas sensors with microscale stripe structures for WO_3-PEDOT: PSS using a gravure printing process (figure 9(b)). Thanks to the larger specific surface area of the microscale stripe structure, the sensor surface can be exposed to gas molecules more effectively. The gas sensor has a maximum response of 6.5 (the ratio of the resistance exposed to NO_2 to that exposed to the atmosphere), a LOD of 30 ppb, and response and recovery times of 45.1 s and 88.7 s, respectively.

5.3.2. Soft lithography. As previously described, soft lithography is a fast patterned micro-nanostructure manufacturing technique suitable for enhancing the active layer sensing area of flexible sensors. The application of soft lithography to gas sensors focuses on the fabrication of structures with specific shapes and sizes. Kim *et al* [342] prepared a gas sensor with micropatterned double-faced ZnO nanostructures using μTM technique (figure 9(c)). The sensor has high selectivity and high sensing characteristics for NO_2, with a responsivity of 218.1 and a response time of 25 s. After 10 000 cyclic bending tests, the sensor still works properly. Also, the application of soft lithography facilitates the device integration of gas sensors, which helps to realise mass production and reduce costs. Tang *et al* [343] prepared a nanowire electronic nose system based on PEDOT: PSS/GO complexes for the detection of low concentrations of VOCs using MIMIC technology. For this sensor array, thanks to the high surface area ratio of the nanowires, the response times were 10 s for p-xylene, 12 s for acetone, 8 s for ethanol, and 10 s for n-hexane, respectively, and the LOD was 1 ppm.

5.3.3. NIL. NIL shows great potential for application in the field of gas sensors due to its advantages of high resolution, high fidelity and high production efficiency. Using NIL technology, it is possible to fabricate micro-nanostructures with high surface area, which can provide more gas channels. Meanwhile, large-area NIL technology can rapidly fabricate large-area micro- nanostructures, which can help realise mass production and cost reduction of gas sensor arrays. Kim *et al* [380] prepared flexible gas sensors that can sense four gases by combining a patterned graphene layer with a polyimide film using a photolithography technique and NIL (figure 9(d)). The responsiveness of this sensor was 6%, 8%, 6%, and 1.5% for NO_2, NH_3, H_2, and C_2H_5OH, respectively.

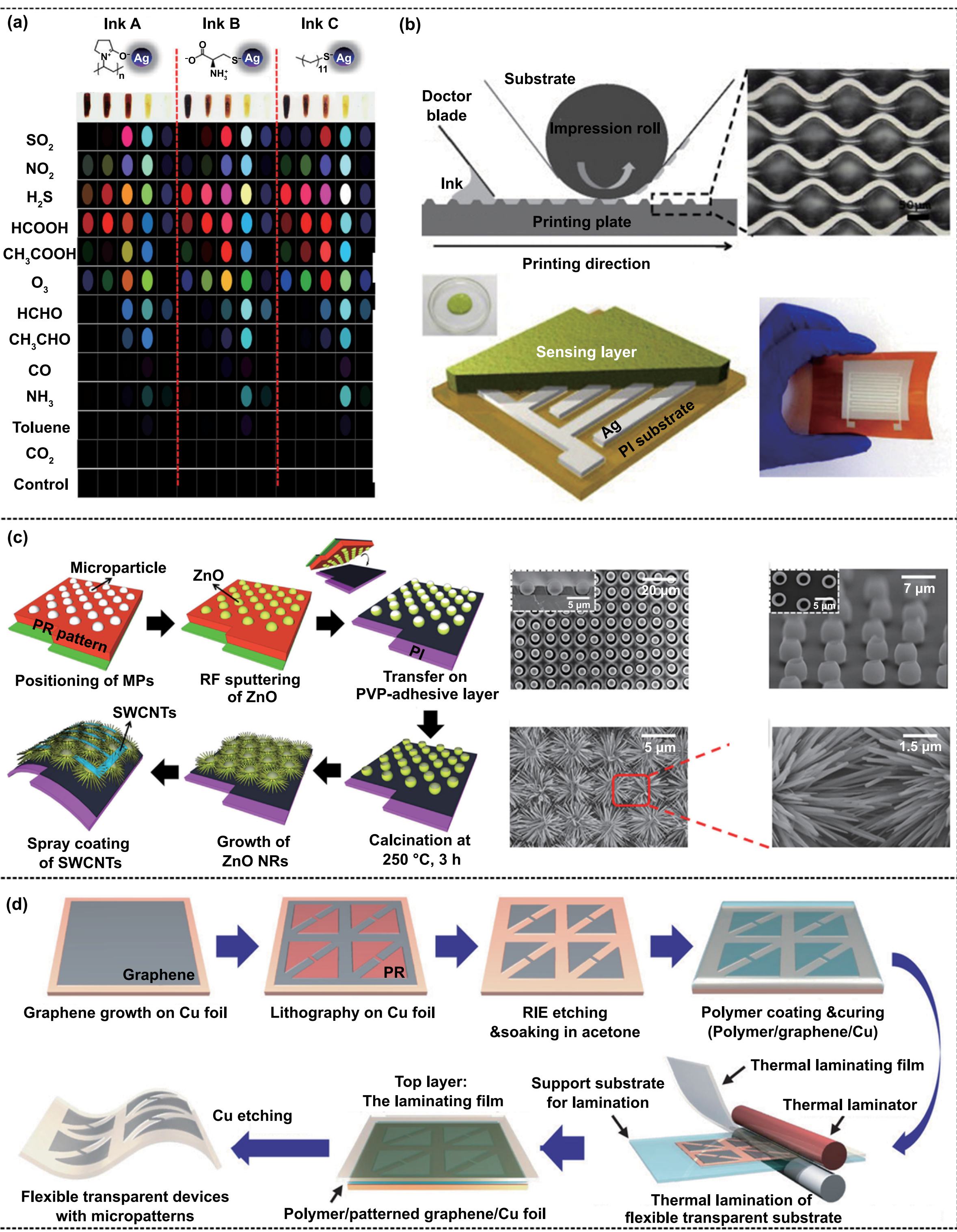

Figure 9. Gas sensor. (a) A gas sensor array prepared by inkjet printing. Reprinted with permission from [340]. Copyright (2020) American Chemical Society. (b) Gas sensors with microscale stripe structures for WO_3-PEDOT: PSS using a gravure printing process. Reprinted from [341], Copyright © 2015 Elsevier B.V. All rights reserved. (c) Gas sensor with micropatterned double-faced ZnO nanostructures using μTM technique. Reprinted with permission from [342]. Copyright (2017) American Chemical Society. (d) The flexible gas sensors prepared by photolithography and NIL. [380] John Wiley & Sons. © 2020 Wiley-VCH GmbH.

5.3.4. LDW. Gas sensor that responds via electrical signals are usually associated with adsorption of gas by the material. Therefore, increasing the contact area between the gas molecules and the material through a patterned manufacturing process can greatly improve the sensitivity of the sensor. Qin *et al* [339] obtained patterned enhanced current gas sensors by patterned ablation of polytetrafluoroethylene films using UV laser etching. The patterned construction of the

polytetrafluoroethylene membrane electrode enhances the three-phase boundary of the sensor and achieves a minimum of 10 ppb SO_2 detection. Meanwhile, the sensor sensitivity was 0.63 μA ppm^{-1}, and the response time and recovery time were 6 s and 9 s, respectively.

5.4. Light sensor

A light sensor is a device that detects and analyses light parameters such as light intensity, frequency, and phase. It is used in a wide variety of applications including, but not limited to, environmental monitoring, medical imaging, industrial automation, and communications technology [381–383]. In 2023, Tang *et al* [384] presented a metal halide chalcogenide-based photoconductive flexible photodetector that can be used to construct a low-power, high-SNR wearable optoelectronic volumetric pulse sensing system for real-time assessment of human cardiopulmonary function. Photodetectors, which convert optical signals into electrical signals, are the most commonly used light detection devices. The operating mechanisms of photodetectors include photoconductivity and photovoltaic effects, with the fundamental principle being that external light generates photo-generated carriers within the material, leading to changes in the material's conductivity or potential difference [385–387]. In addition, photodetectors use photothermoelectric technology, the basic principle is the conversion between optical, thermal and electrical signals [388]. Detection of light intensity is achieved by sensing the changes in voltage and current caused by changes in temperature [389]. In practical applications, effective monitoring of light in specific wavelength bands is often realised by hybrid mechanisms [390]. Meanwhile, sensor arrays can be constructed to realise the imaging function [391]. Next, we will describe the application of patterned manufacturing process for light sensor.

5.4.1. Printing. Printing technology has the advantages of high material utilisation, low cost, and parallel processing with multiple nozzles, which is suitable for combining multiple materials on the same substrate to prepare full-colour flexible light sensor. Wang *et al* [344] prepared full-colour flexible photodetectors using high-resolution E-jet printing (figure 10(a)). The smallest printed feature size for perovskite applications was achieved. The responsivity and specific detectivity were 14.97 AW^{-1} and 1.41 $\times$ 10^{12} Jones, respectively. Zumeit *et al* [345] prepared flexible photodetectors based on GaAs microstructures using a direct roll-to-roll printing process (figure 10(b)). This preparation method combines high throughput and high accuracy. The photodetector obtained has a responsivity of $>10^4$ AW^{-1}, D^* of $>10^{14}$ Jones, an external quantum efficiency of $>10^6$, a photoconductivity gain of $>10^4$, and a stable performance output after 500 bending tests.

5.4.2. Soft lithography. Soft lithography is an important technique for the preparation of patterned micro-nanostructures, which allows flexible preparation of the desired material morphology using solution filling. Li *et al* [284] prepared chalcogenide heterojunction photodetector arrays using MIMIC in a soft lithography process (figure 10(c)). PDMS moulds with microstructures were placed in close contact by the substrate, and $MAPbI_3$ and $MAPbBr_3$ were injected from both ends of the moulds, respectively. After being evaporated and crystallised, the chalcogenide heterojunction photodetector arrays were prepared. The photodetector has a responsivity of 1207 AW^{-1}, a detectivity of 2.78 $\times$ 10^{13} Jones, an external quantum efficiency of 230 500%, a linear dynamic response range of 130.2 dB, and response and recovery times of 3.9 ms and 2.0 ms, respectively.

5.4.3. Mould method. In device using photovoltaic effect, regular micro-nanostructures are important for enhancing the light absorption efficiency [392]. The mould method is a simple patterned process for manufacturing micro-nanostructures, with high resolution, and does not require high temperatures or special substrates, making it very suitable for the preparation of flexible sensors. Wu *et al* [346] used the mould method to fabricate a large-scale integrated flexible photodetector array (figure 10(d)). They first patterned the substrate surface with hydrophilic-hydrophobic treatment, and then prepared the patterned perovskite film through a two-step sequential deposition process. This method has high flexibility and the capability for large-scale production. The sensor has a responsivity of 2.17 AW^{-1}, a D^* of 9.4 $\times$ 10^{11} Jones, a response time of 0.48 s, and a recovery time of 0.26 s, showing excellent durability after hundreds of bending cycles. Lu *et al* [347] prepared a flexible solar-blind photodetector array based on CsCu using the mould method. It has high responsivity and ultra-low power density detection limit. The array device has a long-term stable photo switching behaviour of 8 h and can resolve a light intensity of 6.1 nW cm^{-2} with a responsivity of 62 AW^{-1}.

5.5. Temperature sensor

The temperature sensor is a sensor that converts a temperature value into an output signal. It is important in industrial production and healthcare [393]. Zheng *et al* [394] reported a flexible calorimetric flow sensor using a high-sensitivity vanadium oxide thermistor in 2024. The sensor overcomes the difficulty of accurate identification of pressure sensors at low air speed, and can realise good flight parameter measurement based on a single device, which has a broad application prospect in micro-airflow sensing and micro air vehicle control. Temperature sensors operate based on various physical effects, including but not limited to the thermoelectric effect, thermistor effect, thermal expansion effect, and optical effect [395]. Among them, high-precision temperature sensing is usually measured based on changes in electrical and electromagnetic wave signals [396].

5.5.1. Printing. In temperature sensors that rely on electrical signal measurements, the two primary principles are the change in resistance and the generation of thermal voltage

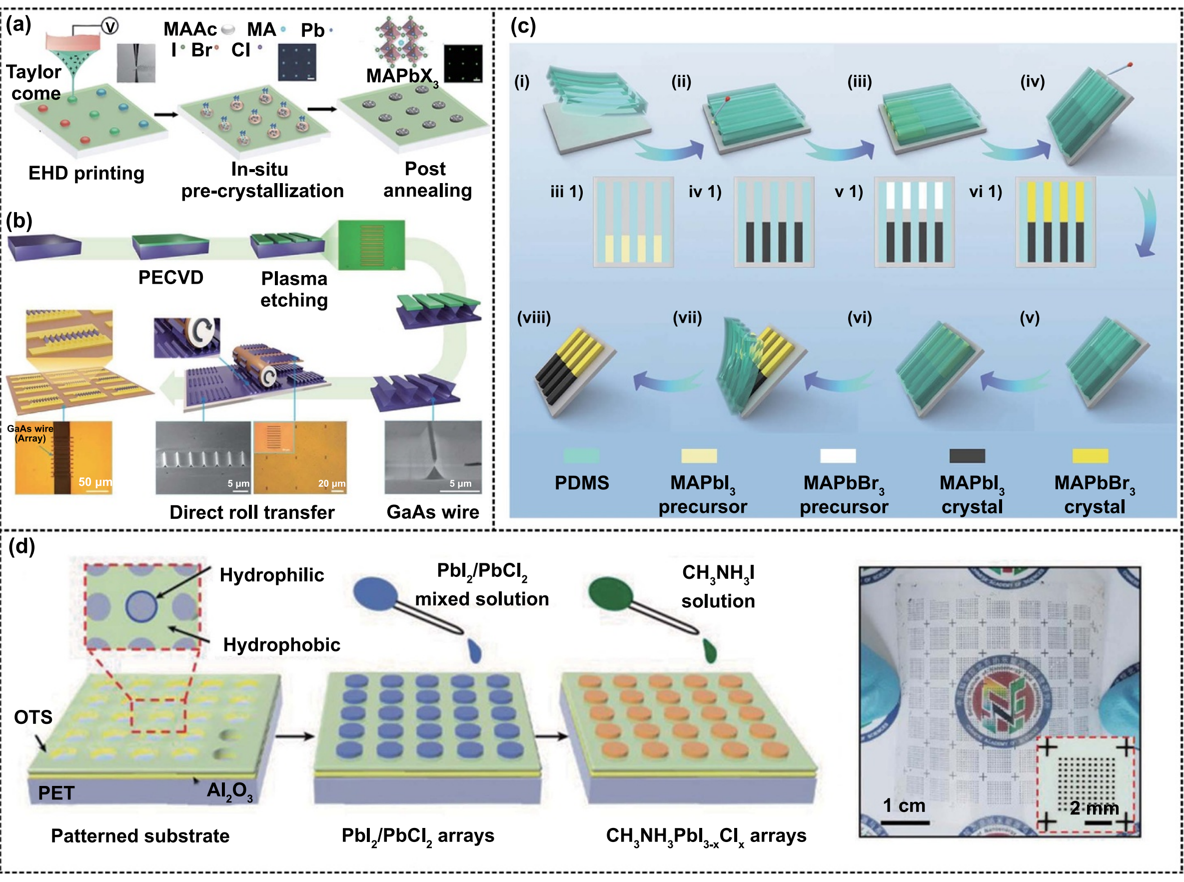

Figure 10. Light sensor. (a) Full-colour flexible photodetectors using high-resolution E-jet printing. [344] John Wiley & Sons. © 2021 Wiley-VCH GmbH. (b) Flexible photodetectors based on GaAs microstructures using a direct roll-to-roll printing process. Reproduced from [345]. CC BY 4.0. (c) Chalcogenide heterojunction photodetector array prepared by MIMIC. [284] John Wiley & Sons. © 2022 Wiley-VCH GmbH. (d) MoS_2 photodetectors prepared by sacrificial mould method. [346] John Wiley & Sons. © 2018 WILEY-VCH Verlag GmbH & Co. KGaA, Weinheim.

through the Seebeck effect. The patterned manufacturing of temperature sensors, which is based on electrical parameters, is typically aimed at enhancing device stability and broadening their applicability. The printing process enables the fabrication of patterns on both rigid and flexible material surfaces, thereby expanding the range of applications for temperature sensors. Choi *et al* [348] prepared resistive temperature sensors on flexible substrates using DOD E-Jet technology, and the printed completed temperature sensors had a resistivity of 25.35 $\mu\Omega\cdot$cm and a resistance temperature coefficient of 0.000 7687 $^{\circ}C^{-1}$.

5.5.2. Exposure lithography. Exposure lithography processes can be customised to fabricate sophisticated electrode patterns, thereby augmenting the deformability resistance of the electrode materials. Liu *et al* [349] prepared thermocouple temperature sensors based on bent thermal electrodes by photolithography process (figure 11(a)). By patterning the electrode design, the deformation resistance of the device is improved. Meanwhile, patterning for the substrate material further enhances the deformation resistance of the device. The sensor had a maximum sensitivity of 76.5 μV $^{\circ}C^{-1}$ at a temperature difference of 100 °C. The sensor exhibited good stability under a pulling force of 0–10 N, and did not degrade the sensitivity of the sensor after 1000 deformation cycles. Precise and rational structural design can amplify the extent of the impact of temperature on the properties of electromagnetic waves. Such structures are particularly amenable to fabrication via lithography processes.

5.5.3. Mould method. Temperature sensing arrays are constructed to map the flow trajectory of the temperature field, which is important for real-time temperature detection. Reusable high-precision shadow masks can rapidly fabricate large-area sensor arrays. Ren *et al* [221] prepared a flexible temperature sensor array based on 16 × 16 organic field-effect transistors (figure 11(b)). Among them, the transistor array portion was prepared by patterning the array by shadow masks technique. The temperature sensor array operated at 20 °C–100 °C with a temperature response coefficient of 20.4, a temperature resolution of 0.4 °C, and an array yield of 100%.

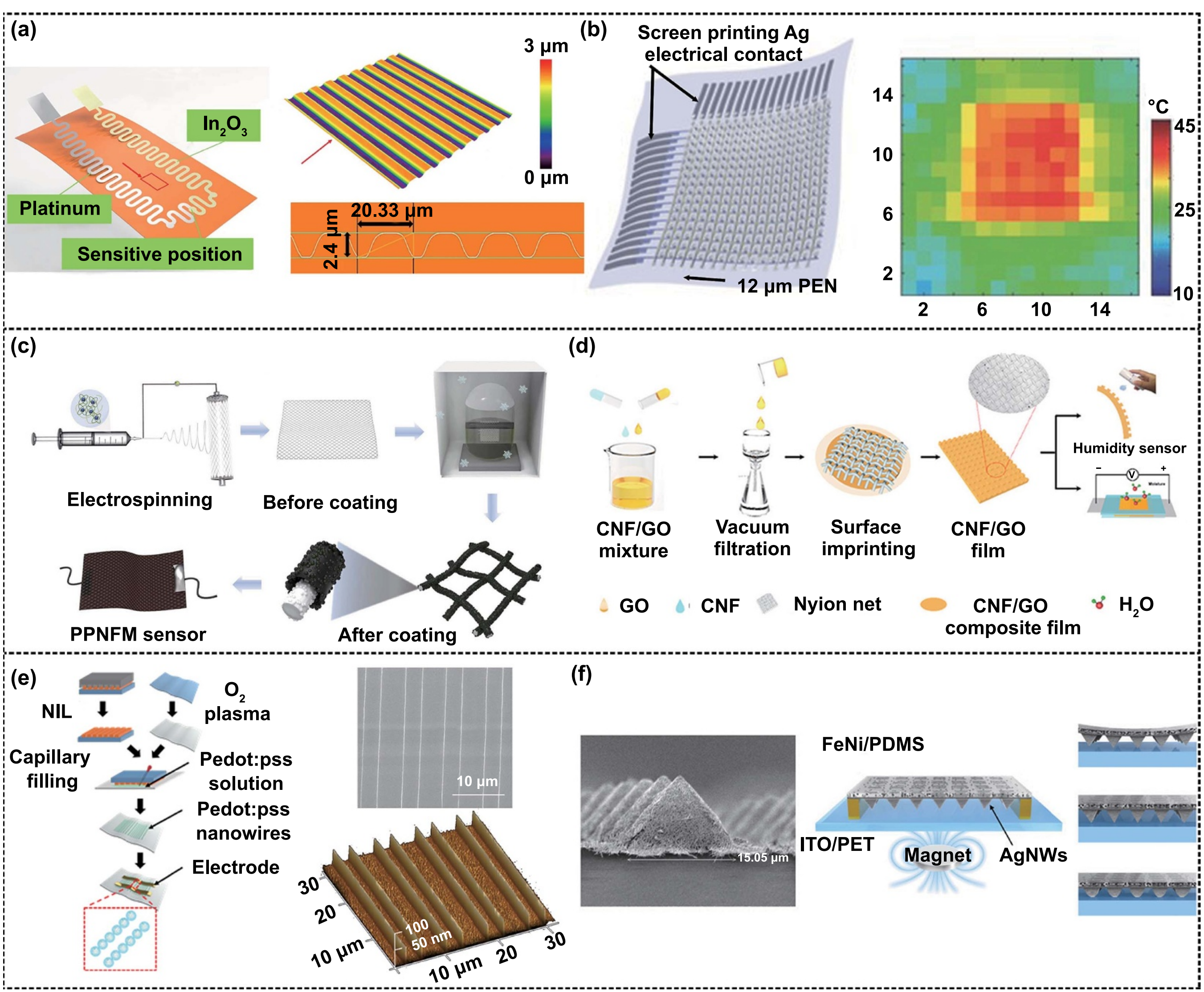

Figure 11. Temperature sensors, humidity sensors and magnetic sensor. (a) Thermocouple temperature sensor prepared by lithography. Reproduced from [349]. CC BY 4.0. (b) A flexible temperature sensor array prepared by shadow masks technique. [221] John Wiley & Sons. © 2016 WILEY-VCH Verlag GmbH & Co. KGaA, Weinheim. (c) Humidity sensors with rhombic electrode structure using mould method. Reprinted from [350], © 2024 Elsevier B.V. All rights reserved. (d) A flexible humidity sensor with cross patterns prepared by mould method. Reprinted with permission from [397]. Copyright (2020) American Chemical Society. (e) Humidity sensors based on large-area PEDOT: PSS nanowires using MIMIC technique. Reproduced from [351]. © IOP Publishing Ltd. All rights reserved. (f) Magnetic sensor based on a pyramidal structure prepared by mould method. Reprinted with permission from [352]. Copyright (2018) American Chemical Society.

5.6. Other sensors

In addition to the aforementioned types of sensors, investigations have also been partially conducted into humidity and magnetism sensors for enhancing single device patterning techniques as well as array manufacturing techniques. Yan *et al* [350] prepared humidity sensors with rhombic electrode structure using electrostatic spinning technique combined with mould method (figure 11(c)). Thanks to the increased specific surface area of the regular rhombic structure electrodes, the humidity sensor has excellent mechanical flexibility and humidity sensing ability. The humidity sensitivity is 83%, the response time is 38 s, and the performance remains stable after 1000 bending cycles. Li *et al* [397] used the mould method to prepare cross patterns on the surface of cellulose nanofiber-/graphene oxide composite films using a nylon mesh as a mould, and used this to form a humidity sensor (figure 11(d)). The sensor deforms in response to changes in humidity by deformation, and the patterned structure promotes stress concentration and thus enhances the deformation capability of the sensor in humidity environments compared to the unpatterned one. Zhou *et al* [351] prepared humidity sensors based on large-area PEDOT: PSS nanowires using MIMIC technique (figure 11(e)). The humidity-sensitive PSS particles in the nanowires were more exposed to moisture compared to the thin film material, resulting in a fast response time and high sensitivity as well as better linearity of this humidity sensor. The response time and recovery time of the sensor were

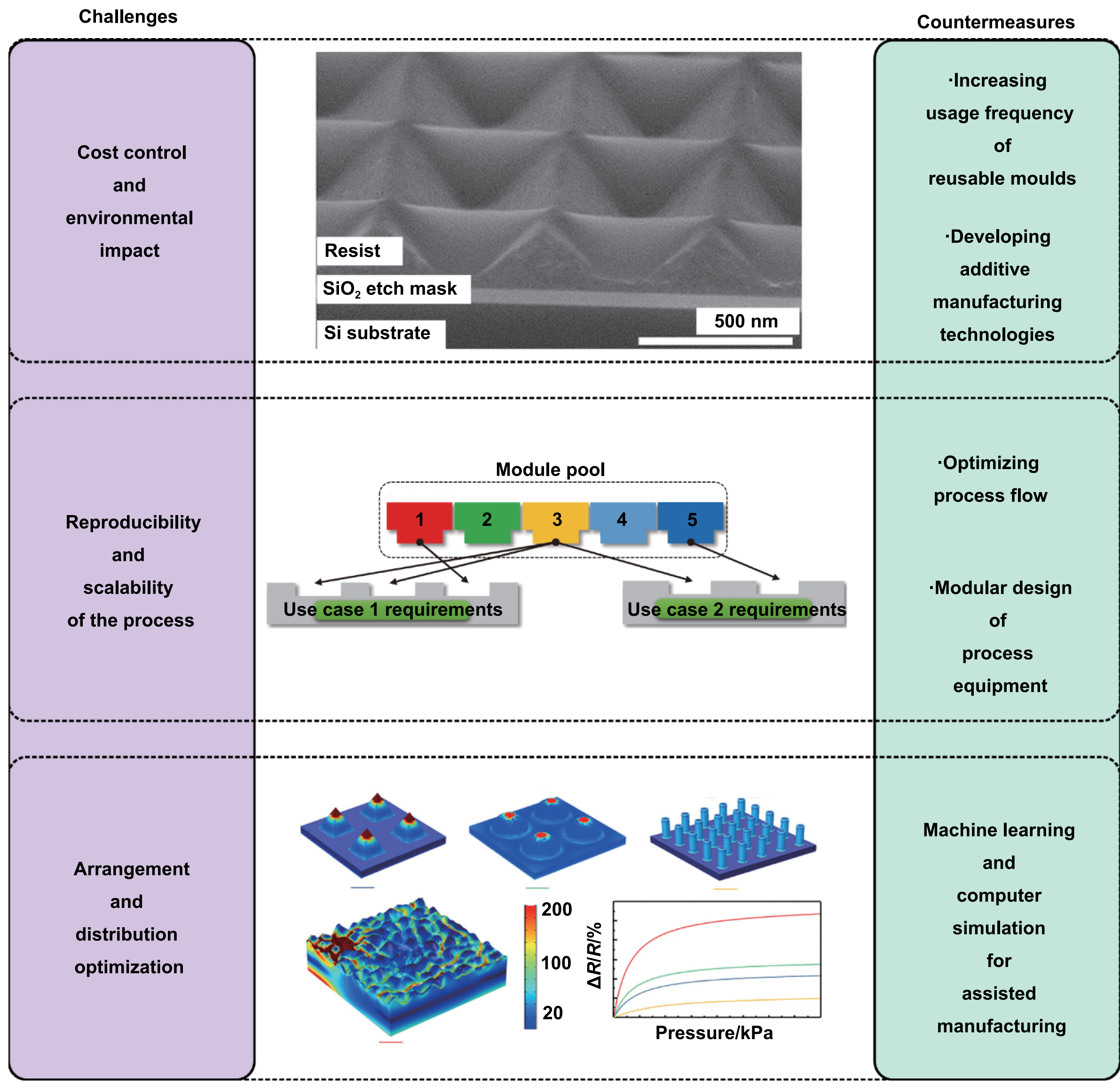

Figure 12. Challenges and countermeasures in the manufacturing technology of patterned micro-nanostructures for flexible sensors. Reprinted from [400], © 2017 Elsevier B.V. All rights reserved. Reprinted from [401], Copyright © 2014 Published by Elsevier Ltd. Reprinted with permission from [402]. Copyright (2018) American Chemical Society.

0.63 s and 2.05 s, respectively, and the response was almost unchanged in 1000 bending cycles, which proved the excellent mechanical properties of the flexible sensor. Cai *et al* [352] designed a magnetic sensor based on a pyramidal structure (figure 11(f)), in which the pyramidal structure of the PDMS was prepared by the mould method. Its surface was covered with an Fe/Ni alloy powder, and a change in the external magnetic field caused a change in the current. The sensitivity of the sensor was as high as 1507.9% mT^{-1} with a response time of 1 ms, and the performance of the device remained almost unchanged after 5000 bending cycles.

6. Conclusions and outlook

Nowadays, sensors play a crucial role in various fields, including industrial production, basic science, medical diagnosis, environmental detection, cosmic development and cultural relics protection [398, 399], and have already realised a depth and breadth far beyond human perception. This is due to advances in materials science and patterned manufacturing processes. In this review, we describe in detail the patterned micro-nanostructure manufacturing process for sensor performance enhancement and provide a comparative analysis of the different processes. Among the patterned manufacturing techniques used for flexible sensors, exposure lithography combines the advantages of high resolution and high scalability, and despite the high cost and complexity of the process, it is still the main choice for the large-scale production of patterned micro- and nanostructures today and is gradually being used on a large scale in the field of flexible materials. Printing process is low cost, compatible, fast and can meet most of the requirements for the manufacturing of patterned structures with low resolution. NIL, as a promising alternative to lithography, offers

the advantages of high resolution, low cost, high speed, and high scalability, but still relies on exposure lithography to prepare high-precision moulds. Soft lithography technology, similar to NIL, offers a lower resolution but is highly compatible with various materials and can prepare the patterned micro-nanostructure on the surfaces of materials with complex structures. The mould method has a long history and has evolved to become an important option for the preparation of complex three-dimensional structures. Standardizing the preparation process can enhance the scalability of the mould method. High-precision LDW technology boasts high material compatibility, technological stability, and minimal environmental requirements, making it more suitable for the fabrication of patterned structures in laboratory settings.

In addition, we discuss practical applications of the patterned manufacturing process based on the type of sensor. The patterned structure of the sensitive element enhances the interaction between the matter to be measured and the material, and increases the contact area and amplifies the signal changes caused by the matter to be measured [403]. Therefore, the construction of patterned structures can enhance the performance of the sensor, including sensitivity and response/relaxation time. In addition, sensor arrays prepared by the patterning process can enhance the density and expand the range of information sensing, which is of great significance at the present time when miniaturisation and integration are pursued [327]. It is foreseeable that the role played by sensors will become more and more important along with the increasing demand for information by the whole society. Currently, various types of sensors are developing towards higher performance, lower cost, greater integration, digitisation, miniaturisation and wearability, which puts higher requirements on the patterned manufacturing process. However, the current manufacturing processes for micro-nano structures face challenges, such as high cost, low uniformity, low flexibility and unsuitable matching mechanisms, which have become bottlenecks that limit the optimisation of sensor performance. To overcome these issues, optimizing the sensor patterned micro-nanostructure manufacturing process is essential in the following aspects (figure 12):

- Cost control and environmental impact. The production environment and process equipment utilised for the manufacturing of nanoscale pattern structures are expensive, and the manufacturing process is time-consuming. Therefore, in the large-scale and standardised manufacturing process of sensors, increasing the usage frequency of reusable moulds can significantly reduce processing time while ensuring precision [400]. For example, a small number of high-precision moulds are prepared using EUV lithography or EBL techniques, followed by bulk fabrication of flexible sensors with micro-nanostructure using NIL or shadow mask techniques [31, 262]. Concurrently, developing additive manufacturing technologies to reduce the proportion of subtractive manufacturing processes in the fabrication workflow can mitigate resource wastage and environmental pollution [404].
- Reproducibility and scalability of the process. The specific shape of micro-nanostructures directly influences the performance of sensors. As the complexity of the fabrication patterns increases, ensuring the process's reproducibility and the uniformity of structures poses a significant challenge. By establishing a standard procedural sequence for the relevant micro-nanostructures, optimizing the process flow, and reducing the number of process steps and operations, the impact of subsequent processes on existing structures can be minimised, enhancing the process's reproducibility [405]. Furthermore, by selecting more appropriate interfacial materials and optimizing the interfacial effects between the processing equipment and the substrate materials, the uniformity of micro-nanostructures can be improved [406]. For high-resolution but low-throughput technologies such as Scanning Probe Lithography, EBL, IBL, and LDW, moulds can be used to link the aforementioned technologies with scaled-up production processes [261]. At the same time, the scalability of the process also implies that the technology can meet the continuous updates of sensor active materials and sensor structures. An appropriate solution is the modular design of process equipment, which facilitates the construction of flexible production lines as well as the transformation and maintenance of production lines [407, 408].
- Arrangement and distribution optimisation. To meet the design requirements of sensors with complex sensing mechanisms for the future, machine learning algorithms and computational simulation will become an essential part of the sensor patterned manufacturing process [409, 410]. Precise patterning structures can enhance sensor performance [411]. Moreover, the design of sensor patterned micro-nanostructures, integrated with disciplines such as biology, chemistry, and physics, can continuously optimise the shape and size of the patterned structures [412]. In the future, combining methods for obtaining high-quality pattern structures through precise calculations with the optimisation of manufacturing processes will propel the comprehensive performance of sensors to a new level [402, 413–416].

The variety of patterned micro-nanostructure manufacturing technologies applied to sensors is vast and complex. In the sensor fabrication process, mature and commonly used technologies are often prioritised. We hope that this review can promote innovation and integration of patterned manufacturing technologies, optimise the process workflow, and achieve the best strategies for the manufacturing of various sensor patterned micro-nanostructures.

Acknowledgments

The authors sincerely acknowledge financial support from the National Key Research and Development Program of China (Grant 2024YFB3212100), National Natural Science Foundation of China (NSFC Grant Nos. 62422409, 62174152 and 62374159) and from the Youth Innovation Promotion Association of Chinese Academy of Sciences (No. 2020115).

ORCID iDs

Kaichen Xu https://orcid.org/0000-0003-4957-3144
Lili Wang https://orcid.org/0000-0002-0422-4277

References

[1] Culler D, Estrin D and Srivastava M 2004 Guest editors' introduction: overview of sensor networks *Computer* **37** 41–49
[2] Wilson J S 2004 *Sensor Technology Handbook* (Elsevier)
[3] Currie E H 2021 *Sensors and Sensing. In Mixed-Signal Embedded Systems Design* ed E H Currie (Springer)
[4] Nag A, Mukhopadhyay S C and Kosel J 2017 Wearable flexible sensors: a review *IEEE Sens. J.* **17** 3949–60
[5] Liu E Z, Cai Z M, Ye Y W, Zhou M Y, Liao H and Yi Y 2023 An overview of flexible sensors: development, application, and challenges *Sensors* **23** 817
[6] Shi X *et al* 2021 Large-area display textiles integrated with functional systems *Nature* **591** 240–5
[7] Wang X F, Zhong B W, Lou Z, Han W and Wang L L 2024 The advancement of intelligent dressings for monitoring chronic wound infections *Chem. Eng. J.* **484** 149643
[8] Zhang H C *et al* 2023 Recent advances in nanofiber-based flexible transparent electrodes *Int. J. Extrem. Manuf.* **5** 032005
[9] Han S T, Peng H Y, Sun Q J, Venkatesh S, Chung K S, Lau S C, Zhou Y and Roy V A L 2017 An overview of the development of flexible sensors *Adv. Mater.* **29** 1700375
[10] Wang J F, Suo J, Song Z X, Li W J and Wang Z B 2023 Nanomaterial-based flexible sensors for metaverse and virtual reality applications *Int. J. Extrem. Manuf.* **5** 032013
[11] Wang C X, Yin L W, Zhang L Y, Xiang D and Gao R 2010 Metal oxide gas sensors: sensitivity and influencing factors *Sensors* **10** 2088–106
[12] Gauglitz G 2018 Analytical evaluation of sensor measurements *Anal. Bioanal. Chem.* **410** 5–13
[13] Steele J J, Taschuk M T and Brett M J 2009 Response time of nanostructured relative humidity sensors *Sens. Actuators* B **140** 610–5
[14] Sun H B, Kuchenbecker K J and Martius G 2022 A soft thumb-sized vision-based sensor with accurate all-round force perception *Nat. Mach. Intell.* **4** 135–45
[15] Li J, Bao R R, Tao J, Peng Y Y and Pan C F 2018 Recent progress in flexible pressure sensor arrays: from design to applications *J. Mater. Chem.* C **6** 11878–92
[16] Lian Z X, Zhou J H, Ren W F, Chen F Z, Xu J K, Tian Y L and Yu H D 2024 Recent progress in bio-inspired macrostructure array materials with special wettability—from surface engineering to functional applications *Int. J. Extrem. Manuf.* **6** 012008
[17] Peng S H, Blanloeuil P, Wu S Y and Wang C H 2018 Rational design of ultrasensitive pressure sensors by tailoring microscopic features *Adv. Mater. Interfaces* **5** 1800403
[18] Chou H H, Nguyen A, Chortos A, To J W F, Lu C E, Mei J G, Kurosawa T, Bae W G, Tok J B H and Bao Z N 2015 A chameleon-inspired stretchable electronic skin with interactive colour changing controlled by tactile sensing *Nat. Commun.* **6** 8011
[19] Li Z and Suslick K S 2021 The optoelectronic nose *Acc. Chem. Res.* **54** 950–60
[20] Chen Z H, Fan Q X, Han X Y, Shi G Y and Zhang M 2020 Design of smart chemical 'tongue' sensor arrays for pattern-recognition-based biochemical sensing applications *TrAC Trends Anal. Chem.* **124** 115794
[21] Lee J Y, Ju J E, Lee C, Won S M and Yu K J 2024 Novel fabrication techniques for ultra-thin silicon based flexible electronics *Int. J. Extrem. Manuf.* **6** 042005
[22] Lee M and Fauchet P M 2007 Two-dimensional silicon photonic crystal based biosensing platform for protein detection *Opt. Express* **15** 4530–5
[23] Pan H Y, Zhou L H, Zheng W, Liu X H, Zhang J and Pinna N 2023 Atomic layer deposition to heterostructures for application in gas sensors *Int. J. Extrem. Manuf.* **5** 022008
[24] Zhao Y J, Zhao X W, Hu J, Xu M, Zhao W J, Sun L G, Zhu C, Xu H and Gu Z Z 2009 Encoded porous beads for label-free multiplex detection of tumor markers *Adv. Mater.* **21** 569–72
[25] Zheng F Y, Cheng Y, Wang J, Lu J, Zhang B, Zhao Y J and Gu Z Z 2014 Aptamer-functionalized barcode particles for the capture and detection of multiple types of circulating tumor cells *Adv. Mater.* **26** 7333–8
[26] Mannsfeld S C B, Tee B C K, Stoltenberg R M, Chen C V H H, Barman S, Muir B V O, Sokolov A N, Reese C and Bao Z N 2010 Highly sensitive flexible pressure sensors with microstructured rubber dielectric layers *Nat. Mater.* **9** 859–64
[27] Park J, Lee Y, Hong J, Ha M, Jung Y D, Lim H, Kim S Y and Ko H 2014 Giant tunneling piezoresistance of composite elastomers with interlocked microdome arrays for ultrasensitive and multimodal electronic skins *ACS Nano* **8** 4689–97
[28] Tee B C K, Chortos A, Dunn R R, Schwartz G, Eason E and Bao Z N 2014 Tunable flexible pressure sensors using microstructured elastomer geometries for intuitive electronics *Adv. Funct. Mater.* **24** 5427–34
[29] Park J, Kim Y S and Hammond P T 2005 Chemically nanopatterned surfaces using polyelectrolytes and ultraviolet-cured hard molds *Nano Lett.* **5** 1347–50
[30] Sayed S and Selvaganapathy P R 2022 High-resolution fabrication of nanopatterns by multistep iterative miniaturization of hot-embossed prestressed polymer films and constrained shrinking *Microsyst. Nanoeng.* **8** 20
[31] Sayed S and Selvaganapathy P R 2020 Multi-step proportional miniaturization to sub-micron dimensions using pre-stressed polymer films *Nanoscale Adv.* **2** 5461–7
[32] Kim K K, Ha I, Kim M, Choi J, Won P, Jo S and Ko S H 2020 A deep-learned skin sensor decoding the epicentral human motions *Nat. Commun.* **11** 2149
[33] Li M H, Lu Y, Wang Y J, Huang S and Feng K 2024 Synergistically biomimetic platform that enables droplets to be self-propelled *Int. J. Extrem. Manuf.* **6** 055503
[34] Wijshoff H 2010 The dynamics of the piezo inkjet printhead operation *Phys. Rep.* **491** 77–177
[35] Bohandy J, Kim B F and Adrian F J 1986 Metal deposition from a supported metal film using an excimer laser *J. Appl. Phys.* **60** 1538–9
[36] Li H, Ling J Y, Lin J M, Lu X and Xu W G 2023 Interface engineering in two-dimensional heterostructures towards novel emitters *J. Semicond.* **44** 011001
[37] Cooper C and Hughes B 2020 Aerosol jet printing of electronics: an enabling technology for wearable devices *Proc. 2020 Pan Pacific Microelectronics Symp.* (IEEE) pp 1–11
[38] Taylor G I 1964 Disintegration of water drops in an electric field *Proc. R. Soc.* A **280** 383–97
[39] Schirmer N C, Kullmann C, Schmid M S, Burg B R, Schwamb T and Poulikakos D 2010 On ejecting colloids against capillarity from sub-micrometer openings: on-demand dielectrophoretic nanoprinting *Adv. Mater.* **22** 4701–5
[40] Bommineedi L K, Upadhyay N and Minnes R 2023 Screen printing: an ease thin film technique *Simple Chemical Methods for Thin Film Deposition* ed B R Sankapal,

A Ennaoui, R B Gupta and C D Lokhande (Springer) pp 449–507
[41] Cope B and Kalantzis D 2001 *Print and Electronic Text Convergence: Technology Drivers Across the Book Production Supply Chain, from Creator to Consumer* (Common Ground Publishing)
[42] Podhajny R M 2004 Aniline printing-100 years later *Paper Film Foil Converter* **78** 20
[43] Piner R D, Zhu J, Xu F, Hong S and Mirkin C A 1999 "Dip-pen" nanolithography *Science* **283** 661–3
[44] Kinoshita H 2005 History of extreme ultraviolet lithography *J. Vac. Sci. Technol.* B **23** 2584–8
[45] Maldonado J R and Peckerar M 2016 x-ray lithography: some history, current status and future prospects *Microelectron. Eng.* **161** 87–93
[46] Pfeiffer H C 2010 Direct write electron beam lithography: a historical overview *Proc. SPIE* **7823** 782316
[47] Watt F, Bettiol A A, Van Kan J A, Teo E J and Breese M B H 2005 Ion beam lithography and nanofabrication: a review *Int. J. Nanosci.* **4** 269–86
[48] Quist A P, Pavlovic E and Oscarsson S 2005 Recent advances in microcontact printing *Anal. Bioanal. Chem.* **381** 591–600
[49] Frank W E and Gibson R J 1954 A new pressure-sensing instrument *J. Franklin Inst.* **258** 21–30
[50] Wang S, Zhou Z, Li B, Wang C and Liu Q 2021 Progresses on new generation laser direct writing technique *Mater. Today Nano* **16** 100142
[51] Chou S Y, Krauss P R and Renstrom P J 1995 Imprint of sub-25 nm vias and trenches in polymers *Appl. Phys. Lett.* **67** 3114–6
[52] Jeon H J, Kim K H, Baek Y K, Kim D W and Jung H T 2010 New top-down approach for fabricating high-aspect-ratio complex nanostructures with 10 nm scale features *Nano Lett.* **10** 3604–10
[53] Song T E, Oh S A, Ahn C W, Oh I K and Jeon H J 2023 Effective approach for fabricating highly precise high-curvature structural patterns via air-bubble induction *Langmuir* **39** 15785–91
[54] Guo M M, Qu Z Y, Min F Y, Li Z, Qiao Y L and Song Y L 2022 Advanced unconventional techniques for sub-100 nm nanopatterning *InfoMat* **4** e12323
[55] Luo Y F *et al* 2023 Technology roadmap for flexible sensors *ACS Nano* **17** 5211–95
[56] Gomes T C, Constantino C J L, Lopes E M, Job A E and Alves N 2012 Thermal inkjet printing of polyaniline on paper *Thin Solid Films* **520** 7200–4
[57] Delrot P, Modestino M A, Gallaire F, Psaltis D and Moser C 2016 Inkjet printing of viscous monodisperse microdroplets by laser-induced flow focusing *Phys. Rev. Appl.* **6** 024003
[58] Chen K K, Jiang E H, Wei X Y, Xia Y, Wu Z Z, Gong Z Y, Shang Z J and Guo S S 2021 The acoustic droplet printing of functional tumor microenvironments *Lab Chip* **21** 1604–12
[59] Wilkinson N J, Smith M A A, Kay R W and Harris R A 2019 A review of aerosol jet printing—a non-traditional hybrid process for micro-manufacturing *Int. J. Adv. Manuf. Technol.* **105** 4599–619
[60] Park J-U *et al* 2007 High-resolution electrohydrodynamic jet printing *Nat. Mater.* **6** 782–9
[61] Ng L W T, Hu G H, Howe R C T, Zhu X X, Yang Z Y, Jones C G and Hasan T 2019 *Printing of Graphene and Related 2D Materials* (Springer)
[62] Harrey P M, Evans P S A, Ramsey B J and Harrison D 1999 A novel manufacturing process for capacitors using offset lithography *Proc. 1st Int. Symp. on Environmentally Conscious Design and Inverse Manufacturing* (IEEE) pp 842–6
[63] Martens J A 1992 Flexographic printing plate process *U.S. Patent. No.* 2047428A1
[64] Liu G Q, Petrosko S H, Zheng Z J and Mirkin C A 2020 Evolution of dip-pen nanolithography (DPN): from molecular patterning to materials discovery *Chem. Rev.* **120** 6009–47
[65] Okazaki S 2015 High resolution optical lithography or high throughput electron beam lithography: the technical struggle from the micro to the nano-fabrication evolution *Microelectron. Eng.* **133** 23–35
[66] Groves T R, Pickard D, Rafferty B, Crosland N, Adam D and Schubert G 2002 Maskless electron beam lithography: prospects, progress, and challenges *Microelectron. Eng.* **61–62** 285–93
[67] Melngailis J 1993 Focused ion beam lithography *Nucl. Instrum. Methods Phys. Res.* B **80–81** 1271–80
[68] Tandon U S 1992 An overview of ion beam lithography for nanofabrication *Vacuum* **43** 241–51
[69] Perl A, Reinhoudt D N and Huskens J 2009 Microcontact printing: limitations and achievements *Adv. Mater.* **21** 2257–68
[70] Tseng A A, Chen K, Chen C D and Ma K J 2003 Electron beam lithography in nanoscale fabrication: recent development *IEEE Trans. Electron Packag. Manuf.* **26** 141–9
[71] Xia Y N and Whitesides G M 1998 Soft lithography *Annu. Rev. Mater. Sci.* **28** 153–84
[72] Kim E, Xia Y N and Whitesides G M 1996 Micromolding in capillaries: applications in materials science *J. Am. Chem. Soc.* **118** 5722–31
[73] Gates B D, Xu Q B, Stewart M, Ryan D, Willson C G and Whitesides G M 2005 New approaches to nanofabrication: molding, printing, and other techniques *Chem. Rev.* **105** 1171–96
[74] Kim J O, Kwon S Y, Kim Y, Choi H B, Yang J C, Oh J, Lee H S, Sim J Y, Ryu S and Park S 2019 Highly ordered 3D microstructure-based electronic skin capable of differentiating pressure, temperature, and proximity *ACS Appl. Mater. Interfaces* **11** 1503–11
[75] Min F Y *et al* 2023 Humidity-controlled molecular assembly and photoisomerization behavior with a bubble-assisted patterning approach *Small* **19** 2301362
[76] Thouti E, Nagaraju A, Chandran A, Prakash P V B S S, Shivanarayanamurthy P, Lal B, Kumar P, Kothari P and Panwar D 2020 Tunable flexible capacitive pressure sensors using arrangement of polydimethylsiloxane micro-pyramids for bio-signal monitoring *Sens. Actuators* A **314** 112251
[77] Yang J, Luo S, Zhou X, Li J L, Fu J T, Yang W D and Wei D P 2019 Flexible, tunable, and ultrasensitive capacitive pressure sensor with microconformal graphene electrodes *ACS Appl. Mater. Interfaces* **11** 14997–5006
[78] Chong T C, Hong M H and Shi L P 2010 Laser precision engineering: from microfabrication to nanoprocessing *Laser Photon. Rev.* **4** 123–43
[79] Kuscer D, Drnovšek S and Levassort F 2021 Inkjet-printing-derived lead-zirconate-titanate-based thick films for printed electronics *Mater. Des.* **198** 109324
[80] Kamarudin S F, Abdul Aziz N H, Lee H W, Jaafar M and Sulaiman S 2024 Inkjet printing optimization: toward realization of high-resolution printed electronics *Adv. Mater. Technol.* **9** 2301875
[81] Uddin M J, Hassan J and Douroumis D 2022 Thermal inkjet printing: prospects and applications in the development of medicine *Technologies* **10** 108
[82] Zhu W, Ma X Y, Gou M L, Mei D Q, Zhang K and Chen S C 2016 3D printing of functional biomaterials for tissue engineering *Curr. Opin. Biotechnol.* **40** 103–12

[83] Wang Y C, Xu C Y, Liu J W, Pan H M, Li Y and Mei D Q 2022 Acoustic-assisted 3D printing based on acoustofluidic microparticles patterning for conductive polymer composites fabrication *Addit. Manuf.* **60** 103247

[84] Seiti M, Degryse O and Ferraris E 2022 Aerosol Jet® printing 3D capabilities for metal and polymeric inks *Mater. Today Proc.* **70** 38–44

[85] Zhang J, Geng B W, Duan S M, Huang C C, Xi Y, Mu Q, Chen H P, Ren X C and Hu W P 2020 High-resolution organic field-effect transistors manufactured by electrohydrodynamic inkjet printing of doped electrodes *J. Mater. Chem.* C **8** 15219–23

[86] Hyun W J, Lim S, Ahn B Y, Lewis J A, Frisbie C D and Francis L F 2015 Screen printing of highly loaded silver inks on plastic substrates using silicon stencils *ACS Appl. Mater. Interfaces* **7** 12619–24

[87] Lemarchand J, Bridonneau N, Battaglini N, Carn F, Mattana G, Piro B, Zrig S and Noël V 2022 Challenges, prospects, and emerging applications of inkjet-printed electronics: a chemist's point of view *Angew. Chem., Int. Ed.* **61** e202200166

[88] Kitsomboonloha R, Morris S J S, Rong X Y and Subramanian V 2012 Femtoliter-scale patterning by high-speed, highly scaled inverse gravure printing *Langmuir* **28** 16711–23

[89] Wen Z X, Liu X Y, Chen W X, Zhou R L, Wu H, Xia Y M and Wu L B 2024 Progress in polyhedral oligomeric silsesquioxane (POSS) photoresists: a comprehensive review across lithographic systems *Polymers* **16** 846

[90] Xia D Y, Zhu X L, Khanom F and Runt D 2020 Neon and helium focused ion beam etching of resist patterns *Nanotechnology* **31** 475301

[91] Greer A I M *et al* 2020 Nanopatterned titanium implants accelerate bone formation *in vivo ACS Appl. Mater. Interfaces* **12** 33541–9

[92] Ito S, Nakamura T and Nakagawa M 2020 Organic–inorganic hybrid replica molds with high mechanical strength for step-and-repeat ultraviolet nanoimprinting *Bull Chem. Soc. Jpn.* **93** 862–9

[93] Sabahi-Kaviani R and Luttge R 2021 Investigating the pattern transfer fidelity of Norland Optical Adhesive 81 for nanogrooves by microtransfer molding *J. Vac. Sci. Technol.* B **39** 062810

[94] Veldhuis S A, George A, Nijland M and ten Elshof J E 2012 Concentration dependence on the shape and size of sol-gel-derived yttria-stabilized zirconia ceramic features by soft lithographic patterning *Langmuir* **28** 15111–7

[95] Zeng Z F, Shi G, Petrescu F I T, Ungureanu L M and Li Y 2021 Micro-nano machining TiO_2 patterns without residual layer by unconventional imprinting *Appl. Sci.* **11** 10097

[96] He Q X and Tang L H 2022 Sub-5 nm nanogap electrodes towards single-molecular biosensing *Biosens. Bioelectron.* **213** 114486

[97] Raza A, Saeed Z, Aslam A, Nizami S M, Habib K and Malik A N 2024. Advances, application and challenges of lithography techniques *Proc. 2024 5th Int. Conf. on Advancements in Computational Sciences* (IEEE) pp 1–6

[98] Li M J, Chen Y L, Luo W X and Cheng X 2021 Interfacial interactions during demolding in nanoimprint lithography *Micromachines* **12** 349

[99] Lio G E, Ferraro A, Ritacco T, Aceti D M, De Luca A, Giocondo M and Caputo R 2021 Leveraging on ENZ metamaterials to achieve 2D and 3D hyper-resolution in two-photon direct laser writing *Adv. Mater.* **33** 2008644

[100] Singh M, Haverinen H M, Dhagat P and Jabbour G E 2010 Inkjet printing-process and its applications *Adv. Mater.* **22** 673–85

[101] Lyu Z Y, Wang J L and Chen Y F 2023 4D printing: interdisciplinary integration of smart materials, structural design, and new functionality *Int. J. Extrem. Manuf.* **5** 032011

[102] Roy S 2007 Fabrication of micro- and nano-structured materials using mask-less processes *J. Phys. D: Appl. Phys.* **40** R413–R26

[103] Cummins G and Desmulliez M P Y 2012 Inkjet printing of conductive materials: a review *Circuit World* **38** 193–213

[104] Calvert P 2001 Inkjet printing for materials and devices *Chem. Mater.* **13** 3299–305

[105] Fromm J E 1984 Numerical calculation of the fluid dynamics of drop-on-demand jets *IBM J. Res. Dev.* **28** 322–33

[106] Jang D, Kim D and Moon J 2009 Influence of fluid physical properties on ink-jet printability *Langmuir* **25** 2629–35

[107] Deegan R D, Bakajin O, Dupont T F, Huber G, Nagel S R and Witten T A 1997 Capillary flow as the cause of ring stains from dried liquid drops *Nature* **389** 827–9

[108] Torrisi F *et al* 2012 Inkjet-printed graphene electronics *ACS Nano* **6** 2992–3006

[109] Lin X D, Feng Z Y, Xiong Y, Sun W W, Yao W C, Wei Y C, Wang Z L and Sun Q J 2024 Piezotronic neuromorphic devices: principle, manufacture, and applications *Int. J. Extrem. Manuf.* **6** 032011

[110] Shah M A, Lee D G, Lee B Y and Hur S 2021 Classifications and applications of inkjet printing technology: a review *IEEE Access* **9** 140079–102

[111] Kwon K S, Rahman K, Phung T H, Hoath S D, Jeong S and Kim J S 2020 Review of digital printing technologies for electronic materials *Flex. Print. Electron.* **5** 043003

[112] Li H Y, Liu J K, Li K and Liu Y X 2019 Piezoelectric micro-jet devices: a review *Sens. Actuators* A **297** 111552

[113] Zhou Z X, Ruiz Cantu L, Chen X S, Alexander M R, Roberts C J, Hague R, Tuck C, Irvine D and Wildman R 2019 High-throughput characterization of fluid properties to predict droplet ejection for three-dimensional inkjet printing formulations *Addit. Manuf.* **29** 100792

[114] Bernasconi R, Brovelli S, Viviani P, Soldo M, Giusti D and Magagnin L 2022 Piezoelectric drop-on-demand inkjet printing of high-viscosity inks *Adv. Eng. Mater.* **24** 2100733

[115] Chen P H, Chen W C and Chang S H 1997 Bubble growth and ink ejection process of a thermal ink jet printhead *Int. J. Mech. Sci.* **39** 683–95

[116] Dou C R, Perez V, Qu J, Tsin A, Xu B and Li J Z 2021 A state-of-the-art review of laser-assisted bioprinting and its future research trends *ChemBioEng Rev.* **8** 517–34

[117] Tsui L K, Ven Chase Kayser S, Strong S A and Lavin J M 2021 High resolution aerosol jet printed components with electrodeposition-enhanced conductance *ECS J. Solid State Sci. Technol* **10** 047001

[118] Abdolmaleki H, Kidmose P and Agarwala S 2021 Droplet-based techniques for printing of functional inks for flexible physical sensors *Adv. Mater.* **33** 2006792

[119] Blayo A and Pineaux B 2005 Printing processes and their potential for RFID printing *Proc. 2005 Joint Conf. on Smart Objects and Ambient Intelligence: Innovative Context-Aware Services: Usages and Technologies* (Association for Computing Machinery) pp 27–30

[120] Grau G, Cen J L, Kang H K, Kitsomboonloha R, Scheideler W J and Subramanian V 2016 Gravure-printed electronics: recent progress in tooling development, understanding of printing physics, and realization of printed devices *Flex. Print. Electron.* **1** 023002

[121] Metters J P, Kadara R O and Banks C E 2011 New directions in screen printed electroanalytical sensors: an overview of recent developments *Analyst* **136** 1067–76

[122] Setti L, Fraleonimorgera A, Mencarelli I, Filippini A, Ballarin B and Dibiase M 2007 An HRP-based

amperometric biosensor fabricated by thermal inkjet printing *Sens. Actuators* B **126** 252–7
[123] Sen A K and Darabi J 2007 Droplet ejection performance of a monolithic thermal inkjet print head *J. Micromech. Microeng.* **17** 1420–7
[124] Setti L, Fraleoni-Morgera A, Ballarin B, Filippini A, Frascaro D and Piana C 2005 An amperometric glucose biosensor prototype fabricated by thermal inkjet printing *Biosens. Bioelectron.* **20** 2019–26
[125] Yan J Y, Huang Y and Chrisey D B 2013 Laser-assisted printing of alginate long tubes and annular constructs *Biofabrication* **5** 015002
[126] Keriquel V *et al* 2017 *In situ* printing of mesenchymal stromal cells, by laser-assisted bioprinting, for *in vivo* bone regeneration applications *Sci. Rep.* **7** 1778
[127] Brown M S, Brasz C F, Ventikos Y and Arnold C B 2012 Impulsively actuated jets from thin liquid films for high-resolution printing applications *J. Fluid Mech.* **709** 341–70
[128] Makrygianni M, Milionis A, Kryou C, Trantakis I, Poulikakos D and Zergioti I 2018 On-demand laser printing of picoliter-sized, highly viscous, adhesive fluids: beyond inkjet limitations *Adv. Mater. Interfaces* **5** 1800440
[129] Elrod S A, Hadimioglu B, Khuri-Yakub B T, Rawson E G, Richley E, Quate C F, Mansour N N and Lundgren T S 1989 Nozzleless droplet formation with focused acoustic beams *J. Appl. Phys.* **65** 3441–7
[130] Hadimioglu B, Elrod S A, Steinmetz D L, Lim M, Zesch J C, Khuri-Yakub B T, Rawson E G and Quate C F 1992 Acoustic ink printing *Proc. 1992 Ultrasonics Symp. Proc.* (IEEE) pp 929–35
[131] Guo Q, Su X, Zhang X G, Shao M C, Yu H X and Li D C 2021 A review on acoustic droplet ejection technology and system *Soft Matter* **17** 3010–21
[132] Lei Y L and Hu H 2020 SAW-driven droplet jetting technology in microfluidic: a review *Biomicrofluidics* **14** 061505
[133] McKibben N, Ryel B, Manzi J, Muramutsa F, Daw J, Subbaraman H, Estrada D and Deng Z X 2023 Aerosol jet printing of piezoelectric surface acoustic wave thermometer *Microsyst. Nanoeng.* **9** 51
[134] Foresti D, Kroll K T, Amissah R, Sillani F, Homan K A, Poulikakos D and Lewis J A 2018 Acoustophoretic printing *Sci. Adv.* **4** eaat1659
[135] Morales-Rodriguez M E, Joshi P C, Humphries J R, Fuhr P L and Mcintyre T J 2018 Fabrication of low cost surface acoustic wave sensors using direct printing by aerosol inkjet *IEEE Access* **6** 20907–15
[136] Bappy M O, Jiang Q, Atampugre S and Zhang Y L 2024 Aerosol jet printing of high-temperature bimodal sensors for simultaneous strain and temperature sensing using gold and indium tin oxide nanoparticle inks *ACS Appl. Nano Mater.* **7** 9453–9
[137] Barton K, Mishra S, Alex Shorter K, Alleyne A, Ferreira P and Rogers J 2010 A desktop electrohydrodynamic jet printing system *Mechatronics* **20** 611–6
[138] Yin Z P, Wang D Z, Guo Y L, Zhao Z Y, Li L Q, Chen W and Duan Y Q 2024 Electrohydrodynamic printing for high resolution patterning of flexible electronics toward industrial applications *InfoMat* **6** e12505
[139] Wang D Z, Zhao X J, Lin Y G, Ren T Q, Liang J S, Liu C and Wang L D 2017 Fabrication of micro/nano-structures by electrohydrodynamic jet technique *Front. Mech. Eng.* **12** 477–89
[140] Onses M S, Sutanto E, Ferreira P M, Alleyne A G and Rogers J A 2015 Mechanisms, capabilities, and applications of high-resolution electrohydrodynamic jet printing *Small* **11** 4237–66
[141] Guo H J, Zou W H, Zhao T M, Liang J W, Zhong Y, Zhou P L, Zhao Y, Liu L Q and Yu H B 2024 Multimodal electrohydrodynamic jet printing-based microstructure-sensitized flexible pressure sensor *Compos. Sci. Technol.* **254** 110686
[142] Suh J, Han B, Okuyama K and Choi M 2005 Highly charging of nanoparticles through electrospray of nanoparticle suspension *J. Colloid Interface Sci.* **287** 135–40
[143] Mondal K and McMurtrey M D 2020 Present status of the functional advanced micro-, nano-printings—a mini review *Mater. Today Chem.* **17** 100328
[144] Ru C H, Luo J, Xie S R and Sun Y 2014 A review of non-contact micro- and nano-printing technologies *J. Micromech. Microeng.* **24** 053001
[145] Chen H P, Yang C M and Lu M S C 2024 Development of a CMOS dielectrophoresis and microbead-based capacitive immunosensor array *IEEE Sens. J.* **24** 23454–61
[146] Harrey P M, Ramsey B J, Evans P S A and Harrison D J 2002 Capacitive-type humidity sensors fabricated using the offset lithographic printing process *Sens. Actuators* B **87** 226–32
[147] Nguyen H A D, Lee C, Shin K H and Lee D 2015 An investigation of the ink-transfer mechanism during the printing phase of high-resolution roll-to-roll gravure printing *IEEE Trans. Compon. Packag. Manuf. Technol.* **5** 1516–24
[148] Bariya M *et al* 2018 Roll-to-roll gravure printed electrochemical sensors for wearable and medical devices *ACS Nano* **12** 6978–87
[149] Leach R 2012 *The Printing Ink Manual* 4th edn (Springer)
[150] Tudorache M and Bala C 2007 Biosensors based on screen-printing technology, and their applications in environmental and food analysis *Anal. Bioanal. Chem.* **388** 565–78
[151] Beniwal A, Ganguly P, Aliyana A K, Khandelwal G and Dahiya R 2023 Screen-printed graphene-carbon ink based disposable humidity sensor with wireless communication *Sens. Actuators* B **374** 132731
[152] Eigler D M and Schweizer E K 1990 Positioning single atoms with a scanning tunnelling microscope *Nature* **344** 524–6
[153] Fan P F, Gao J, Mao H, Geng Y Q, Yan Y D, Wang Y Z, Goel S and Luo X C 2022 Scanning probe lithography: state-of-the-art and future perspectives *Micromachines* **13** 228
[154] Xie Z, Zhou X C, Tao X M and Zheng Z J 2012 Polymer nanostructures made by scanning probe lithography: recent progress in material applications *Macromol. Rapid Commun.* **33** 359–73
[155] Pires D, Hedrick J L, De Silva A, Frommer J, Gotsmann B, Wolf H, Despont M, Duerig U and Knoll A W 2010 Nanoscale three-dimensional patterning of molecular resists by scanning probes *Science* **328** 732–5
[156] Wouters D and Schubert U S 2004 Nanolithography and nanochemistry: probe-related patterning techniques and chemical modification for nanometer-sized devices *Angew. Chem., Int. Ed.* **43** 2480–95
[157] Wouters D, Hoeppener S and Schubert U S 2009 Local probe oxidation of self-assembled monolayers: templates for the assembly of functional nanostructures *Angew. Chem., Int. Ed.* **48** 1732–9
[158] Krämer S, Fuierer R R and Gorman C B 2003 Scanning probe lithography using self-assembled monolayers *Chem. Rev.* **103** 4367–418
[159] Song J Q, Liu Z F, Li C Z, Chen H F and He H X 1998 SPM-based nanofabrication using a synchronization technique *Appl. Phys.* A **66** S715–S7
[160] Bouchiat V and Esteve D 1996 Lift-off lithography using an atomic force microscope *Appl. Phys. Lett.* **69** 3098–100

[161] Liu X L, Chen K S, Wells S A, Balla I, Zhu J, Wood J D and Hersam M C 2017 Scanning probe nanopatterning and layer-by-layer thinning of black phosphorus *Adv. Mater.* **29** 1604121
[162] Braunschweig A B, Huo F W and Mirkin C A 2009 Molecular printing *Nat. Chem.* **1** 353–8
[163] Saban D, Shamir D, Zohar M and Burg A 2023 Glucose oxidase patterned meta-chemical surface for sensing glucose using dip-pen nanolithography *ChemElectroChem* **10** e202300424
[164] Chiu G L T and Shaw J M 1997 Optical lithography: introduction *IBM J. Res. Dev.* **41** 3–6
[165] Yuan H Y *et al* 2024 Spatial and energetic mapping of traps in FeFET during endurance process by advanced trap characterization platform *IEEE Electron Device Lett.* **12** 2371–4
[166] Levinson H J 2005 *Principles of Lithography* 2nd edn (SPIE Press)
[167] Harriott L R 2001 Limits of lithography *Proc. IEEE* **89** 366–74
[168] Ito T and Okazaki S 2000 Pushing the limits of lithography *Nature* **406** 1027–31
[169] Born M and Wolf E 2013 *Principles of Optics: Electromagnetic Theory of Propagation, Interference and Diffraction of Light* (Elsevier)
[170] Thompson L F, Willson C G and Bowden M J 1983 *Introduction to Microlithography: Theory, Materials, and Processing* (American Chemical Society)
[171] Pease R F and Chou S Y 2008 Lithography and other patterning techniques for future electronics *Proc. IEEE* **96** 248–70
[172] Bloomstein T M, Horn M W, Rothschild M, Kunz R R, Palmacci S T and Goodman R B 1997 Lithography with 157 nm lasers *J. Vac. Sci. Technol.* B **15** 2112–6
[173] Kim J, Yoon Y K and Allen M G 2016 Computer numerical control (CNC) lithography: light-motion synchronized UV-LED lithography for 3D microfabrication *J. Micromech. Microeng.* **26** 035003
[174] Sasago M, Endo M, Hirai Y, Ogawa K and Ishihara T 1986 Half-micron photolithography using a KrF excimer laser stepper *Proc. 1986 International Electron Devices Meeting* (IEEE) pp 316–9
[175] Kakizaki K, Saito T, Mitsuhashi K I, Arai M, Tada A, Kasahara S, Igarashi T and Hotta K 2000 High-repetition-rate ArF excimer laser for 193-nm lithography *Proc. SPIE* **4000** 1397–404
[176] Vogler K, Klaft I, Voss F, Bragin I, Bergmann E, Nagy T, Niemoeller N, Paetzel R, Govorkov S V and Hua G X 2001 Advanced F_2-lasers for 157-nm lithography *Proc. SPIE* **4346** 1175–82
[177] Li Z W, Zhang J F, Zheng Z P, Feng P F, Yu D W and Wang J J 2024 Elliptical vibration chiseling: a novel process for texturing ultra-high-aspect-ratio microstructures on the metallic surface *Int. J. Extrem. Manuf.* **6** 025102
[178] Cerrina F 2000 x-ray imaging: applications to patterning and lithography *J. Phys. D: Appl. Phys.* **33** R103–R16
[179] Xu P *et al* 2024 Demonstration of large MW and prominent endurance in a $Hf_{0.5}Zr_{0.5}O_2$ FeFET with IGZO channel utilizing postdeposition annealing *IEEE Electron Device Lett.* **45** 2110–3
[180] Wang Y *et al* 2023 A stable rhombohedral phase in ferroelectric $Hf(Zr)_{1+x}O_2$ capacitor with ultralow coercive field *Science* **381** 558–63
[181] Feng Z F, Giubertoni D, Cian A, Valt M, Ardit M, Pedrielli A, Vanzetti L, Fabbri B, Guidi V and Gaiardo A 2023 Fabrication of a highly NO_2-sensitive gas sensor based on a defective ZnO nanofilm and using electron beam lithography *Micromachines* **14** 1908
[182] Groves T R 2014 Electron beam lithography *Nanolithography* ed M Feldman (Woodhead Publishing) pp 80–115
[183] Cui B 2011 *Recent Advances in Nanofabrication Techniques and Applications* (IntechOpen)
[184] Joshi-Imre A and Bauerdick S 2014 Direct-write ion beam lithography *J. Nanotechnol.* **2014** 170415
[185] Gao M 2016 *Direct-Writing Nanolithography* (Chemical Industry Press) (https://doi.org/10.1002/9783527696406.ch10)
[186] Kang H, Joo H, Choi J, Kim Y J, Lee Y, Cho S Y and Jung H T 2022 Top-down approaches for 10 nm-scale nanochannel: toward exceptional H_2S detection *ACS Nano* **16** 17210–9
[187] Petrzelka J E and Hardt D E 2012 Static load-displacement behavior of PDMS microfeatures for soft lithography *J. Micromech. Microeng.* **22** 075015
[188] Wissman J, Lu T and Majidi C 2013 Soft-matter electronics with stencil lithography *Proc. Sensors, 2013 IEEE* (IEEE) pp 1–4
[189] Chen H P, Lentz D M, Rhoades A M, Pyles R A, Haider K W, Vanapalli S A, Nunley R K and Hedden R C 2012 Surface infusion micropatterning of elastomeric substrates *Microfluid. Nanofluid.* **12** 451–64
[190] Rolland J P, Hagberg E C, Denison G M, Carter K R and De Simone J M 2004 High-resolution soft lithography: enabling materials for nanotechnologies *Angew. Chem., Int. Ed.* **43** 5796–9
[191] Rogers J A and Nuzzo R G 2005 Recent progress in soft lithography *Mater. Today* **8** 50–56
[192] Qin D, Xia Y N and Whitesides G M 2010 Soft lithography for micro- and nanoscale patterning *Nat. Protocols* **5** 491–502
[193] Larsen N B, Biebuyck H, Delamarche E and Michel B 1997 Order in microcontact printed self-assembled monolayers *J. Am. Chem. Soc.* **119** 3017–26
[194] Du B R, Lu J Y, Wang G T, Han M G, Gao Y and Luo S D 2024 Combined laser-induced graphene and microcontact printing for processing scalable and stackable micro-stripe patterns toward multifunctional electronic devices *Carbon* **225** 119148
[195] Poirier G E, Tarlov M J and Rushmeier H E 1994 Two-dimensional liquid phase and the $px\sqrt{3}$ phase of alkanethiol self-assembled monolayers on Au(111) *Langmuir* **10** 3383–6
[196] Torres C M S 2012 *Alternative Lithography: Unleashing the Potentials of Nanotechnology* (Springer)
[197] Helmuth J A, Schmid H, Stutz R, Stemmer A and Wolf H 2006 High-speed microcontact printing *J. Am. Chem. Soc.* **128** 9296–7
[198] Brehmer M, Conrad L and Funk L 2003 New developments in soft lithography *J. Dispersion Sci. Technol.* **24** 291–304
[199] Xia Y N, Kim E, Zhao X M, Rogers J A, Prentiss M and Whitesides G M 1996 Complex optical surfaces formed by replica molding against elastomeric masters *Science* **273** 347–9
[200] Dervisevic M, Jara Fornerod M J, Harberts J, Zangabad P S and Voelcker N H 2024 Wearable microneedle patch for transdermal electrochemical monitoring of urea in interstitial fluid *ACS Sens.* **9** 932–41
[201] Zhao X M, Xia Y N and Whitesides G M 1996 Fabrication of three-dimensional micro-structures: microtransfer molding *Adv. Mater.* **8** 837–40
[202] Park M J, Choi W M and Park O O 2006 Patterning polymer light-emitting diodes by micromolding in capillary *Curr. Appl. Phys.* **6** 627–31
[203] Heule M and Gauckler L J 2003 Miniaturised arrays of tin oxide gas sensors on single microhotplate substrates

fabricated by micromolding in capillaries *Sens. Actuators* B **93** 100–6
[204] King E, Xia Y N, Zhao X M and Whitesides G M 1997 Solvent-assisted microcontact molding: a convenient method for fabricating three-dimensional structures on surfaces of polymers *Adv. Mater.* **9** 651–4
[205] Wang S L *et al* 2023 Body-area sensor network featuring micropyramids for sports healthcare *Nano Res.* **16** 1330–7
[206] Hassanin H and Jiang K 2011 Multiple replication of thick PDMS micropatterns using surfactants as release agents *Microelectron. Eng.* **88** 3275–7
[207] Qi J L, Wu Z X, Wang W B, Bao K, Wang L Z, Wu J K, Ke C X, Xu Y and He Q Y 2023 Fabrication and applications of van der Waals heterostructures *Int. J. Extrem. Manuf.* **5** 022007
[208] Pattnaik S, Karunakar D B and Jha P K 2012 Developments in investment casting process—A review *J. Mater. Process. Technol.* **212** 2332–48
[209] Li T, Xu Z Z, Xu B B, Guo Z H, Jiang Y H, Zhang X H, Bayati M, Liu T X and Liu Y H 2023 Advancing pressure sensors performance through a flexible MXene embedded interlocking structure in a microlens array *Nano Res.* **16** 10493–9
[210] Miranda I, Souza A, Sousa P, Ribeiro J, Castanheira E M S, Lima R and Minas G 2022 Properties and applications of PDMS for biomedical engineering: a review *J. Funct. Biomater.* **13** 2
[211] Alderighi T, Malomo L, Auzinger T, Bickel B, Cignoni P and Pietroni N 2022 State of the art in computational mould design *Comput. Graph. Forum* **41** 435–52
[212] Kang S B, Lee J, Lee S, Kim S, Kim J K, Algadi H, Al-sayari S, Kim D E, Kim D and Lee T 2016 Highly sensitive pressure sensor based on bioinspired porous structure for real-time tactile sensing *Adv. Electron. Mater.* **2** 1600356
[213] Zhang X F, Tang G L, Yang S H and Benattar J J 2010 Two-dimensional self-assemblies of silica nanoparticles formed using the "bubble deposition technique" *Langmuir* **26** 16828–32
[214] Tang G L, Zhang X F, Yang S H, Derycke V and Benattar J J 2010 New confinement method for the formation of highly aligned and densely packed single-walled carbon nanotube monolayers *Small* **6** 1488–91
[215] Qu Z *et al* 2023 Bubble wall confinement-driven molecular assembly toward sub-12 nm and beyond precision patterning *Sci. Adv.* **9** eadf3567
[216] Wang L Y, Wang Z W, Bakhtiyari A N and Zheng H Y 2020 A comparative study of laser-induced graphene by CO_2 infrared laser and 355 nm ultraviolet (UV) laser *Micromachines* **11** 1094
[217] Yin B S, Liu F R, Chen Q Y, Liu M and Wang F Y 2024 Flexible strain sensors based on bionic parallel vein-like structures for human motion monitoring *Sensors* **24** 468
[218] Schallenberg T, Schumacher C, Gundel S and Faschinger W 2002 Shadow mask technology *Thin Solid Films* **412** 24–29
[219] Tixier A, Mita Y, Gouy J P and Fujita H 2000 A silicon shadow mask for deposition on isolated areas *J. Micromech. Microeng.* **10** 157–62
[220] Nouhi A, Sookhak Lari M R, Spelt J K and Papini M 2015 Implementation of a shadow mask for direct writing in abrasive jet micro-machining *J. Mater. Process. Technol.* **223** 232–9
[221] Ren X C, Pei K, Peng B Y, Zhang Z C, Wang Z R, Wang X Y and Chan P K L 2016 A low-operating-power and flexible active-matrix organic-transistor temperature-sensor array *Adv. Mater.* **28** 4832–8
[222] Resnick D 2014 Nanoimprint lithography *Nanolithography* ed M Feldman (Woodhead Publishing) pp 315–47
[223] Wu D X, Rajput N S and Luo X C 2016 Nanoimprint lithography—the past, the present and the future *Curr. Nanosci.* **12** 712–24
[224] Fan Y, Wang C H, Sun J X, Peng X G, Tian H M, Li X M, Chen X L, Chen X M and Shao J Y 2023 Electric-driven flexible-roller nanoimprint lithography on the stress-sensitive warped wafer *Int. J. Extrem. Manuf.* **5** 035101
[225] Chou S Y, Krauss P R and Renstrom P J 1996 Nanoimprint lithography *J. Vac. Sci. Technol.* B **14** 4129–33
[226] Nie Z H and Kumacheva E 2008 Patterning surfaces with functional polymers *Nat. Mater.* **7** 277–90
[227] Zanut A, Cian A, Cefarin N, Pozzato A and Tormen M 2020 Nanoelectrode arrays fabricated by thermal nanoimprint lithography for biosensing application *Biosensors* **10** 90
[228] Alkaisi M M, Blaikie R J, McNab S J, Cheung R and Cumming D R S 1999 Sub-diffraction-limited patterning using evanescent near-field optical lithography *Appl. Phys. Lett.* **75** 3560–2
[229] Wang J S, Fang F Z, An H J, Wu S, Qi H M, Cai Y X and Guo G Y 2023 Laser machining fundamentals: micro, nano, atomic and close-to-atomic scales *Int. J. Extrem. Manuf.* **5** 012005
[230] Thiel M, Fischer J, von Freymann G and Wegener M 2010 Direct laser writing of three-dimensional submicron structures using a continuous-wave laser at 532 nm *Appl. Phys. Lett.* **97** 221102
[231] Zhou J, Shen H, Pan Y Q and Ding X H 2016 Experimental study on laser microstructures using long pulse *Opt. Lasers Eng.* **78** 113–20
[232] Kiisk V, Kahro T, Kozlova J, Matisen L and Alles H 2013 Nanosecond laser treatment of graphene *Appl. Surf. Sci.* **276** 133–7
[233] Audouard E and Mottay E 2023 High efficiency GHz laser processing with long bursts *Int. J. Extrem. Manuf.* **5** 015003
[234] Li X R, Zhang B Y, Jakobi T, Yu Z L, Ren L Q and Zhang Z H 2024 Laser-based bionic manufacturing *Int. J. Extrem. Manuf.* **6** 042003
[235] Cui S Y, Lu Y Y, Kong D P, Luo H Y, Peng L, Yang G, Yang H Y and Xu K C 2023 Laser direct writing of Ga_2O_3/liquid metal-based flexible humidity sensors *Opto-Electron. Adv.* **6** 220172
[236] Luo Y, Miao Y P, Wang H M, Dong K, Hou L, Xu Y Y, Chen W C, Zhang Y, Zhang Y and Fan W 2023 Laser-induced Janus graphene/poly(p-phenylene benzobisoxazole) fabrics with intrinsic flame retardancy as flexible sensors and breathable electrodes for fire-fighting field *Nano Res.* **16** 7600–8
[237] Chu G L, Zhang Y Y, Zhou Z R, Zeng W X, Chen D F, Yu S P, Wang J M, Guo Y M, Sun X and Li M 2023 Rapid CO_2-laser scribing fabrication of an electrochemical sensor for the direct detection of Pb^{2+} and Cd^{2+} *Nano Res.* **16** 7671–81
[238] Lin J, Peng Z W, Liu Y Y, Ruiz-Zepeda F, Ye R Q, Samuel E L G, Yacaman M J, Yakobson B I and Tour J M 2014 Laser-induced porous graphene films from commercial polymers *Nat. Commun.* **5** 5714
[239] Xu K C *et al* 2023 Laser direct writing of flexible thermal flow sensors *Nano Lett.* **23** 10317–25
[240] Yang L *et al* 2022 Intrinsically breathable and flexible NO_2 gas sensors produced by laser direct writing of self-assembled block copolymers *ACS Appl. Mater. Interfaces* **14** 17818–25
[241] Lu Y Y *et al* 2024 Stretchable graphene–hydrogel interfaces for wearable and implantable bioelectronics *Nat. Electron.* **7** 51–65
[242] Zhong B W, Xu H, Qin X K, Liu L C, Wang H L and Wang L L 2024 A crosstalk-free dual-mode sweat sensing

system for naked-eye sweat loss quantification via changes in structural reflectance *Bio-Des. Manuf.* **7** 428–38

[243] Shaheen M E, Gagnon J E and Fryer B J 2013 Laser ablation of iron: a comparison between femtosecond and picosecond laser pulses *J. Appl. Phys.* **114** 083110

[244] Chichkov B N, Momma C, Nolte S, von Alvensleben F and Tünnermann A 1996 Femtosecond, picosecond and nanosecond laser ablation of solids *Appl. Phys.* A **63** 109–15

[245] Son S, Park J E, Lee J, Yang M Y and Kang B 2016 Laser-assisted fabrication of single-layer flexible touch sensor *Sci. Rep.* **6** 34629

[246] Li Z Y, Zhang B, Li K, Zhang T and Yang X N 2020 A wide linearity range and high sensitivity flexible pressure sensor with hierarchical microstructures via laser marking *J. Mater. Chem.* C **8** 3088–96

[247] Huang Y S, Chen K Y, Cheng Y T, Lee C K and Tsai H E 2020 An inkjet-printed flexible non-enzymatic lactate sensor for clinical blood plasma test *IEEE Electron Device Lett.* **41** 597–600

[248] Zhou K *et al* 2023 Manufacturing of graphene based synaptic devices for optoelectronic applications *Int. J. Extrem. Manuf.* **5** 042006

[249] Gao L, Wu M G, Yu X G and Yu J S 2024 Device design principles and bioelectronic applications for flexible organic electrochemical transistors *Int. J. Extrem. Manuf.* **6** 012005

[250] Khan Y, Thielens A, Muin S, Ting J, Baumbauer C and Arias A C 2020 A new frontier of printed electronics: flexible hybrid electronics *Adv. Mater.* **32** 1905279

[251] Marquez C *et al* 2023 Direct ink-write printing of ceramic clay with an embedded wireless temperature and relative humidity sensor *Sensors* **23** 3352

[252] Sui Y K and Zorman C A 2020 Review—inkjet printing of metal structures for electrochemical sensor applications *J. Electrochem. Soc.* **167** 037571

[253] Jung W B, Jang S, Cho S Y, Jeon H J and Jung H T 2020 Recent progress in simple and cost-effective top-down lithography for ≈10 nm scale nanopatterns: from edge lithography to secondary sputtering lithography *Adv. Mater.* **32** 1907101

[254] Salim A and Lim S 2017 Review of recent inkjet-printed capacitive tactile sensors *Sensors* **17** 2593

[255] Huang Y Q *et al* 2024 Deep insights into the mechanism of nitrogen on the endurance enhancement in ferroelectric field effect transistors: trap behavior during memory window degradation *Appl. Phys. Lett.* **124** 133504

[256] Lawson R A and Robinson A P G 2016 Overview of materials and processes for lithography *Front. Nanosci.* **11** 1–90

[257] Hasan R M M and Luo X 2018 Promising lithography techniques for next-generation logic devices *Nanomanuf. Metrol.* **1** 67–81

[258] Giannopoulos I, Mochi I, Vockenhuber M, Ekinci Y and Kazazis D 2024 Extreme ultraviolet lithography reaches 5 nm resolution *Nanoscale* **16** 15533–43

[259] Zhang J H and Yang B 2010 Patterning colloidal crystals and nanostructure arrays by soft lithography *Adv. Funct. Mater.* **20** 3411–24

[260] Moonen P F, Yakimets I and Huskens J 2012 Fabrication of transistors on flexible substrates: from mass-printing to high-resolution alternative lithography strategies *Adv. Mater.* **24** 5526–41

[261] Mackenzie D M A, Smistrup K, Whelan P R, Luo B R, Shivayogimath A, Nielsen T, Petersen D H, Messina S A and Bøggild P 2017 Batch fabrication of nanopatterned graphene devices via nanoimprint lithography *Appl. Phys. Lett.* **111** 193103

[262] Ifuku T *et al* 2024 Nanoimprint lithography performance advances for new application spaces *Proc. SPIE* **12956** 1295603

[263] Nakayama T, Yonekawa M, Matsuoka Y, Azuma H, Takabayashi Y, Aghili A, Mizuno M, Choi J and Jones C E 2017 Improved defectivity and particle control for nanoimprint lithography high-volume semiconductor manufacturing *Proc. SPIE* **10144** 1014407

[264] Schift H and Kristensen A 2017 Nanoimprint lithography *Springer Handbook of Nanotechnology* ed B Bhushan (Springer)

[265] Martinez-Perdiguero J, Retolaza A, Otaduy D, Juarros A and Merino S 2013 Real-time label-free surface plasmon resonance biosensing with gold nanohole arrays fabricated by nanoimprint lithography *Sensors* **13** 13960–8

[266] Stratakis E, Ranella A, Farsari M and Fotakis C 2009 Laser-based micro/nanoengineering for biological applications *Prog. Quantum Electron.* **33** 127–63

[267] Lu Y Y, Kong D P, Yang G, Wang R H, Pang G Y, Luo H Y, Yang H Y and Xu K C 2023 Machine learning-enabled tactile sensor design for dynamic touch decoding *Adv. Sci.* **10** 2303949

[268] Wang L H, Liu J X, Qi X J, Zhang X J, Wang H, Tian M W and Qu L J 2024 Flexible micro/nanopatterned pressure tactile sensors: technologies, morphology and applications *J. Mater. Chem.* A **12** 8065–99

[269] Liu M M *et al* 2023 Patterning two-dimensional semiconductors with thermal etching *InfoMat* **5** e12474

[270] Ma S M *et al* 2024 Ultra-sensitive and stable multiplexed biosensors array in fully printed and integrated platforms for reliable perspiration analysis *Adv. Mater.* **36** 2311106

[271] Shi J D, Wang L, Dai Z H, Zhao L Y, Du M D, Li H B and Fang Y 2018 Multiscale hierarchical design of a flexible piezoresistive pressure sensor with high sensitivity and wide linearity range *Small* **14** 1800819

[272] Špačková B, Lynn N S, Slabý J, Šípová H and Homola J 2018 A route to superior performance of a nanoplasmonic biosensor: consideration of both photonic and mass transport aspects *ACS Photonics* **5** 1019–25

[273] Manfrinato V R, Zhang L H, Su D, Duan H G, Hobbs R G, Stach E A and Berggren K K 2013 Resolution limits of electron-beam lithography toward the atomic scale *Nano Lett.* **13** 1555–8

[274] Liu T S, Chen P, Qiu F, Yang H Y, Jin N T Y, Chew Y, Wang D, Li R D, Jiang Q C and Tan C L 2024 Review on laser directed energy deposited aluminum alloys *Int. J. Extrem. Manuf.* **6** 022004

[275] Hong M H, Chen Z C, Tang M, Shi L P and Chong T C 2009 Femtosecond laser irradiation for functional micro-/nanostructure fabrication *Proc. 2009 Conf. on Lasers & Electro Optics & The Pacific Rim Conf. on Lasers and Electro-Optics* (IEEE)

[276] Zheng S J, Zhu Y N and Krishnaswamy S 2013 Fiber humidity sensors with high sensitivity and selectivity based on interior nanofilm-coated photonic crystal fiber long-period gratings *Sens. Actuators* B **176** 264–74

[277] Li H H, Zhan Q F, Liu Y W, Liu L P, Yang H L, Zuo Z H, Shang T, Wang B M and Li R W 2016 Stretchable spin valve with stable magnetic field sensitivity by ribbon-patterned periodic wrinkles *ACS Nano* **10** 4403–9

[278] Liu G G, Han M and Hou W L 2015 High-resolution and fast-response fiber-optic temperature sensor using silicon Fabry-Pérot cavity *Opt. Express* **23** 7237–47

[279] Sharma R K, Chan P C H, Tang Z N, Yan G Z, Hsing I M and Sin J K O 2001 Investigation of stability and reliability of tin oxide thin-film for integrated micro-machined gas sensor devices *Sens. Actuators* B **81** 9–16

[280] Lin L, Xie Y N, Wang S H, Wu W Z, Niu S M, Wen X N and Wang Z L 2013 Triboelectric active sensor array for self-powered static and dynamic pressure detection and tactile imaging *ACS Nano* **7** 8266–74

[281] Saadeldin A S, Hameed M F O, Elkaramany E M A and Obayya S S A 2019 Highly sensitive terahertz metamaterial sensor *IEEE Sens. J.* **19** 7993–9

[282] Li N *et al* 2023 The measurement of responsivity of infrared photodetectors using a cavity blackbody *J. Semicond.* **44** 102301

[283] Li Z X, Xu H, Zheng Y Q, Liu L C, Li L L, Lou Z and Wang L L 2025 A reconfigurable heterostructure transistor array for monocular 3D parallax reconstruction *Nat. Electron.* (https://doi.org/10.1038/s41928-024-01261-6)

[284] Li S X, Xia H, Wang L, Sun X C, An Y, Zhu H, Bai B F and Sun H B 2022 Self-powered and flexible photodetector with high polarization sensitivity based on $MAPbBr_3$–$MAPbI_3$ microwire lateral heterojunction *Adv. Funct. Mater.* **32** 2206999

[285] Liu F, Piao Y, Choi J S and Seo T S 2013 Three-dimensional graphene micropillar based electrochemical sensor for phenol detection *Biosens. Bioelectron.* **50** 387–92

[286] Xu R, Chen C Q, Sun J P, He Y L, Li X, Lu M H and Chen Y F 2023 The design, manufacture and application of multistable mechanical metamaterials-a state-of-the-art review *Int. J. Extrem. Manuf.* **5** 042013

[287] Koala R A S D, Fujita M and Nagatsuma T 2022 Nanophotonics-inspired all-silicon waveguide platforms for terahertz integrated systems *Nanophotonics* **11** 1741–59

[288] Yu H Y, Sun X Y, Liu G L, Fateh U, Ban D S, Deng N P and Qiu F 2021 Gas environment independent temperature sensor via double-metal surface plasmon resonance *Opt. Express* **29** 15393–402

[289] Piliarik M, Šípová H, Kvasnička P, Galler N, Krenn J R and Homola J 2012 High-resolution biosensor based on localized surface plasmons *Opt. Express* **20** 672–80

[290] Gao W C, Huang J Y, He J, Zhou R H, Li Z M, Chen Z Y, Zhang Y F and Pan C F 2023 Recent advances in ultrathin materials and their applications in e-skin *InfoMat* **5** e12426

[291] Huang X H, Liu L S, Lin Y H, Feng R, Shen Y Y, Chang Y N and Zhao H B 2023 High-stretchability and low-hysteresis strain sensors using origami-inspired 3D mesostructures *Sci. Adv.* **9** eadh9799

[292] Zhang Y, Xu Y, Guan S, Zheng J, Gu H, Li L, Xiao R, Fang T, Zou H and Chen X 2023 Modulation bandwidth enhancement in monolithic integrated two-section DFB lasers based on the detuned loading effect *J. Semicond.* **44** 112301

[293] Wu W T, Li L L, Li Z X, Sun J Z and Wang L L 2023 Extensible integrated system for real-time monitoring of cardiovascular physiological signals and limb health *Adv. Mater.* **35** 2304596

[294] Li L L, Zhao S F, Ran W H, Li Z X, Yan Y X, Zhong B W, Lou Z, Wang L L and Shen G Z 2022 Dual sensing signal decoupling based on tellurium anisotropy for VR interaction and neuro-reflex system application *Nat. Commun.* **13** 5975

[295] Yu Z J, Gao H, Wang Y, Yu Y, Tsang H K, Sun X K and Dai D X 2023 Fundamentals and applications of photonic waveguides with bound states in the continuum *J. Semicond.* **44** 101301

[296] Wu L, Ji Y, Dan H Y, Bowen C R and Yang Y 2023 A multifunctional optical-thermal logic gate sensor array based on ferroelectric $BiFeO_3$ thin films *InfoMat* **5** e12414

[297] Xu C H *et al* 2024 A physicochemical-sensing electronic skin for stress response monitoring *Nat. Electron.* **7** 168–79

[298] Niu H S, Yin F F, Kim E S, Wang W X, Yoon D Y, Wang C, Liang J G, Li Y and Kim N Y 2023 Advances in flexible sensors for intelligent perception system enhanced by artificial intelligence *InfoMat* **5** e12412

[299] Hu W D, Ye Z H, Liao L, Chen H L, Chen L, Ding R J, He L, Chen X S and Lu W 2014 128 x 128 long-wavelength/mid-wavelength two-color HgCdTe infrared focal plane array detector with ultralow spectral cross talk *Opt. Lett.* **39** 5184–7

[300] Liu W J *et al* 2023 Integrating 2D layered materials with 3D bulk materials as van der Waals heterostructures for photodetections: current status and perspectives *InfoMat* **5** e12470

[301] Li Y, Yang L, Deng S H, Huang H, Wang Y Y, Xiong Z P, Feng S M, Wang S Q, Li T and Zhang T 2023 A machine learning-assisted multifunctional tactile sensor for smart prosthetics *InfoMat* **5** e12463

[302] Ma R, Zhang X D, Sutherland D, Bochenkov V and Deng S K 2024 Nanofabrication of nanostructure lattices: from high-quality large patterns to precise hybrid units *Int. J. Extrem. Manuf.* **6** 062004

[303] Sánchez-Pastor J, Kaděra P, Sakaki M, Jakoby R, Lacik J, Benson N and Jiménez-Sáez A 2024 A wireless W-band 3D-printed temperature sensor based on a three-dimensional photonic crystal operating beyond 1000 °C *Commun. Eng.* **3** 137

[304] Duan Y Q, Xie W S, Yin Z P and Huang Y A 2024 Multi-material 3D nanoprinting for structures to functional micro/nanosystems *Int. J. Extrem. Manuf.* **6** 063001

[305] Zheludev N I and Kivshar Y S 2012 From metamaterials to metadevices *Nat. Mater.* **11** 917–24

[306] Huang Y H *et al* 2023 A direct laser-synthesized magnetic metamaterial for low-frequency wideband passive microwave absorption *Int. J. Extrem. Manuf.* **5** 035503

[307] Kumar A, Gupta M, Pitchappa P, Tan T C, Chattopadhyay U, Ducournau G, Wang N, Chong Y D and Singh R 2022 Active ultrahigh-Q (0.2×10^6) THz topological cavities on a chip *Adv. Mater.* **34** 2202370

[308] Li Z Y, Chang H N, Lai J M, Song F L, Yao Q F, Liu H Q, Ni H Q, Niu Z C and Zhang J 2023 Terahertz phononic crystal in plasmonic nanocavity *J. Semicond.* **44** 082901

[309] Chen H T, Cao H Y, Yu Z J, Zhao W K and Dai D X 2023 Waveguide-integrated optical modulators with two-dimensional materials *J. Semicond.* **44** 111301

[310] Zhou W, Shen X Y, Yang X L, Wang J J and Zhang W 2024 Fabrication and integration of photonic devices for phase-change memory and neuromorphic computing *Int. J. Extrem. Manuf.* **6** 022001

[311] Zhao Y J, Zhao X W and Gu Z Z 2010 Photonic crystals in bioassays *Adv. Funct. Mater.* **20** 2970–88

[312] Yu Z *et al* 2023 Swarming magnetic photonic-crystal microrobots with on-the-fly visual pH detection and self-regulated drug delivery *InfoMat* **5** e12464

[313] Li J X, Madiyar F, Ghate S, Kumar K S and Thomas J 2023 Plasmonic organic electrochemical transistors for enhanced sensing *Nano Res.* **16** 3201–6

[314] Peng J P, Liu P J, Chen Y T, Guo Z H, Liu Y H and Yue K 2023 Templated synthesis of patterned gold nanoparticle assemblies for highly sensitive and reliable SERS substrates *Nano Res.* **16** 5056–64

[315] Hu Y D, Hu Y L, Wang Z Y, Yong J L, Xiong W, Wu D and Xu S X 2024 Efficient concentration of trace analyte with ordered hotspot construction for a robust and sensitive SERS platform *Int. J. Extrem. Manuf.* **6** 035505

[316] Cai M, Jiao Z D, Nie S, Wang C J, Zou J and Song J Z 2021 A multifunctional electronic skin based on patterned metal films for tactile sensing with a broad linear response range *Sci. Adv.* **7** eabl8313

[317] Melik R, Unal E, Kosku Perkgoz N, Puttlitz C and Demir H V 2009 Flexible metamaterials for wireless strain sensing *Appl. Phys. Lett.* **95** 181105
[318] Choong C-L *et al* 2014 Highly stretchable resistive pressure sensors using a conductive elastomeric composite on a micropyramid array *Adv. Mater.* **26** 3451–8
[319] Chhetry A, Kim J, Yoon H and Park J Y 2019 Ultrasensitive interfacial capacitive pressure sensor based on a randomly distributed microstructured iontronic film for wearable applications *ACS Appl. Mater. Interfaces* **11** 3438–49
[320] Wan Y B, Qiu Z G, Hong Y, Wang Y, Zhang J M, Liu Q X, Wu Z G and Guo C F 2018 A highly sensitive flexible capacitive tactile sensor with sparse and high-aspect-ratio microstructures *Adv. Electron. Mater.* **4** 1700586
[321] Jing Q S, Choi Y S, Smith M, Ćatić N, Ou C L and Kar-Narayan S 2019 Aerosol-jet printed fine-featured triboelectric sensors for motion sensing *Adv. Mater. Technol.* **4** 1800328
[322] Zhao S F, Ran W H, Wang D P, Yin R Y, Yan Y X, Jiang K, Lou Z and Shen G Z 2020 3D dielectric layer enabled highly sensitive capacitive pressure sensors for wearable electronics *ACS Appl. Mater. Interfaces* **12** 32023–30
[323] Xiong Y X, Shen Y K, Tian L, Hu Y G, Zhu P L, Sun R and Wong C P 2020 A flexible, ultra-highly sensitive and stable capacitive pressure sensor with convex microarrays for motion and health monitoring *Nano Energy* **70** 104436
[324] Yang J C, Kim J O, Oh J, Kwon S Y, Sim J Y, Kim D W, Choi H B and Park S 2019 Microstructured porous pyramid-based ultrahigh sensitive pressure sensor insensitive to strain and temperature *ACS Appl. Mater. Interfaces* **11** 19472–80
[325] Yan Z G *et al* 2021 Flexible high-resolution triboelectric sensor array based on patterned laser-induced graphene for self-powered real-time tactile sensing *Adv. Funct. Mater.* **31** 2100709
[326] Zhang C J, Li Z K, Li H Y, Yang Q, Wang H, Shan C, Zhang J Z, Hou X and Chen F 2022 Femtosecond laser-induced supermetalphobicity for design and fabrication of flexible tactile electronic skin sensor *ACS Appl. Mater. Interfaces* **14** 38328–38
[327] Woo S J, Kong J H, Kim D G and Kim J M 2014 A thin all-elastomeric capacitive pressure sensor array based on micro-contact printed elastic conductors *J. Mater. Chem.* C **2** 4415–22
[328] Li L L, Pan L J, Ma Z, Yan K, Cheng W, Shi Y and Yu G H 2018 All inkjet-printed amperometric multiplexed biosensors based on nanostructured conductive hydrogel electrodes *Nano Lett.* **18** 3322–7
[329] Yadav K K, Shamir D, Kornweitz H, Peled Y, Zohar M and Burg A 2024 Development of meta-chemical surface by dip-pen nanolithography for precise electrochemical lead sensing *Small Methods* **8** 2301118
[330] Xu X L, Peng B, Li D H, Zhang J, Wong L M, Zhang Q, Wang S J and Xiong Q H 2011 Flexible visible–infrared metamaterials and their applications in highly sensitive chemical and biological sensing *Nano Lett.* **11** 3232–8
[331] Wang D X, Luo S Y and Xu K D 2024 A flexible terahertz metamaterial sensor for pesticide sensing and detection *ACS Appl. Mater. Interfaces* **16** 27969–78
[332] Liang L J *et al* 2023 Metamaterial Flexible GaN/graphene heterostructure-enabled multidimensional terahertz sensor for femtogram-level detection of aspartic acid *IEEE Sens. J.* **23** 16814–22
[333] Yao H Y *et al* 2022 Patterned graphene and terahertz metasurface-enabled multidimensional ultra-sensitive flexible biosensors and bio-assisted optical modulation amplification *Results Phys.* **40** 105884
[334] Tao H *et al* 2011 Metamaterials on paper as a sensing platform *Adv. Mater.* **23** 3197–201
[335] He Q Y, Sudibya H G, Yin Z Y, Wu S X, Li H, Boey F, Huang W, Chen P and Zhang H 2010 Centimeter-long and large-scale micropatterns of reduced graphene oxide films: fabrication and sensing applications *ACS Nano* **4** 3201–8
[336] Kim B Y, Lee H B and Lee N E 2019 A durable, stretchable, and disposable electrochemical biosensor on three-dimensional micro-patterned stretchable substrate *Sens. Actuators* B **283** 312–20
[337] Saito M, Kitamura A, Murahashi M, Yamanaka K, Hoa L Q, Yamaguchi Y and Tamiya E 2012 Novel gold-capped nanopillars imprinted on a polymer film for highly sensitive plasmonic biosensing *Anal. Chem.* **84** 5494–500
[338] Yao H Z, Mei H Y, Zhang W W, Zhong S C and Wang X F 2022 Theoretical and experimental research on terahertz metamaterial sensor with flexible substrate *IEEE Photon. J.* **14** 3700109
[339] Qin Z Y, Wang P N and Wang Y J 2005 Enhanced sensing performance of the amperometric gas sensor by laser-patterning of the polymer membrane electrode *Sens. Actuators* B **107** 805–11
[340] Li Z, Wang Z W, Khan J, LaGasse M K and Suslick K S 2020 Ultrasensitive monitoring of museum airborne pollutants using a silver nanoparticle sensor array *ACS Sens.* **5** 2783–91
[341] Lin Y J, Huang L, Chen L, Zhang J K, Shen L, Chen Q and Shi W Z 2015 Fully gravure-printed NO_2 gas sensor on a polyimide foil using WO_3-PEDOT:PSS nanocomposites and Ag electrodes *Sens. Actuators* B **216** 176–83
[342] Kim J W, Porte Y, Ko K Y, Kim H and Myoung J M 2017 Micropatternable double-faced ZnO nanoflowers for flexible gas sensor *ACS Appl. Mater. Interfaces* **9** 32876–86
[343] Tang N, Jiang Y, Qu H M and Duan X X 2018 Graphene oxide-doped conducting polymer nanowires fabricated by soft lithography for gas sensing applications *IEEE Sens. J.* **18** 7765–71
[344] Wang Q L, Zhang G N, Zhang H Y, Duan Y Q, Yin Z P and Huang Y A 2021 High-resolution, flexible, and full-color perovskite image photodetector via electrohydrodynamic printing of ionic-liquid-based ink *Adv. Funct. Mater.* **31** 2100857
[345] Zumeit A, Dahiya A S, Christou A, Mukherjee R and Dahiya R 2022 Printed GaAs microstructures-based flexible high-performance broadband photodetectors *Adv. Mater. Technol.* **7** 2200772
[346] Wu W Q, Wang X D, Han X, Yang Z, Gao G Y, Zhang Y F, Hu J F, Tan Y W, Pan A L and Pan C F 2019 Flexible photodetector arrays based on patterned $CH_3NH_3PbI_{3-x}Cl_x$ perovskite film for real-time photosensing and imaging *Adv. Mater.* **31** 1805913
[347] Lu Q C *et al* 2023 Large-scale, uniform-patterned $CsCu_2I_3$ films for flexible solar-blind photodetectors array with ultraweak light sensing *Small* **19** 2300364
[348] Choi K H, Zubair M and Dang H W 2014 Characterization of flexible temperature sensor fabricated through drop-on-demand electrohydrodynamics patterning *Jpn. J. Appl. Phys.* **53** 05HB02
[349] Liu Z J *et al* 2021 A thin-film temperature sensor based on a flexible electrode and substrate *Microsyst. Nanoeng.* **7** 42
[350] Yan S Z, Shen D D, Newton A A, Zhu S Y and Xin B J 2024 Patterned, flexible, self-supporting humidity sensor with core-sheath structure for real-time sensing of human-related humidity *Colloids Surf.* A **695** 134198
[351] Zhou C, Zhang X S, Tang N, Fang Y, Zhang H N and Duan X X 2020 Rapid response flexible humidity sensor for respiration monitoring using nano-confined strategy *Nanotechnology* **31** 125302
[352] Cai S-Y *et al* 2018 Ultrahigh sensitive and flexible magnetoelectronics with magnetic nanocomposites:

toward an additional perception of artificial intelligence *ACS Appl. Mater. Interfaces* **10** 17393–400
[353] Wang J, Xu S Y, Zhang C C, Yin A L, Sun M Y, Yang H R, Hu C G and Liu H 2023 Field effect transistor-based tactile sensors: from sensor configurations to advanced applications *InfoMat* **5** e12376
[354] Qiu A D, Li P L, Yang Z K, Yao Y, Lee I and Ma J 2019 A path beyond metal and silicon: polymer/nanomaterial composites for stretchable strain sensors *Adv. Funct. Mater.* **29** 1806306
[355] Feng Z P, Hao Y N, Qin J, Zhong S L, Bi K, Zhao Y, Yin L J, Pei J Y and Dang Z M 2023 Ultrasmall barium titanate nanoparticles modulated stretchable dielectric elastomer sensors with large deformability and high sensitivity *InfoMat* **5** e12413
[356] Luo Y S, Chen X L, Li X M, Tian H M, Wang L and Shao J Y 2023 A flexible dual-function capacitive sensor enhanced by loop-patterned fibrous electrode and doped dielectric pillars for spatial perception *Nano Res.* **16** 7550–8
[357] Shi Y J *et al* 2023 A self-powered piezoelectret sensor based on foamed plastic garbage for monitoring human motions *Nano Res.* **16** 1269–76
[358] Wu M G *et al* 2023 Stretchable, skin-conformable neuromorphic system for tactile sensory recognizing and encoding *InfoMat* **5** e12472
[359] Gong W, Hou C Y, Zhou J, Guo Y B, Zhang W, Li Y G, Zhang Q H and Wang H Z 2019 Continuous and scalable manufacture of amphibious energy yarns and textiles *Nat. Commun.* **10** 868
[360] Dai S F, Li X J, Jiang C M, Ping J F and Ying Y B 2023 Triboelectric nanogenerators for smart agriculture *InfoMat* **5** e12391
[361] Liu F, Feng Y, Qi Y C, Liu G X, Zhou H, Lin Y, Fan B B, Zhang Z, Dong S C and Zhang C 2023 Self-powered wireless body area network for multi-joint movements monitoring based on contact-separation direct current triboelectric nanogenerators *InfoMat* **5** e12428
[362] Yang W F, Gong W, Hou C Y, Su Y, Guo Y B, Zhang W, Li Y G, Zhang Q H and Wang H Z 2019 All-fiber tribo-ferroelectric synergistic electronics with high thermal-moisture stability and comfortability *Nat. Commun.* **10** 5541
[363] Yin F F, Niu H S, Kim E S, Shin Y K, Li Y and Kim N Y 2023 Advanced polymer materials-based electronic skins for tactile and non-contact sensing applications *InfoMat* **5** e12424
[364] Ma H D *et al* 2023 Robust hydrogel sensors for unsupervised learning enabled sign-to-verbal translation *InfoMat* **5** e12419
[365] Zhong B W *et al* 2024 Interindividual- and blood-correlated sweat phenylalanine multimodal analytical biochips for tracking exercise metabolism *Nat. Commun.* **15** 624
[366] Qin X K, Zhong B W, Lv S X, Long X, Xu H, Li L L, Xu K C, Lou Z, Luo Q and Wang L L 2024 A zero-voltage-writing artificial nervous system based on biosensor integrated on ferroelectric tunnel junction *Adv. Mater.* **36** 2404026
[367] Lee C W *et al* 2023 Rationally designed graphene channels for real-time sodium ion detection for electronic tongue *InfoMat* **5** e12427
[368] Wang M H, Wu P X, Yang S, Wu G L, Li N, Tan X F and Yang Q L 2023 β-cyclodextrin-modified AuBi metallic aerogels enable efficient peroxidase mimicking for colorimetric sensing of urease-positive pathogenic bacteria *Nano Res.* **16** 9663–71
[369] Xue H L, Gao W S, Gao J W, Schneider G F, Wang C and Fu W Y 2023 Radiofrequency sensing systems based on emerging two-dimensional materials and devices *Int. J. Extrem. Manuf.* **5** 032010
[370] Liu Y Q, Lian M R, Chen W and Chen H P 2024 Recent advances in fabrication and functions of neuromorphic system based on organic field effect transistor *Int. J. Extrem. Manuf.* **6** 022008
[371] Wu J, Liu H, Chen W W, Ma B and Ju H X 2023 Device integration of electrochemical biosensors *Nat. Rev. Bioeng.* **1** 346–60
[372] Hu Y X, Zhou Y, Luo G H, Li D G and Qu M N 2024 Femtosecond laser-induced nanoparticle implantation into flexible substrate for sensitive and reusable microfluidics SERS detection *Int. J. Extrem. Manuf.* **6** 045005
[373] Zhu J F, Wang Z Y, Lin S W, Jiang S, Liu X Y and Guo S S 2020 Low-cost flexible plasmonic nanobump metasurfaces for label-free sensing of serum tumor marker *Biosens. Bioelectron.* **150** 111905
[374] Zhang S Z, Rao S L, Li Y F, Wang S, Sun D Y, Liu F and Cheng G J 2024 Laser-forged transformation and encapsulation of nanoalloys: pioneering robust wideband electromagnetic wave absorption and shielding from GHz to THz *Int. J. Extrem. Manuf.* **6** 055501
[375] Yu Y C, Joshi P C, Wu J and Hu A M 2018 Laser-induced carbon-based smart flexible sensor array for multiflavors detection *ACS Appl. Mater. Interfaces* **10** 34005–12
[376] Yang Z, Xu T T, Zhang S B, Li H, Ji Y L, Jia X D and Li J L 2023 Multifunctional N, S-doped and methionine functionalized carbon dots for on-off-on Fe^{3+} and ascorbic acid sensing, cell imaging, and fluorescent ink applying *Nano Res.* **16** 5401–11
[377] Zhang X Y, Chen P F, He S W X, Jiang B W, Wang Y, Cheng Y H, Peng J, Verpoort F, Wang J and Kou Z K 2023 Single-atom metal-nitrogen-carbon catalysts energize single molecule detection for biosensing *InfoMat* **5** e12421
[378] Pasupuleti K S, Chougule S S, Vidyasagar D, Bak N H, Jung N, Kim Y H, Lee J H, Kim S G and Kim M D 2023 UV light driven high-performance room temperature surface acoustic wave NH_3 gas sensor using sulfur-doped g-C_3N_4 quantum dots *Nano Res.* **16** 7682–95
[379] Wang C *et al* 2024 Biomimetic olfactory chips based on large-scale monolithically integrated nanotube sensor arrays *Nat. Electron.* **7** 157–67
[380] Kim Y *et al* 2021 Tailored graphene micropatterns by wafer-scale direct transfer for flexible chemical sensor platform *Adv. Mater.* **33** 2004827
[381] Li X L, Zhu Y P, Liu Z, Peng L Z, Liu X Q, Niu C Q, Zheng J, Zuo Y H and Cheng B W 2023 75 GHz germanium waveguide photodetector with 64 Gbps data rates utilizing an inductive-gain-peaking technique *J. Semicond.* **44** 012301
[382] Li Z X, Zheng Y Q, Li L L, Liu L C, Lou Z and Wang L L 2024 Parallel photoelectron storage and visual preprocessing based on nanowire defect engineering for image degradation *Adv. Funct. Mater.* **34** 2304119
[383] Tao H Y, Wang T L, Li D Y, Xing J and Li G W 2023 Preparation, properties, and applications of Bi_2O_2Se thin films: a review *J. Semicond.* **44** 031001
[384] Tang Y J *et al* 2023 Enabling low-drift flexible perovskite photodetectors by electrical modulation for wearable health monitoring and weak light imaging *Nat. Commun.* **14** 4961
[385] Yan S L, Huang J L, Xue T, Zhang Y H and Ma W Q 2023 Long wavelength interband cascade photodetector with type II InAs/GaSb superlattice absorber *J. Semicond.* **44** 042301
[386] He T J, Liu S P, Li W, Zhong L, Ma X Y, Xiong C, Lin N and Wang Z N 2023 Study of quantum well mixing induced by impurity-free vacancy in the primary epitaxial wafers of a 915 nm semiconductor laser *J. Semicond.* **44** 102302
[387] Hu W D, Chen X S, Ye Z H and Lu W 2011 A hybrid surface passivation on HgCdTe long wave infrared detector with

in-situ CdTe deposition and high-density hydrogen plasma modification *Appl. Phys. Lett.* **99** 091101
[388] Zhong Y J, Fang H Y, Ran Y T and Zhu H W 2023 Fast optical-writing recognition based on two-dimensional photothermoelectric effect assisted with deep learning *InfoMat* **5** e12384
[389] Dai W, Liu W K, Yang J, Xu C, Alabastri A, Liu C, Nordlander P, Guan Z Q and Xu H X 2020 Giant photothermoelectric effect in silicon nanoribbon photodetectors *Light Sci. Appl.* **9** 120
[390] Dong Z *et al* 2023 Wafer-scale patterned growth of type-II Dirac semimetal platinum ditelluride for sensitive room-temperature terahertz photodetection *InfoMat* **5** e12403
[391] Li L L, Xu H, Li Z X, Liu L C, Lou Z and Wang L L 2023 CMOS-compatible tellurium/silicon ultra-fast near-infrared photodetector *Small* **19** 2303114
[392] Long Z H, Ding Y C, Qiu X, Zhou Y, Kumar S and Fan Z Y 2023 A dual-mode image sensor using an all-inorganic perovskite nanowire array for standard and neuromorphic imaging *J. Semicond.* **44** 092604
[393] Qu X Y, Sun H J, Kan X L, Lei B, Shao J J, Wang Q, Wang W J, Ni Z H and Dong X C 2023 Temperature-sensitive and solvent-resistance hydrogel sensor for ambulatory signal acquisition in "moist/hot environment" *Nano Res.* **16** 10348–57
[394] Gong Z *et al* 2024 Flexible calorimetric flow sensor with unprecedented sensitivity and directional resolution for multiple flight parameter detection *Nat. Commun.* **15** 3091
[395] Hou C Y and Zhu M F 2022 Semiconductors flex thermoelectric power *Science* **377** 815–6
[396] Liu Z J, Tian B, Jiang Z D, Li S M, Lei J M, Zhang Z K, Liu J J, Shi P and Lin Q J 2023 Flexible temperature sensor with high sensitivity ranging from liquid nitrogen temperature to 1200 °C *Int. J. Extrem. Manuf.* **5** 015601
[397] Li Z X, Wang J, Dai L, Sun X H, An M, Duan C, Li J and Ni Y H 2020 Asymmetrically patterned cellulose nanofibers/graphene oxide composite film for humidity sensing and moist-induced electricity generation *ACS Appl. Mater. Interfaces* **12** 55205–14
[398] Bal M 2014 An industrial Wireless Sensor Networks framework for production monitoring *Proc. 2014 IEEE 23rd Int. Symp. on Industrial Electronics* (IEEE) pp 1442–7
[399] Kozitsina A N, Svalova T S, Malysheva N N, Okhokhonin A V, Vidrevich M B and Brainina K Z 2018 Sensors based on bio and biomimetic receptors in medical diagnostic, environment, and food analysis *Biosensors* **8** 35
[400] Si S H, Dittrich L and Hoffmann M 2017 The *NanoTuFe*—fabrication of large area periodic nanopatterns with tunable feature sizes at low cost *Microelectron. Eng.* **180** 71–80
[401] Scheifele S, Friedrich J, Lechler A and Verl A 2014 Flexible, self-configuring control system for a modular production system *Proc. Technol.* **15** 398–405
[402] Pang Y *et al* 2018 Epidermis microstructure inspired graphene pressure sensor with random distributed spinosum for high sensitivity and large linearity *ACS Nano* **12** 2346–54
[403] Chen L, Hu Y Z, Huang H X, Liu C, Wu D and Xia J L 2023 Direct laser patterning of organic semiconductors for high performance OFET-based gas sensors *J. Mater. Chem.* C **11** 7088–97
[404] Sui X Y, Downing J R, Hersam M C and Chen J H 2021 Additive manufacturing and applications of nanomaterial-based sensors *Mater. Today* **48** 135–54
[405] Wang X P, Zhang M J, Zhang L W, Xu J C, Xiao X Q and Zhang X S 2022 Inkjet-printed flexible sensors: from function materials, manufacture process, and applications perspective *Mater. Today Commun.* **31** 103263
[406] Wang J R, Li Z Y and Gu Z Y 2021 A comprehensive review of template-synthesized multi-component nanowires: from interfacial design to sensing and actuation applications *Sens. Actuators Rep.* **3** 100029
[407] Scholz S, Mueller T, Plasch M, Limbeck H, Adamietz R, Iseringhausen T, Kimmig D, Dickerhof M and Woegerer C 2016 A modular flexible scalable and reconfigurable system for manufacturing of Microsystems based on additive manufacturing and e-printing *Robot. Comput. Integr. Manuf* **40** 14–23
[408] Zhang W L, Schneider J, Prodanov M F, Vashchenko V V, Rogach A L, Yuan X C and Srivastava A K 2023 Photo-induced flexible semiconductor CdSe/CdS quantum rods alignment *J. Semicond.* **44** 092605
[409] Wang S *et al* 2024 Flexible pressure sensors with ultrahigh stress tolerance enabled by periodic microslits *Microsyst. Nanoeng.* **10** 24
[410] Li C and Zheng K 2023 Methods, progresses, and opportunities of materials informatics *InfoMat* **5** e12425
[411] Zhao S F, Ran W H, Lou Z, Li L L, Poddar S, Wang L L, Fan Z Y and Shen G Z 2022 Neuromorphic-computing-based adaptive learning using ion dynamics in flexible energy storage devices *Natl Sci. Rev.* **9** nwac158
[412] Hu S Q, Huan X, Liu Y, Cao S X, Wang Z R and Kim J T 2023 Recent advances in meniscus-on-demand three-dimensional micro- and nano-printing for electronics and photonics *Int. J. Extrem. Manuf.* **5** 032009
[413] Cai Z M *et al* 2024 Bio-inspired hybrid laser direct writing of interfacial adhesion for universal functional coatings *Adv. Funct. Mater.* **34** 2408354
[414] Dong C Y, An X, Wu Z C, Zhu Z G, Xie C, Huang J A and Luo L B 2023 Multilayered $PdTe_2$/thin Si heterostructures as self-powered flexible photodetectors with heart rate monitoring ability *J. Semicond.* **44** 112001
[415] Kim Y, Hwang E, Kai C, Xu K C, Pan H and Hong S 2024 Recent developments in selective laser processes for wearable devices *Bio-Des. Manuf.* **7** 517–47
[416] Xu K C, Cai Z M, Luo H Y, Lin X Y, Yang G, Xie H B, Ko S H and Yang H Y 2024 An *in-situ* hybrid laser-induced integrated sensor system with antioxidative copper *Int. J. Extrem. Manuf.* **6** 065501